ALUMINUM-CATALYZED COUPLING OF CARBON DIOXIDE AND CYCLIC ETHERS

Jeroen Rintjema Tanger

UNIVERSITAT ROVIRA I VIRGILI
ALUMINUM-CATALYZED COUPLING OF CARBON DIOXIDE AND CYCLIC ETHERS
Jeroen Rintjema Tanger

UNIVERSITAT ROVIRA I VIRGILI
ALUMINUM-CATALYZED COUPLING OF CARBON DIOXIDE AND CYCLIC ETHERS
Jeroen Rintjema Tanger

Jeroen Rintjema

Aluminum-Catalyzed Coupling of Carbon Dioxide and Cyclic Ethers

DOCTORAL THESIS

Supervised by Prof. Arjan W. Kleij

ICIQ – Institut Català d'Investigació Química

UNIVERSITAT ROVIRA I VIRGILI

Tarragona 2017

UNIVERSITAT ROVIRA I VIRGILI
ALUMINUM-CATALYZED COUPLING OF CARBON DIOXIDE AND CYCLIC ETHERS
Jeroen Rintjema Tanger

UNIVERSITAT ROVIRA I VIRGILI

Avinguda Països Catalans 16
43007 Tarragona
Tel: +34977920847
E-mail: akleij@iciq.es

Prof. Dr. Arjan W. Kleij, Group leader at the Institute of Chemical Research of Catalonia (ICIQ) and Research Professor of the Catalan Institution for Research and Advanced Studies (ICREA),

I state that the present study, entitled `*Aluminum-Catalyzed Coupling of Carbon Dioxide and Cyclic Ethers´*, presented by Jeroen Rintjema to receive the degree of Doctor, has been carried out under my supervision at the Institut Català d'Investigació Química (ICIQ).

Tarragona, October 2017

Doctoral thesis supervisor

Prof. Dr. Arjan W. Kleij

UNIVERSITAT ROVIRA I VIRGILI
ALUMINUM-CATALYZED COUPLING OF CARBON DIOXIDE AND CYCLIC ETHERS
Jeroen Rintjema Tanger

UNIVERSITAT ROVIRA I VIRGILI
ALUMINUM-CATALYZED COUPLING OF CARBON DIOXIDE AND CYCLIC ETHERS
Jeroen Rintjema Tanger

моей Катюше

UNIVERSITAT ROVIRA I VIRGILI
ALUMINUM-CATALYZED COUPLING OF CARBON DIOXIDE AND CYCLIC ETHERS
Jeroen Rintjema Tanger

"Not all chemicals are bad. Without chemicals such as hydrogen and oxygen, for example, there would be no way to make water, a vital ingedrient in beer."

Dave Barry

UNIVERSITAT ROVIRA I VIRGILI
ALUMINUM-CATALYZED COUPLING OF CARBON DIOXIDE AND CYCLIC ETHERS
Jeroen Rintjema Tanger

Acknowledgements

It is now almost four years ago that I left from Holland to start my PhD studies here in Tarragona. Over the years I have seen many people defending their thesis and now it is my turn to show the chemistry I have developed during my doctorate. First of all, I would like to thank Arjan for giving me the opportunity to join his group, providing useful advice and discussing chemistry (I quickly noticed you like to talk… a lot). Especially I appreciate your focus when it comes to defining projects, you always seem to know which experiments will bring the chemistry to the next level.

All of the research that builds up my manuscript would not have been possible without the aid of ICIQ´s support unit. Thanks to the guys from NMR, Chromatography, X-ray and in particular to Marta and Cristina for all your patience and help in setting up reactions with CO_2.

Many thanks to all the former and present members of the group, especially to Luis, Leticia, Victor and Sergio. We all started our PhD around the same time and therefore spent quite some time together both in- and outside the lab. Also the other people that joined the group afterwards Wusheng, Kike, Aijie, Nicole, Rui, Alex and Jianing, you have been good labmates. Special mention to Roel for working with me on our project focused on product divergence. You always had a lot of interesting suggestions and ideas for new projects, although at times you were maybe diverging a bit too much. Thanks to Claudia for enlightening us with your visit to Tarragona not just once, but twice! Also for showing me the "golden elephant", how I could have missed this awesome bar for all these years. Giulia, thanks for all those amazing tiramisu you made for the lab. Chris, our paths crossed only for a couple weeks in the lab, but I am thankful for accepting the invitiation to be part of my committee and I am curious to hear your opinion.

Outside the lab I spent most of my time practising different kinds of sports. In the summer season (March-October in Tarragona) we spent many weekends on the beach playing volleyball with a rather large group from ICIQ, thanks everyone! Thanks to Bart for not having to give up my atlethics routine when moving to Spain, as well as being my flatmate. For the last couple of years my variety in sport has been reducing drastically down to one: climbing! Thanks to all who joined the various climbing trips throughout the past two years: Marino, Victor, Hanna, Ani, Fedor, Pablo, Franziska, Ilario, Evgeny, Masaki and others.

I would like to thank all my friends in Holland, you always made sure I had a busy schedule whenever I was coming over. Also its is nice to see that most of you managed to spend some days of vacation in Tarragona, although I feel that was not much of a sacrifice. Thanks to Katia´s parents for inviting me over to St. Petersburg. Though it is very very cold in winter, I am looking forward to my next visit this summer when temperatures will move above zero. I also would like to thank my parents for their support and frequent visits to Tarragona, I feel like you know more about the city than I do. Thanks to my brother, I still owe you a lot of good weather that you did not get on your previous visits. I hope that your next trip to Spain will make up for that!

Finally a very big thanks to my Katusha. We have been together basically since the start of my PhD and I have enjoyed every moment of it, dankjewel!

Curriculum Vitae

Jeroen Rintjema was born on May 31, **1988** in Heemskerk (Netherlands). He started studying chemistry at the University of Amsterdam in **2006**, obtaining his BSc degree in **2009** where he worked on rhodium catalyzed enantioselective hydroformylation. In **2011** he received his MSc degree in "*Molecular Design, Synthesis and Catalysis*" from the same university where he worked in the group of Professor Joost N. H. Reek on supramolecular gold chemistry. In **2013** he started his PhD under the supervision of Professor Arjan W. Kleij at the Institute of Chemical research of Catalonia (ICIQ) in Tarragona where he performed the research that is described in this thesis. His PhD research was financially supported with a pre-doctoral fellowship from the ICIQ Foundation. Results described in this thesis have been communicated at several international conferences including the Zing conference on Carbon Dioxide Catalysis (Albufeira, **2016**) and the American Chemical Society National Meeting and Exposition (San Fransisco, **2017**).

UNIVERSITAT ROVIRA I VIRGILI
ALUMINUM-CATALYZED COUPLING OF CARBON DIOXIDE AND CYCLIC ETHERS
Jeroen Rintjema Tanger

List of publications

1. *Unique insight into the Halide-Free Coupling of Epoxides with CO_2 via an Alkyl Carbonate Intermediate*
   Huang, R.[#]; **Rintjema, J.**[#]; González-Fabra, J.; Martín, E.; Escudero-Adán, E. C.; Bo, C.; Urakawa, A.; Kleij, A. W. *manuscript in preparation*. [#] Equal contributions.

2. *Vanadium(V) Catalysts with High Activity for the Coupling of Epoxides and CO_2: Characterization of a Putative Catalytic Intermediate*
   Miceli, C.; **Rintjema, J.**; Martin, E.; Escudero-Adán, E. M.; Zonta, C.; Licini, G.; Kleij, A. W. *ACS Catal.* **2017**, *7*, 2367–2373. (*Not part of this thesis)*

3. *Aluminum-Mediated Formation of Cyclic Carbonates: Benchmarking Catalytic Performance Metrics*
   Rintjema, J.; Kleij, A. W. *ChemSusChem* **2017**, *10,* 1274–1282.

4. *Substrate-Controlled Product Divergence: Conversion of CO_2 into Heterocyclic Products*
   Rintjema, J.; Epping, R.; Fiorani, G.; Martin, E.; Escudero-Adán, E. M.; Kleij, A. W. *Angew. Chem. Int. Ed.* **2016**, *55*, 3972–3976.

5. *Catalytic One-Pot Oxetane to Carbamate Conversions: Formal Synthesis of Drug Relevant Molecules*
   Guo, W.: Laserna, V.; **Rintjema, J.**; Kleij, A. W. *Adv. Synth. Catal.* **2016**, *358*, 1602–1607. *Selected as very important paper (VIP), featured on the front cover of this issue*.

6. *Highly Chemoselective Catalytic Coupling of Substituted Oxetanes and Carbon Dioxide*
   Rintjema, J.; Guo, W.; Martin, E.; Escudero-Adán, E. M.; Kleij, A. W. *Chem. Eur. J.* **2015**, *21*, 10754–10762.

Reviews and book chapters

7. *Metal Complexes Catalyzed Cyclization with CO_2*
   Rintjema, J.; Peña-Carrodeguas, L.; Laserna, V.; Sopeña, S.; Kleij, A. W. *Top. Organomet. Chem.* **2016**, *53,* 39-72.

8. *Substrate-Assisted Carbon Dioxide Activation as a Versatile Approach for Heterocyclic Synthesis*
   Rintjema, J.; Kleij, A. W. *Synthesis* **2016**, *48*, 3863–3878.

Publications not related to this thesis

9. *Supramolecular Ligands in Gold(I) Catalysis*
   Gramage-Doria, R.; Bellini, R.; **Rintjema, J.;** Reek, J. N. H. *ChemCatChem* **2013**, *5*, 1084–1087.

Table of contents

UNIVERSITAT ROVIRA I VIRGILI
ALUMINUM-CATALYZED COUPLING OF CARBON DIOXIDE AND CYCLIC ETHERS
Jeroen Rintjema Tanger

Summary

Utilization of carbon dioxide as a C1-building block for organic chemistry has become increasingly popular over the last decades. **Chapter 1** provides an overview of the general applications of CO_2 and more specifically its reaction with epoxides to form cyclic carbonates. Furthermore, the aluminum aminotriphenolate catalyst is introduced as a highly potent system to activate epoxides and facilitate cyclic carbonate formation.

A detailed comparative study on the synthesis of five-membered cyclic carbonates is reported in **Chapter 2**, where the activity of 15 different binary catalytic systems is compared in the conversion of several terminal and internal epoxides into their respective cyclic carbonate products. The aluminum aminotriphenolate system proved to be an attractive option both in terms of catalytic activity and low cost.

In **Chapter 3** the first general methodology for the coupling of oxetanes and CO_2 is presented, leading to the formation of various six-membered cyclic carbonates in high yield and selectivity. The latter are useful monomers for polymer synthesis or as building blocks in organic synthesis. We have applied the developed method in the formal synthesis of two linear carbamate based drug molecules.

Chapter 4 describes the halide-free conversion of epoxides containing alcohol or amine functionalities, that mediate *in-situ* formation of linear carbonate or carbamate nucleophiles that can ring-open the epoxide. This strategy gave access to a broad scope of cyclic carbonate and carbamate structures, including the 5-oxazolidinone based antidepressant Toloxatone. In addition, by selectively triggering either the conventional and the newly developed reaction mechanism we were able to induce product divergence from a single substrate using the same catalyst.

Chapter 5 provides an in-depth study on the *in-situ* formation of an alkyl carbonate species from epoxy alcohols and CO_2, along with their subsequent conversion to cyclic carbonates under *operando* conditions. This chapter combines classical mechanistic experiments, X-ray analysis, *in-situ* IR spectroscopy and DFT-analysis, resulting in a comprehensive description of the reaction mechanism with a special focus on a linear carbonate, that acts as an internal nucleophile to ring-open the epoxide.

UNIVERSITAT ROVIRA I VIRGILI
ALUMINUM-CATALYZED COUPLING OF CARBON DIOXIDE AND CYCLIC ETHERS
Jeroen Rintjema Tanger

List of abbreviations

In this manuscript, the abbreviations and acronyms most commonly used in organic and organometallic chemistry have been used following the recommendations from "Guidelines for authors" of *Journal of Organic Chemistry*.

Additional abbreviations and acronyms used in this manuscript are referenced in the list below:

5MCC: 5-membered cyclic carbonate
6MCC: 6-membered cyclic carbonate
TON: Turn over number
TOF: Turn over frequency
m-CPBA: *meta*-chloroperbenzoic acid
DMAP: 4-(Dimethylamino)pyridine
DIPEA: N,N-Diisopropylethylamine
TBACl: Tetrabutylammonium chloride
TBAB: Tetrabutylammonium bromide
TBAI: Tetrabutylammonium iodide
PPNCl: Bis(triphenylphosphine)iminium chloride
PPNBr: Bis(triphenylphosphine)iminium bromide
PPNI: Bis(triphenylphosphine)iminium iodide
DCM: Dichloromethane
MEK: Methyl ethyl ketone
Mes: Mesitylene
PO: Propylene oxide
HBD: Hydrogen bond donor
TPA: Aminotriphenolate
CHO: Cyclohexene oxide
PC: Propylene carbonate
ee: enantiomeric excess
er: enantiomeric ratio
DMC: Dimethylcarbonate
NIS: N-iodo succinimide

UNIVERSITAT ROVIRA I VIRGILI
ALUMINUM-CATALYZED COUPLING OF CARBON DIOXIDE AND CYCLIC ETHERS
Jeroen Rintjema Tanger

Chapter 1.

Al-catalyzed Formation of Cyclic Carbonates from Epoxides and CO_2
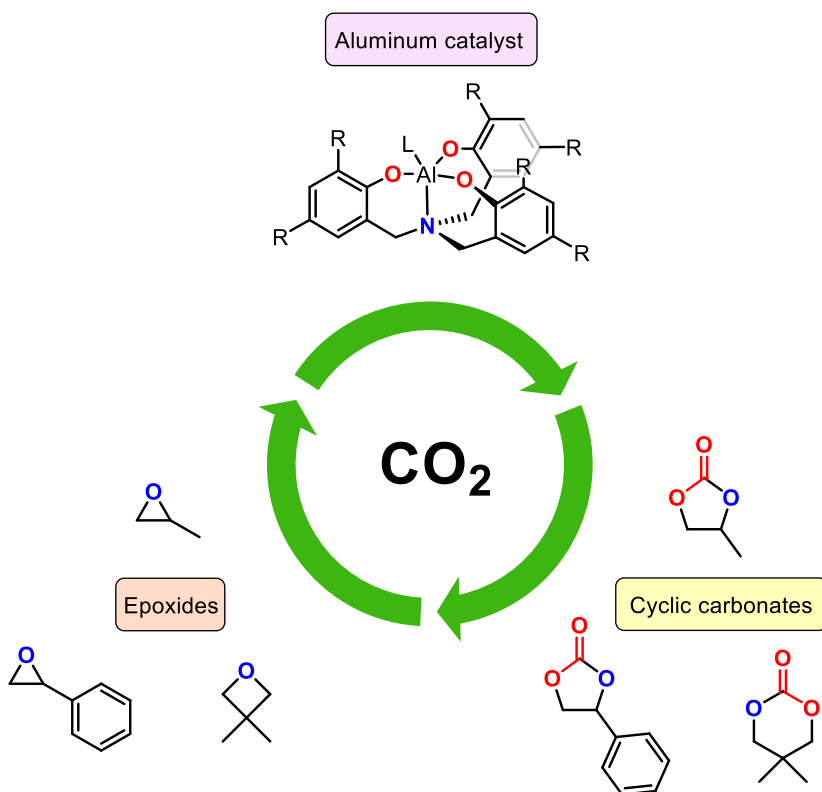
UNIVERSITAT ROVIRA I VIRGILI
ALUMINUM-CATALYZED COUPLING OF CARBON DIOXIDE AND CYCLIC ETHERS
Jeroen Rintjema Tanger

Chapter 1

1.1 Carbon dioxide

The use of CO_2 in chemistry and other applications dates back many centuries, starting with its discovery by Joseph Black in 1754.[1] He found that by heating calcium carbonate, a gas was produced that was heavier than air. Also he showed that passing CO_2 through a saturated aqueous solution of calcium hydroxide produced calcium carbonate, a principle he used to demonstrate that humans exhale carbon dioxide. In the following century, carbon dioxide became known in a completely different way with the start of the industrial revolution. The years after the industrial revolution in the early 19th century witnessed a drastic increase in global carbon emissions accompanied by climate change and rising temperatures around the world. These effects can be ascribed to the release of greenhouse gasses into the atmosphere, of which carbon dioxide is one of the main contributors. The majority of CO_2 comes from industrial processes, annually releasing billions of tons into the earth´s atmosphere.[2] While carbon dioxide levels fluctuate throughout history, they have never been above 300 ppm since the beginning of mankind. Last year, the 400 ppm threshold (see Figure 1) was surpassed and studies indicate that the current trend is far from over.[3]
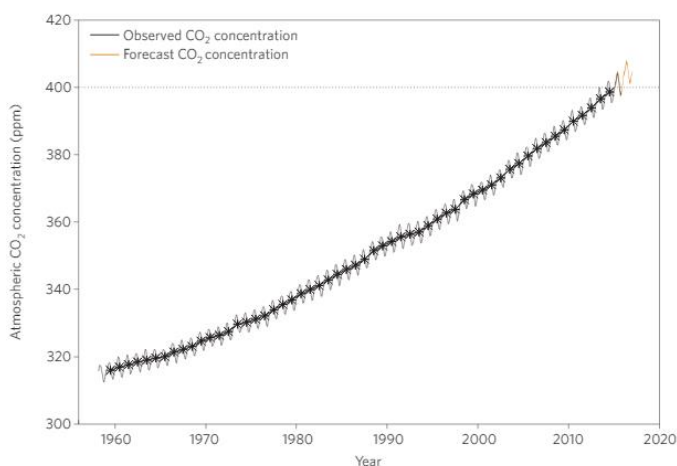
Figure 1. Rising atmospheric CO_2 levels.[3]

Apart from being a pollutant, the scientific community has developed ways to make use of CO_2 and nowadays it finds application in many industrial branches (see Figure 2). Due to its inert properties it is a relatively safe gas to handle and can for instance be used for pneumatic systems and fire extinguishers. The solid form is called "dry ice" and is frequently employed in the food industry or in wine-making. Most of these

Chapter 1

processes only temporarily store CO_2, where it is released again after use. In the chemical industry however, processes have been developed to transform it into useful compounds.
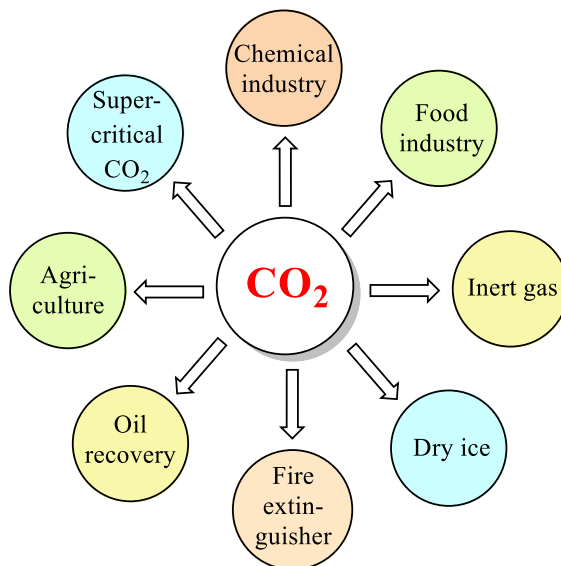
Figure 2. Utilization of CO₂ in a variety of applications.

An early example of CO_2 transformation is the Kolbe-Schmitt reaction invented by Herman Kolbe and Rudolf Schmitt in 1860.[4] This reaction describes the carboxylation of sodium phenoxide (the sodium salt of phenol) under 100 bar of CO_2 at 125 $^{\circ}$C. Treatment of the subsequent product with acid yields salicylic acid, which is the precursor for aspirin. Currently there are several CO_2-derived compounds being synthesized (even industrially) including urea, methanol, carbonates, carbamates, and polyurethanes among others. Whereas urea is mainly made using carbon dioxide gas, the synthesis of most CO_2 derived compounds relies on the use of activated derivatives of CO_2 such as dimethylcarbonate or phosgene. Ideally, one would like to completely replace the use of reagents as phosgene with carbon dioxide. The latter is not only safer to work with, it is also an abundant and cheap feedstock. The limiting factor here is, however, the relatively inert nature of carbon dioxide making its transformation into organic compounds a challenging task. Carbon dioxide is a thermodynamically very stable molecule with the carbon center in the highest (+4) oxidation state. In addition, it adopts a linear conformation and does not posses any dipole moment, further adding to the stability of CO_2. Therefore, in order to tranform CO_2 into useful organic molecules, a reactive coupling partner (with a relative high free energy) is required.

Chapter 1

1.2 Epoxides

Cyclic ethers comprising of a three-atom ring, also known as epoxides, have a long history in the field of synthetic chemistry. The most simple example of an epoxide, ethylene oxide, was first synthesized by Charles-Adolphe Wurtz in 1859 through the cyclization of 2-chloroethanol in the presence of a base.[5] An alternative method allowed for direct oxidation by air using a silver based catalyst, and was patented in 1931 by Lefort and six years later industrialized by Union Carbide. Shell further improved this methodology, which currently accounts for the majority of ethylene oxide production worldwide. Unfortunately, this direct oxidation does not work for other alkenes and is thus limited to ethylene. This has urged the scientific community to develop alternative techniques for epoxide synthesis (see Scheme 1).
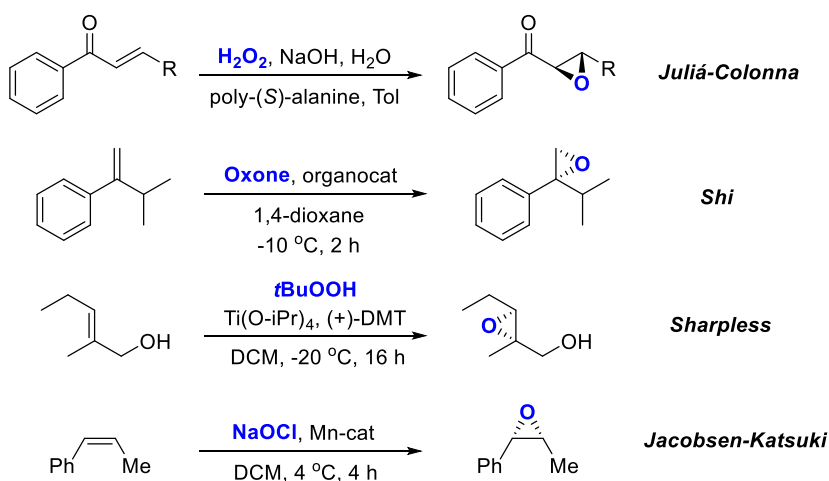
Scheme 1. Methods used for the epoxidation of alkenes.

A typical reagent often used is hydrogen peroxide, which is for instance used in the Juliá-Colonna epoxidation of electron-deficient alkenes.[6] Due to its higher stability and easier handling, *t*BuOOH is often used as an alternative in reactions such as the asymmetric Sharpless epoxidation.[7] While both of the previous approaches allow for enantioselective epoxidation, currently one of the most popular enantioselective methods is the Jacobsen-Katsuki epoxidation, due to its broad substrate scope.[8] Other epoxidation reagents include the use of oxone (Shi epoxidation)[9] or peroxycarboxylic acids. The latter reagent is used in the Prilezhaev reaction,[10] that was first reported in

Chapter 1

1909 where a peroxy acid is utilized to epoxidize the alkene. This chemistry has enabled the development of *m*-CPBA, which is now one of the most commonly used epoxidizing reagents owing to its high stability, good solubility in organic solvents and excellent reactivity in the absence of catalyst. This method follows a concerted pathway yielding the epoxidized alkene along with benzoic acid as a byproduct (see Scheme 2).
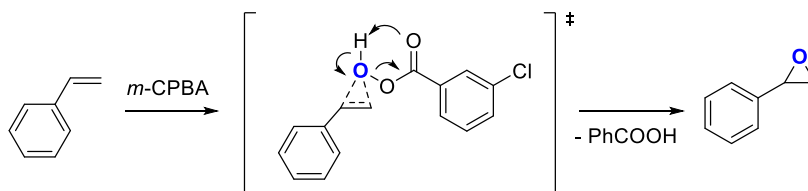
Scheme 2. Formation of styrene oxide through epoxidation of styrene with m-CPBA.

The use of these aforementioned epoxidation techniques provides access to a wide variety of functional compounds, as double bonds can be found in many organic molecules. The resulting epoxides are applied in epoxy glues, aerosols, insecticides and chemical building blocks. Most of the chemical tranformations rely on nucleophilic ring-opening of the strained oxirane, and classes of nucleophiles studied include water,[11] alcohols,[12] amines,[13] halides and several types of carbanions.[14] The reaction with halides is unique in the sense that it represents a reversible process, as the resulting halohydrin intermediate is a common precursor for epoxide formation. Under appropriate conditions however, this principle can be used to trap carbon dioxide (see Scheme 3).
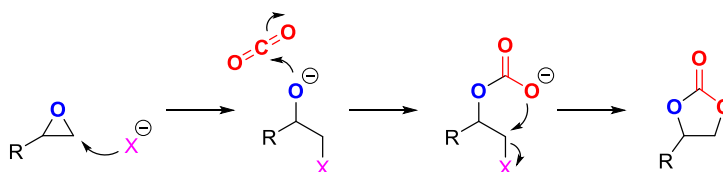
Scheme 3. Epoxide ring-opening by a halide nucleophile (X) and subsequent reaction with CO₂.

In this simplified model, a halide is used to open the epoxide to yield an alkoxide species. The resulting alkoxide allows for nucleophilic activation of CO_2 thereby forming a carbonate intermediate that upon cyclization regenerates the halide and yields the cyclic carbonate product.

Chapter 1

1.3 Cyclic carbonates

The coupling product of epoxides with CO_2 are five-membered cyclic carbonates. Alternatively, oxetanes can be used to obtain the respective six-membered products. Carbonates consisting of larger ring sizes also exist, though they are usually made via other methods.[15] Cyclic carbonates are versatile compounds that have found application within various fields of chemistry (see Figure 3).
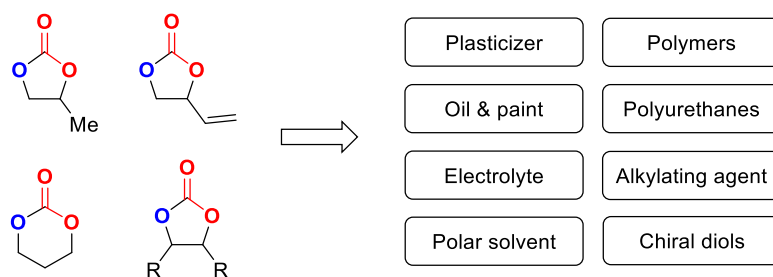
Figure 3. Application of cyclic carbonates in chemistry and commercial processes.

Simple cyclic carbonates such as ethylene and propylene carbonate are used in coatings, paint, electrolytes for lithium ion batteries[16] or applied as polar aprotic solvents.[17] More functionalized structures such as vinyl carbonates are frequently employed as building blocks for asymmetric synthesis.[18] Other uses include the alkylation of aromatic amines, phenols and thiols,[19] synthesis of polyurethanes,[20] biomedical applications,[21] production of herbicides[22] and plasticizers[23] as well as several other minor applications.[24]

Structurally related to the class of organic carbonates are the nitrogen-containing carbamates. Carbamates play an important role in medicinal chemistry and the scaffolds are often found in pharmaceutical drugs.[25] Linear carbamates are typically formed through the coupling of alcohols and isocyanates, such as in the production of polyurethanes.[26] Here we focus specifically on cyclic analogues, of which the five-membered variants are more commonly known as oxazolidinones. There are several ways to prepare cyclic carbamates, including the reaction of amines with cyclic carbonates[27] or directly from a combination of an epoxide, amine and CO_2.[28] Another possibility is the coupling of CO_2 with aziridines.[29] The resulting oxazolidinones are important motifs that are frequently used as chiral auxilaries,[30] as synthetic precursors[31] or as structural elements in active pharmaceuticals[32] and fungicides (see Scheme 4).[33]

Chapter 1
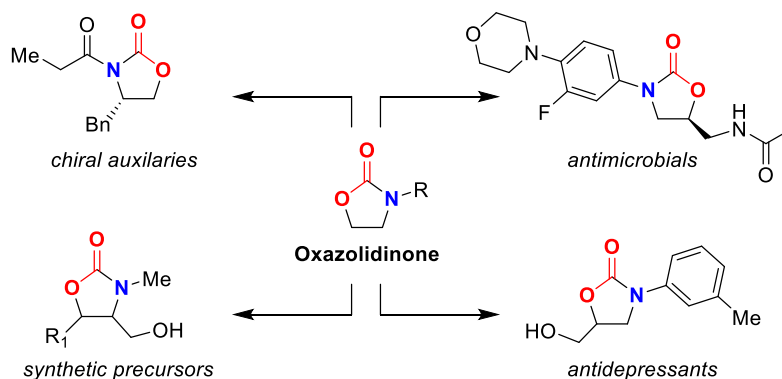
Scheme 4. The oxazolidinone motif plays an important role in organic synthesis and medicinal chemistry.

Industrial formation of ethylene and propylene carbonate dates back to 1958,[34] where tetraethylammonium bromide was used to catalyze the coupling of epoxides and carbon dioxide following the mechanism outlined in Scheme 3. Although this reaction required high temperatures and high pressure of CO_2, it was a promising step towards a greener and more sustainable alternative. Replacing phosgene with carbon dioxide reduces the dangers associated with exposure to human beings or the environment as well as safer operating procedures. Moreover, the coupling of CO_2 with epoxides is 100% atom efficient and thus does not produce any byproducts. A limiting factor, however, is the high temperatures that are needed, which reduces the range of products that can be obtained by this method. In order to achieve cyclic carbonate formation at low(er) temperatures, a more efficient catalytic system is thus necessary.

1.4 Aluminum aminotriphenolate

Over the years several catalysts have emerged able to efficiently mediate the insertion of CO_2 into epoxides. The most prominent systems are based on alkali metals,[35] metal oxides,[36] organocatalysts,[37] transition metals[38] or ionic liquids[39] (see for examples: Figure 4).
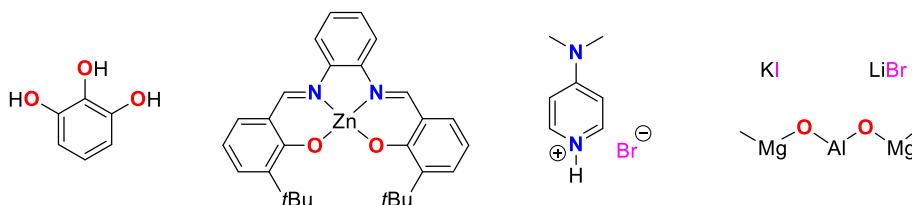
Figure 4. Catalysts used in the activation of epoxides.

12

Chapter 1

An interesting feature related to ionic liquids derived from quaternary amonium salts is that these can be used as both solvent and catalyst, allowing for high conversions at atmospheric or even lower pressures of carbon dioxide. A very recent example was reported by the group of Zhang using an ionic liquid based on DMAP.[40] A downside of this approach, however, is the requisite of a high reaction temperature (usually 120 °C or higher) and the necessity of over-stoichiometric amounts of catalyst. Currently the use of alkali metals and metal oxides has almost completely been replaced by organocatalysts and metal-based catalysts, due to the much better performance of the latter two catalyst categories. Despite the recent advances using organocatalysis,[37a, 37b] the best results are typically obtained with (transition) metal based catalysts. These systems have a stronger potential for epoxide activation, allowing them to be operated at lower catalyst loadings and temperatures, while giving acces to a wide(r) scope of organic carbonates.

The current methodology for metal catalyzed formation of cyclic carbonates relies for a larger part on the use of a binary catalyst system, consisting of a Lewis acid (metal; M) and a nucleophile (usually a quaternary ammonium halide salt; X). A widely accepted mechanism for CO_2 insertion into epoxides catalyzed by binary catalysts is depicted in Scheme 5.
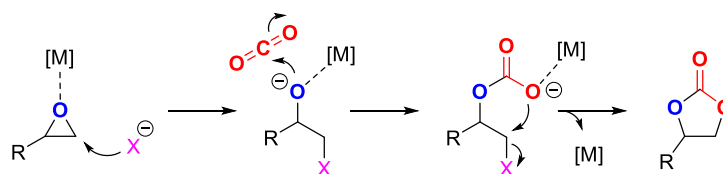
Scheme 5. Cyclic carbonate formation catalyzed by a binary catalytic system.

The reaction mechanism follows the same general principle as the nucleophilic ring-opening by halides outlined in Scheme 3. Coordination of the epoxide to the Lewis acid renders the substrate susceptible towards nucleophilic attack leading to the formation of an alkoxide species that is stabilized by the metal. CO_2 insertion into the metal-alkoxide bond followed by ring-closure yields the final cyclic carbonate product after decoordination from the metal. Pioneering work in this field was done by Inoue in the 1960s, who used Lewis acids to catalyze the coupling of CO_2 with PO. Several simple zinc and aluminum based systems were tested in the copolymerization of propylene oxide with carbon dioxide.[41] This initial work led to the development of the binary catalytic system as we know it, mainly based on metals such as chromium,[42] cobalt[43] and aluminum.[44] Other systems that have been reported include complexes based on zinc,[45] copper,[45] manganese[46] and ruthenium[47] amongst others.

Chapter 1

Of all the previously mentioned metals that have been employed for epoxide conversion, aluminum has proven to be one of the best options. Not only is aluminum the most abundant metal in the earth´s crust, it also has a highly oxophilic nature making it especially suitable for activation of oxygen-containing compounds such as epoxides. Most catalytic systems employ either porphyrins[48] or derivatives of the salen type ligands,[49] in combination with aluminum or other metals. The first example of an aluminum-porphyrin mediated reaction between CO_2 and epoxides was reported by Inoue in 1983.[50] Similar porphyrin-based systems are still widely used due to the ease of synthesis, as just one step is required involving coupling of an aldehyde with pyrrole to access a wide variety of different ligands. Aluminum salen complexes where first used in 1989 for the living polymerization of epoxides.[51] It was not until 2002 that the use of aluminum salens in the formation of cyclic carbonates was investigated by the group of He.[52] Nowadays the most common salen is the chiral Jacobsen´s ligand,[8] which is often used for enantioselective reactions.[53]

A relatively new class of ligands in the field of CO_2 is the aminotriphenolate structure (TPA), which is a potentially tetradentate ligand with C_3-symmetry. While this ligand was synthesized already in 1922,[54] its use in transition metal chemistry emerged less than just 20 years ago.[55] As reported for previouly developed salen/porphyrin ligand systems, the TPA also allows for facile steric and electronic modulation. A common methodology for its synthesis is based on the Mannich reaction of *ortho,para*-disubstituted phenols with HMTA,[56] leading to the formation of the aluminum complex in just two steps (see Scheme 6).
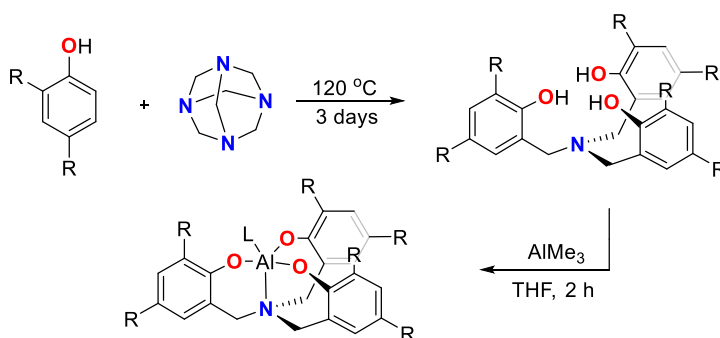
Scheme 6. Two-step synthesis of an aluminum-aminotriphenolate catalyst.

The main drawback of these types of Mannich reactions is the low yield, which is moderate at best. As a consequence additional methodologies to prepare this class of ligands have been developed, the first one relying on a S_N2 alkylation reaction between

Chapter 1

a benzylamine and two equivalents of benzyl bromide.[55] Different aromatic substituents can be used, making this procedure especially suitable for the synthesis of nonsymmetrical ligands. Another strategy was reported by the group of Licini in 2006, which utilizes a three-step procedure including a reductive amination step.[57] Aminotriphenolates have been used in combination with different (transition) metals resulting in a variety of synthetic applications.[58] One of the main differences between these three types of catalysts (porphyrins, salens and TPAs) is that the salen and porphyrin-based metal complexes adopt a relatively planar conformation, while the triphenolate ligand forms trigonal bipyramidal complexes with aluminum. This results in a more open, and importantly, flexible coordination sphere that has proven to be effective in the conversion of sterically challenging epoxides.[59]

1.5 Outline of this thesis

The previous section has shown the importance of organic carbonates in both industrial applications and academical research. Of all the different catalytic systems that exist in the field of epoxide/CO_2 coupling reactions, the aminotriphenolate based complexes are a relatively recent addition. We therefore wanted to compare their activity to the current state of the art Al-catalysts in this field. Furthermore, we intended to apply the Al TPA complexes and derivatives to discover new and unexplored reactivity in the field of CO_2 utilization, thereby extending the current portfolio of cyclic organic carbonates that have been studied and prepared to date.

Chapter 1

1.6 References

[1]   H. Guerlac, *Dictionary of Scientific Biography* **1970-1980**, *2*, 173-183.
[2]   P. Friedlingstein, R. M. Andrew, J. Rogelj, G. P. Peters, J. G. Canadell, R. Knutti, G. Luderer, M. R. Raupach, M. Schaeffer, D. P. van Vuuren, C. Le Quere, *Nature Geosci* **2014**, *7*, 709-715.
[3]   R. A. Betts, C. D. Jones, J. R. Knight, R. F. Keeling, J. J. Kennedy, *Nature Clim. Change* **2016**, *6*, 806-810.
[4]   H. Kolbe, *Justus Liebigs Ann. Chem.* **1860**, *113*, 125-127.
[5]   A. Wurtz, *Comptes rendus* **1859**, *48*, 101-105.
[6]   a) S. Juliá, J. Masana, J. C. Vega, *Angew. Chem. Int. Ed.* **1980**, *19*, 929-931; b) S. Julia, J. Guixer, J. Masana, J. Rocas, S. Colonna, R. Annuziata, H. Molinari, *J. Chem. Soc., Perkin Trans. 1* **1982**, 1317-1324.
[7]   a) T. Katsuki, K. B. Sharpless, *J. Am. Chem. Soc.* **1980**, *102*, 5974-5976; b) B. E. Rossiter, T. Katsuki, K. B. Sharpless, *J. Am. Chem. Soc.* **1981**, *103*, 464-465.
[8]   E. N. Jacobsen, W. Zhang, A. R. Muci, J. R. Ecker, L. Deng, *J. Am. Chem. Soc.* **1991**, *113*, 7063-7064.
[9]   B. Wang, O. A. Wong, M.-X. Zhao, Y. Shi, *J. Org. Chem.* **2008**, *73*, 9539-9543.
[10]   N. Prileschajew, *Ber. Dtsch. Chem. Ges.* **1909**, *42*, 4811-4815.
[11]   L. P. C. Nielsen, C. P. Stevenson, D. G. Blackmond, E. N. Jacobsen, *J. Am. Chem. Soc.* **2004**, *126*, 1360-1362.
[12]   G. D. Yadav, S. Singh, *Tetrahedron Lett.* **2014**, *55*, 3979-3983.
[13]   F. A. Saddique, A. F. Zahoor, S. Faiz, S. A. R. Naqvi, M. Usman, M. Ahmad, *Synth. Commun.* **2016**, *46*, 831-868.
[14]   S. Gil, M. Torres, N. Ortúzar, R. Wincewicz, M. Parra, *Eur. J. Org. Chem.* **2004**, 2160-2165.
[15]   S. Venkataraman, V. W. L. Ng, D. J. Coady, H. W. Horn, G. O. Jones, T. S. Fung, H. Sardon, R. M. Waymouth, J. L. Hedrick, Y. Y. Yang, *J. Am. Chem. Soc.* **2015**, *137*, 13851-13860.
[16]   S.-J. P. H. Zhao, F.i Shi, Y. Fu, V. Battaglia, P. N. Ross Jr. and G. Liu, *J. Electrochem. Soc* **2014**, *161*, A194-A200.
[17]   H. L. Parker, J. Sherwood, A. J. Hunt, J. H. Clark, *ACS Sustain. Chem. Eng.* **2014**, *2*, 1739-1742.
[18]   a) Y. J. Zhang, J. H. Yang, S. H. Kim, M. J. Krische, *J. Am. Chem. Soc.* **2010**, *132*, 4562-4563; b) W. Guo, L. Martínez-Rodríguez, R. Kuniyil, E. Martin, E. C. Escudero-Adán, F. Maseras, A. W. Kleij, *J. Am. Chem. Soc.* **2016**, *138*, 11970-11978.
[19]   J. H. Clements, *Ind. Eng. Chem. Res.* **2003**, *42*, 663-674.
[20]   L. Maisonneuve, O. Lamarzelle, E. Rix, E. Grau, H. Cramail, *Chem. Rev.* **2015**, *115*, 12407-12439.

[21]   C. B. Cooley, B. M. Trantow, F. Nederberg, M. K. Kiesewetter, J. L. Hedrick, R. M. Waymouth, P. A. Wender, *J. Am. Chem. Soc.* **2009**, *131*, 16401-16403.

[22]   V. Rukachaisirikul, N. Rungsaiwattana, S. Klaiklay, S. Phongpaichit, K. Borwornwiriyapan, J. Sakayaroj, *J. Nat. Prod.* **2014**, *77*, 2375-2382.

[23]   M. Polyakov, B. Schäffner, D. Kruse, A. Martin, A. Köckritz, *Tetrahedron Lett.* **2016**, *57*, 964-968.

[24]   A.-A. G. Shaikh, S. Sivaram, *Chem. Rev.* **1996**, *96*, 951-976.

[25]   A. K. Ghosh, M. Brindisi, *J. Med. Chem.* **2015**, *58*, 2895-2940.

[26]   J. O. Akindoyo, M. D. H. Beg, S. Ghazali, M. R. Islam, N. Jeyaratnam, A. R. Yuvaraj, *RSC Adv.* **2016**, *6*, 114453-114482.

[27]   B. Wang, S. Yang, L. Min, Y. Gu, Y. Zhang, X. Wu, L. Zhang, E. H. M. Elageed, S. Wu, G. Gao, *Adv. Synth. Catal.* **2014**, *356*, 3125-3134.

[28]   U. R. Seo, Y. K. Chung, *Green Chem.* **2017**, *19*, 803-808.

[29]   C. Phung, R. M. Ulrich, M. Ibrahim, N. T. G. Tighe, D. L. Lieberman, A. R. Pinhas, *Green Chem.* **2011**, *13*, 3224-3229.

[30]   M. M. Heravi, V. Zadsirjan, *Tetrahedron: Asymmetry* **2013**, *24*, 1149-1188.

[31]   L. Aurelio, R. T. C. Brownlee, A. B. Hughes, *Chem. Rev.* **2004**, *104*, 5823-5846.

[32]   Z. Giovanni, M. Pilar, M. Giuliano Delle, M. Domenico, N. Laura, B. Bruno, *Mini-Rev. Med. Chem.* **2007**, *7*, 389-409.

[33]   A. Sarkar, S. Bhattacharyya, S. K. Dey, S. Karmakar, A. Mukherjee, *New J. Chem.* **2014**, *38*, 817-826.

[34]   W. J. Peppel, *Ind. Eng. Chem.* **1958**, *50*, 767-770.

[35]   a) J. Song, B. Zhang, P. Zhang, J. Ma, J. Liu, H. Fan, T. Jiang, B. Han, *Catal. Today* **2012**, *183*, 130-135; b) B. Barkakaty, K. Morino, A. Sudo, T. Endo, *Green Chem.* **2010**, *12*, 42-44; c) S. Kaneko, S. Shirakawa, *ACS Sustain. Chem. Eng.* **2017**, *5*, 2836-2840.

[36]   a) K. Yamaguchi, K. Ebitani, T. Yoshida, H. Yoshida, K. Kaneda, *J. Am. Chem. Soc.* **1999**, *121*, 4526-4527; b) K. Tomishige, H. Yasuda, Y. Yoshida, M. Nurunnabi, B. Li, K. Kunimori, *Green Chem.* **2004**, *6*, 206-214.

[37]   a) G. Fiorani, W. Guo, A. W. Kleij, *Green Chem.* **2015**, *17*, 1375-1389; b) S. Sopeña, E. Martin, E. C. Escudero-Adán, A. W. Kleij, *ACS Catal.* **2017**, *7*, 3532-3539; c) C. J. Whiteoak, A. Nova, F. Maseras, A. W. Kleij, *ChemSusChem* **2012**, *5*, 2032-2038.

[38]   a) J. W. Comerford, I. D. V. Ingram, M. North, X. Wu, *Green Chem.* **2015**, *17*, 1966-1987; b) C. Martín, G. Fiorani, A. W. Kleij, *ACS Catal.* **2015**, *5*, 1353-1370.

[39]   a) Q. He, J. W. O'Brien, K. A. Kitselman, L. E. Tompkins, G. C. T. Curtis, F. M. Kerton, *Catal. Sci. Technol.* **2014**, *4*, 1513-1528; b) B.-H. Xu, J.-Q. Wang, J. Sun, Y. Huang, J.-P. Zhang, X.-P. Zhang, S.-J. Zhang, *Green Chem.* **2015**, *17*, 108-122.

[40]   Z. Zhang, F. Fan, H. Xing, Q. Yang, Z. Bao, Q. Ren, *ACS Sustain. Chem. Eng.* **2017**, *5*, 2841-2846.

[41]   S. Inoue, H. Koinuma, T. Tsuruta, *J. Polym. Sci. B* **1969**, *7*, 287-292.

[42]   R. L. Paddock, S. T. Nguyen, *J. Am. Chem. Soc.* **2001**, *123*, 11498-11499.

[43]   P. Yan, H. Jing, *Adv. Synth. Catal.* **2009**, *351*, 1325-1332.
[44]   C. J. Whiteoak, N. Kielland, V. Laserna, F. Castro-Gómez, E. Martin, E. C. Escudero-Adán, C. Bo, A. W. Kleij, *Chem. Eur. J.* **2014**, *20*, 2264-2275.
[45]   Y.-M. Shen, W.-L. Duan, M. Shi, *J. Org. Chem.* **2003**, *68*, 1559-1562.
[46]   L. Jin, H. Jing, T. Chang, X. Bu, L. Wang, Z. Liu, *J. Mol. Catal. A: Chem.* **2007**, *261*, 262-266.
[47]   H. Jing, T. Chang, L. Jin, M. Wu, W. Qiu, *Catal. Commun.* **2007**, *8*, 1630-1634.
[48]   Y. Qin, H. Guo, X. Sheng, X. Wang, F. Wang, *Green Chem.* **2015**, *17*, 2853-2858.
[49]   A. Decortes, A. M. Castilla, A. W. Kleij, *Angew. Chem. Int. Ed.* **2010**, *49*, 9822-9837.
[50]   T. Aida, S. Inoue, *J. Am. Chem. Soc.* **1983**, *105*, 1304-1309.
[51]   V. Vincens, A. L. Borgne, N. Spassky, *Makromol. Chem. Rapid. Comm.* **1989**, *10*, 623-628.
[52]   X.-B. Lu, X.-J. Feng, R. He, *Appl. Catal., A* **2002**, *234*, 25-33.
[53]   a) M. S. Taylor, E. N. Jacobsen, *J. Am. Chem. Soc.* **2003**, *125*, 11204-11205; b) G. M. Sammis, H. Danjo, E. N. Jacobsen, *J. Am. Chem. Soc.* **2004**, *126*, 9928-9929.
[54]   G. Zemplén, A. Kunz, *Ber. Dtsch. Chem. Ges.* **1922**, *55*, 979-992.
[55]   J. Hwang, K. Govindaswamy, S. A. Koch, *Chem. Commun.* **1998**, 1667-1668.
[56]   A. Chandrasekaran, R. O. Day, R. R. Holmes, *J. Am. Chem. Soc.* **2000**, *122*, 1066-1072.
[57]   L. J. Prins, M. M. Blázquez, A. Kolarović, G. Licini, *Tetrahedron Lett.* **2006**, *47*, 2735-2738.
[58]   G. Licini, M. Mba, C. Zonta, *Dalton Trans.* **2009**, 5265-5277.
[59]   C. J. Whiteoak, N. Kielland, V. Laserna, E. C. Escudero-Adán, E. Martin, A. W. Kleij, *J. Am. Chem. Soc.* **2013**, *135*, 1228-1231.

Chapter 2.

Aluminum-Mediated Formation of Cyclic Carbonates: Benchmarking Catalytic Performance Metrics
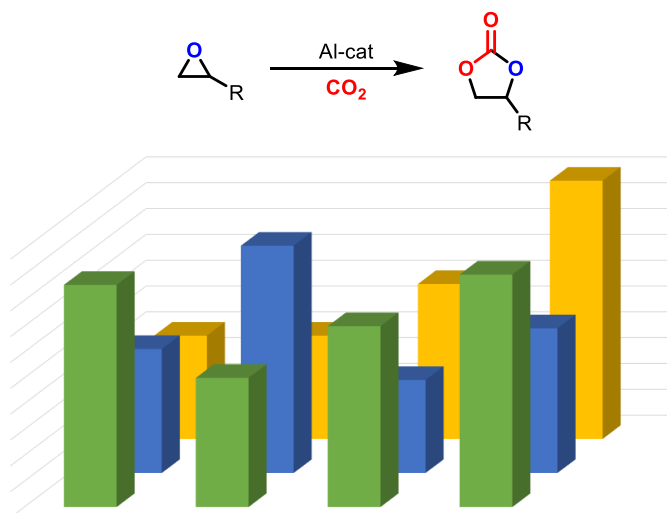
This work has been published in:

Rintjema, J.; Kleij, A. W. *ChemSusChem* **2017**, *10,* 1274–1282.

UNIVERSITAT ROVIRA I VIRGILI
ALUMINUM-CATALYZED COUPLING OF CARBON DIOXIDE AND CYCLIC ETHERS
Jeroen Rintjema Tanger

Chapter 2

2.1 Introduction

Small molecule activation is currently one of the most vibrant topics in modern-day research.[60] Catalysis plays a crucial role by enabling the conversion of molecules such as CO_2 to valuable organic compounds.[61] Many catalytic systems have been developed over the years that can effectively couple CO_2 with epoxides to form cyclic carbonates. Several factors determine the potential of a certain catalytic system for either industrial and/or academical applications. Crucial features are catalyst stability, high activity and the possibility for facile ligand/complex modifications when considering metal catalysts. For commercial applications the cost and ease of synthesis are highly important, as well as a low toxicity and easy handling. These requirements have led to the emergence of catalysts based on abundant and easy to handle metals such as iron,[62] zinc[63] or aluminum.[64]

Mg-porphyrin
TOF up to 46.000 h^{-1}
3 active sites
T = 160 °C
$p(CO_2)$ = 17 bar

Cr-salphen
TOF = <10 h^{-1}
1 active site
T = 25 °C
$p(CO_2)$ = 1 bar
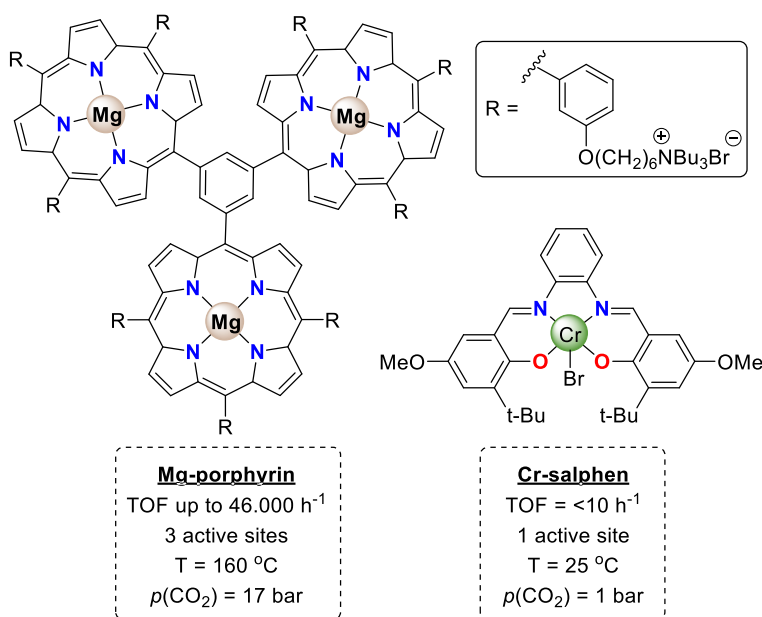
Figure 5. Comparison of two efficient catalytic systems in the conversion of epoxides.

Popular ligands to support these metals are porphyrins and salens/salphens, of which two examples are depicted in Figure 5. The first one is a highly active magnesium based bifunctional catalyst derived from a trinuclear porphyrin and developed by the group of Ema.[65] The second example is a Cr-salophen complex reported by North *et al.* that catalyzes the conversion of epoxides under very mild conditions.[66] While both catalytic

Chapter 2

systems give (near) full conversion of epoxides under the optimized conditions, the activity of a catalyst is often quantified by looking at the turnover number (TON) and frequency (TOF). At first sight, the magnesium based porphyrin seems far more efficient, giving up to 46.000 turnovers per hour compared to less than 10 for the chromium complex. Upon taking a closer look at the reaction conditions, however, there are several important aspects to discuss. The magnesium complex has three active sites compared to only one for chromium, which of course increases the molecular turnover frequency of the catalyst. Furthermore the chromium complex operates at room temperature and atmospheric pressure of CO_2, while the trinuclear porphyrin requires high temperature (160 ºC) and pressure (17 bar) to achieve its high activity.

From this comparison it becomes clear that the activity of different catalytic sytems can not be directly related by looking only at the TON and TOF values of the respective systems. Apart from the number of active sites, differences in temperature and pressure, there are more factors that should be taken into account such as scale of the reaction, reactor volume, gas-to-liquid ratios and heat distribution. This means that in order to make a useful comparison of catalyst performances, proper benchmarking is required and testing the complexes under identical conditions in similar or preferably the same reactor system.
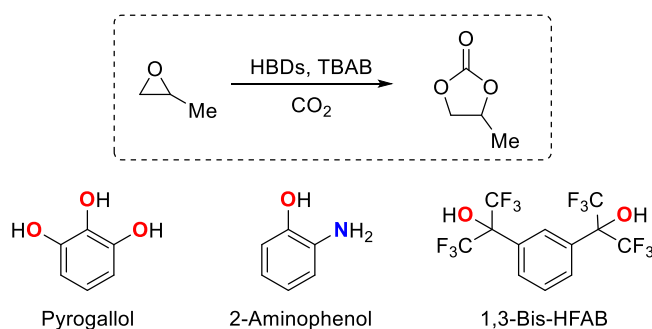
Scheme 7. Several HBDs tested in the conversion of PO to propylene carbonate.

Currently, the literature only reports one example of such benchmarking studies in the field of epoxide/CO_2 couplings, which is a contribution communicated by Jerome and Tassaing in 2015.[67] They presented a comparative study on the influence of several HBDs (HBD = hydrogen bond donor) in the conversion of propylene oxide into its cyclic carbonate product (see Scheme 7). This provided useful insight into the activity of these organocatalysts and revealed that fluorinated alcohols showed superior activity

Chapter 2

compared to previously reported HBD systems. However, to date no comparable studies exist pertinent to metal-based catalystic systems.

2.2 Objectives

The aim of the work described in this chapter is to establish a benchmarking study that compares the activity of different aluminum based binary catalysts in the coupling of various epoxides and CO_2. For these studies we have examined an Al(III) based aminotriphenolate system together with other Al(III) catalysts from the current state of the art and compared their relative kinetics in the conversion of several terminal and internal epoxides. Other factors that have been compared are ease of catalyst synthesis, type of nucleophilic additive and the influence of the reaction temperature. In addition, the different mechanistic manifolds reported for these catalytic systems provide a rationale for the optimal operating window belonging to each catalyst.

2.3 Results and discussion

The aluminum based catalysts that were selected for the benchmarking studies are depicted in Figure 6, consisting of the aminotriphenolate based complexes[59] (**1a-c**), North´s μ-oxo bridged bimetallic Al-salen[68] (**2**) and the mononuclear analogue (**4**), and the porphyrin system reported by Wang and Qin[48] (**3a-b**).

1a, [Al]^{Cl}: R = Cl; L = thf
1b, [Al]^{Me}: R = Me; L = thf
1c, [Al]^{tBu}: R= tBu; L = thf

2, [Al]$_2$O-Salen

3a, [Al]^{TPP}: R = H
3b, [Al]$^{Cl-TPP}$: R = Cl

4, [Al]-Salen
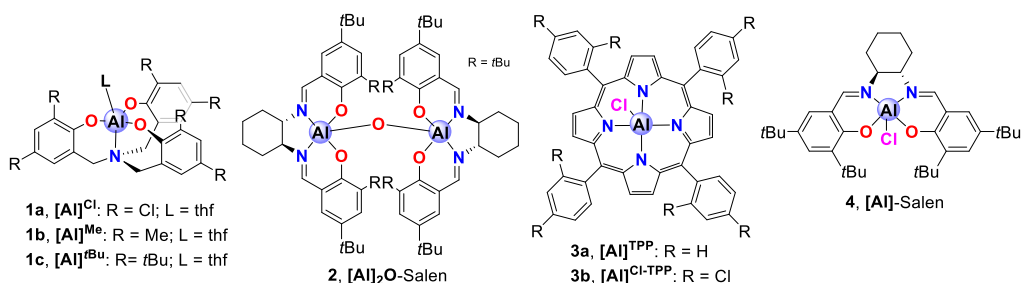
Figure 6. Selected aluminum catalysts for the benchmarking studies.

2.3.1 Conversion of terminal epoxides

First, the activity of complexes **1**-**4** was evaluated using three different types of nucleophiles in the conversion of benchmark terminal epoxides (see Table 1 and 2). A

Chapter 2

parallel reactor system was used (see Experimental section for details) to facilitate these comparative studies.

*Table 1. Comparison of the reactivities of binary Al-catalysts **1**–**4**/X (X = Cl, Br, I) in the conversion of 1,2-epoxyhexane **5** to its cyclic carbonate product **6**.[a]*
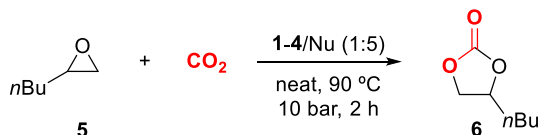
Entry	Cat	Nu	Substrate	Yield [%][b]	TON[c]
1	–	PPNCl	5	3	–
2	1a	PPNCl	5	14	1400
3	2	PPNCl	5	5	250
4	3a	PPNCl	5	35	3500
5	3b	PPNCl	5	33	3300
6	4	PPNCl	5	4	400
7	–	TBAB	5	1	–
8	1a	TBAB	5	19	1900
9	2	TBAB	5	3	150
10	3a	TBAB	5	11	1100
11	3b	TBAB	5	12	1200
12	4	TBAB	5	3	300
13	–	TBAI	5	2	–
14	1a	TBAI	5	13	1300
15	2	TBAI	5	2	100
16	3a	TBAI	5	7	700
17	3b	TBAI	5	7	700
18	4	TBAI	5	3	300

[a] Reaction conditions: epoxide **5** (10.0 mmol), Al-complex (0.001 mmol), nucleophile (Nu: 0.005 mmol), mesitylene (1.0 mmol), 90 ºC, 10 bar, 2 h; [b] Determined by ^{1}H NMR (CDCl$_3$) using mesitylene as internal standard; the average of two runs is reported. Selectivity towards the cyclic carbonate **6** was >99%. [c] TON = total turnover number observed per Al center; note that complex **2** contains two Al centers.

24

Chapter 2

*Table 2. Comparison of the reactivities of binary Al-catalysts **1**–**4**/X (X = Cl, Br, I) in the conversion of terminal epoxides **7** and **8** into their respective cyclic carbonates **9** and **10**.[a]*

7: R = Ph
8: R = Me

9: R = Ph
10: R = Me
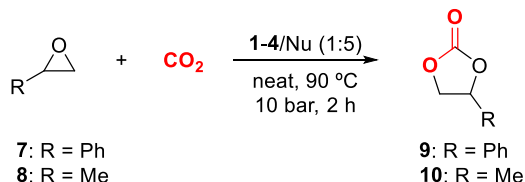
Entry	Cat	Nu	Substrate	Yield **9**, **10** [%][b]	TON **9**, **10**[c]
1	–	PPNCl	**7, 8**	5, 2	–
2	**1a**	PPNCl	**7, 8**	8, 29	800, 2900
3	**2**	PPNCl	**7, 8**	5, 7	250, 350
4	**3a**	PPNCl	**7, 8**	22, 49	2200, 4900
5	**3b**	PPNCl	**7, 8**	24, 53	2400, 5300
6	**4**	PPNCl	**7, 8**	6, 5	600, 500
7	–	TBAB	**7, 8**	2, 3	–
8	**1a**	TBAB	**7, 8**	12, 43	1200, 4300
9	**2**	TBAB	**7, 8**	3, 9	150, 450
10	**3a**	TBAB	**7, 8**	14, 40	1400, 4000
11	**3b**	TBAB	**7, 8**	13, 41	1300, 4100
12	**4**	TBAB	**7, 8**	3, 6	300, 600
13	–	TBAI	**7, 8**	3, 1	–
14	**1a**	TBAI	**7, 8**	11, 26	1100, 2600
15	**2**	TBAI	**7, 8**	3, 6	150, 300
16	**3a**	TBAI	**7, 8**	7, 20	700, 2000
17	**3b**	TBAI	**7, 8**	8, 18	800, 1800
18	**4**	TBAI	**7, 8**	3, 5	300, 500

[a] Reaction conditions: epoxide **7** or **8** (10.0 mmol), Al-complex (0.001 mmol), nucleophile (Nu: 0.005 mmol), mesitylene (1.0 mmol), 90 °C, 10 bar, 2 h; [b] Determined by ^{1}H NMR (CDCl$_3$) using mesitylene as internal standard, first number refers to yield when using **7** as substrate; the average of two runs is reported. Selectivity towards the cyclic carbonates **9** and **10** was >99%. [c] TON = total turnover number observed per Al; note that complex **2** contains two Al centers.

To examine the reactivities of the complexes **1**-**4** upon combination with various nucleophiles, initial kinetics were determined in most of the cases reported here. First, the conversion of three different terminal epoxides (**6**–**8**) was investigated at 90 °C, 10 bar CO$_2$ pressure, and at low complex loading ([Al]= 0.01 mol%). Previous reports on the selected catalysts show high reactivity at 90 °C and this temperature was therefore

used as a starting point for further experiments. As co-catalytic nucleophiles (Nu), tetrabutylammonium halides (TBAX; X=Br, I) and bis(triphenylphosphine)iminium chloride (PPNCl) were used in a five-fold excess with respect to the Al complex. Note that PPNCl is used here as it is much easier to handle than the hygroscopic TBACl. The nature of the cation seems to be of little influence, as several experiments that were repeated with TBACl gave the same results as with PPNCl.

The conversion of 1,2-epoxyhexane (**6**, Table 1) and total TONs were determined for all binary combinations after 2 h on a per reactive center basis, that is, per Al site. The data were compared within each series with the background conversion mediated by the nucleophilic additive alone as a reference (entries 1, 7, and 13). Striking differences were noted for the binary systems based on **1–4** as well as significant changes upon variation of the type of nucleophile (halide). In the presence of PPNCl as nucleophile (entries 1–6), the data clearly demonstrate that the Wang and Qin complex **3b** has excellent activity under these conditions (entry 5), in line with their previous findings.[48] Interestingly, the non-chlorinated version of this Al(porphyrin)-based binary catalyst (Figure 6, **3a**; entry 4) displays similar activity features, suggesting that Lewis acidity for this system under dilute catalyst conditions does not play an significant role. Apart from **3b**, the Kleij system based on **1a** shows significantly better activity compared to the other screened binary catalysts that are derived from **2** and **4**.

A dramatic change in the activity order was observed when changing the nucleophile from PPNCl to TBAB or TBAI (entries 7–18). In the presence of either TBAB or TBAI the most active binary catalyst is the one based on complex **1a**, followed by the porphyrin systems **3a**/TBAX and **3b**/TBAX (X= Br, I). Binary couple **1a**/TBAB shows the highest TON (entry 8; 1900) under these conditions, and these observations align well with previous data in the literature that showed that bromide based nucleophiles give the highest activities when combined with Al(aminotriphenolate) complexes.[59] Additionally, a similar reactivity difference between catalysts based on **1a** and the North system (**2**) has been observed at a ten-fold higher loading of both catalyst components (0.01 mol% [Al], 0.05 mol% TBAI).[44] The combined results for the conversion of terminal epoxide **5** into mono-substituted cyclic carbonate **6** (Table 1) suggest that matching of the Lewis acid complex and nucleophilic additive has a pronounced influence on the overall catalyst performance.

Intrigued by the results presented in Table 1, we decided to screen two other terminal epoxides to see whether the trends observed in the catalytic formation of cyclic carbonate **6** from terminal epoxide **5** were of a more general nature (see Table 2). Indeed, when all results are considered it can be observed that both porphyrin-based binary systems (**3a**/PPNCl and **3b**/PPNCl) have significantly higher activities compared

26

Chapter 2

to the other binary catalysts derived from **1**, **2**, and **4**, for the conversion of styrene oxide (**7**) and propylene oxide (PO, **8**) (Table 2, entries 1–6). After combining complexes **1**–**4** with either TBAB or TBAI, the activities noted in the presence of **3a** and **3b** drop whereas those for the systems based on **1a** specifically become more competitive and reveal similar to slightly improved activities (entries 8 and 14) as noted for the binary combinations comprising of metalloporphyrins **3a** or **3b**.

The somewhat lower conversion kinetics for the styrene oxide substrate compared to 1,2-epoxyhexane and PO is likely a result of an increasing influence of electronic effects as reported previously.[69] This affects the nucleophilic character of the alkoxide intermediate formed after initial ring-opening of the epoxide through a more pronounced charge delocalization. Overall, the results of Table 1 and 2 align well and show clear reproducible trends in the initial conversion kinetics of terminal epoxides and CO_2 at 90 °C catalyzed by binary catalysts derived from Al complexes **1**–**4**.

2.3.2   Influence of reaction temperature

Our next focus was on the influence of the reaction temperature on the catalyst performance and therefore parallel catalysis experiments were performed at 25, 50 and 105 °C in a suitable high-throughput reactor platform (see Experimental for details; see Table 3). TBAB was used as nucleophile as most of the catalysts studied here showed appreciable turnover in the presence of this additive. At 25 °C (entries 1–8), the two porphyrin-based catalysts show the best performance (entries 6 and 7) with nearly quantitative or quantitative conversion, and high TONs. Under these conditions, the North system **2**/TBAB also performs comparatively well (entry 5) whereas the aminotriphenolate complexes **1a**–**1c** show lower activity (entries 2–4). Upon increasing the reaction temperature to 50 °C (entries 9–16), the most notable changes are observed for the binary systems based on **1a**–**1c**, with the combination of Al complex **1a** and TBAB (entry 10) now being the third most efficient catalyst. The results obtained at 105 °C ([Al] = 0.02 mol%, TBAB = 0.10 mol%) reveal that at elevated temperatures the binary combination **1a**/TBAB shows the best catalytic turnover (entry 18, conversion 76%, TON=3800) of all binary catalyst combinations.

Chapter 2

*Table 3. Comparison of the reactivities of binary Al-catalysts **1–4**/TBAB in the conversion of terminal epoxide **5** into cyclic carbonate **6** at different reaction temperatures.[a]*

Entry	Cat	Nu	T [ºC]	Yield [%][b]	TON[c]
1	–	TBAB	25	<1	–
2	1a	TBAB	25	19	190
3	1b	TBAB	25	13	130
4	1c	TBAB	25	19	190
5	2	TBAB	25	30	150
6	3a	TBAB	25	97	970
7	3b	TBAB	25	>99	1000
8	4	TBAB	25	18	180
9	–	TBAB	50	2	–
10	1a	TBAB	50	63	630
11	1b	TBAB	50	43	430
12	1c	TBAB	50	38	380
13	2	TBAB	50	49	245
14	3a	TBAB	50	96	960
15	3b	TBAB	50	97	970
16	4	TBAB	50	36	360
17	–	TBAB	105	6	–
18	1a	TBAB	105	76	3800
19	1b	TBAB	105	47	2350
20	1c	TBAB	105	51	2550
21	2	TBAB	105	12	300
22	3a	TBAB	105	44	2200
23	3b	TBAB	105	52	2600
24	4	TBAB	105	8	400

[a] Reaction conditions at **25** and **50** ºC: epoxide **5** (5.0 mmol), Al-complex (0.005 mmol; 0.1 mol%), nucleophile (Nu: 0.025 mmol; 0.5 mol%), mesitylene (0.5 mmol), 10 bar, 8 h (25ºC) and 3 h (50ºC); Reaction conditions at **105** ºC: epoxide **A** (5.0 mmol), Al-complex (0.001 mmol; 0.02 mol%), nucleophile (Nu: 0.005 mmol; 0.1 mol%), mesitylene (0.5 mmol), 10 bar, 2 h. [b] Determined by ^{1}H NMR (CDCl$_3$) using mesitylene as internal standard; the average of two runs is reported. Selectivity towards the cyclic carbonate **5** was >99%. [c] TON = total turnover number observed per Al; note that complex **2** contains two Al centers.

Chapter 2

Whereas the aminotriphenolate complexes **1a**–**1c** in the presence of TBAB steadily increase their performance at higher reaction temperatures, the data in Table 3 shows that the opposite trend is noted for the porphyrin-based catalysts **3a/3b** and the North system **2** (entries 21–23). The highest TON (3800) was observed for the binary catalyst **1a**/TBAB at 105 °C among the series of catalyst systems tested. Similar order TONs were reached with **3a** (3500) or **3b** (3300) when combined with PPNCl at 90 °C (see Table 1). The reaction temperature is thus one of the decisive process parameters for selection of the most efficient catalyst system.

2.3.3   Internal epoxide conversion

After examination of terminal epoxides **5, 7** and **8** as coupling partners for CO_2 and observing clear trends for the reactivity of binary catalysts derived from complexes **1**–**4**, we then turned our focus to the use of more challenging internal epoxides **11**–**13** (Table 4) and their conversion into cyclic carbonates **14**–**16** to see whether the reactivity and performance of the various binary catalyst systems would follow a similar tendency.

Most of the features observed in the conversion of the terminal epoxides were maintained when using internal epoxides as substrates. The porphyrin-based catalysts derived from **3a/3b** and PPNCl typically give the highest conversions (and consequently TON values; cf. entries 5, 11, and 17), whereas the aminophenolate Al complex **1a** becomes more competitive in the presence of TBAB, displaying similar TONs (entries 2, 8, and 14). However, apart from these similarities, there are also some other observations that add to the overall performance of the binary catalyst systems. For substrate **11** (*trans*-2,3-epoxybutane), the chemoselectivity toward the cyclic carbonate was >99% for all cases except for the binary catalysts **3b**/PPNCl and **3b**/TBAB. For these systems, there was significant formation of a diol product (butane-2,3-diol) of up to 19% of the total amount of product formed. Also, the stereospecificity was not quantitative in these cases, and loss of stereo-information was seen to be more pronounced when PPNCl was present (diastereoselectivity, *d.r.*, was 24:76, *trans* isomer major component). Therefore, despite the higher activity noted for **3b**/PPNCl and **3b**/TBAB, the lower chemoselectivity and stereospecificity makes the binary system based on **1a** the most attractive catalyst alternative.

Chapter 2

*Table 4. Comparison of the reactivities of binary Al-catalysts **1–4**/Nu in the conversion of internal epoxides **11–13** into cyclic carbonates **14–16** at 90 °C.*[a]
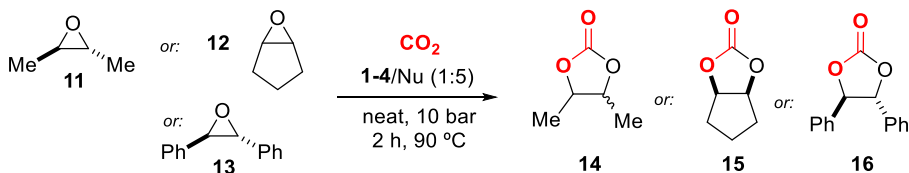
Entry	Cat	Sub.[b]	Yield [%][c]	TON[d]	Sel. [%][e]
1[f]	–	11	<1, <1	–	ND
2[f]	1a	11	8, 12	200, 300	>99
3[f]	2	11	1, 1	13, 13	>99
4[f]	3a	11	5, 3	125, 75	>99
5[f]	3b	11	13, 10	325, 250	24:76[g] 7:93[h]
6[f]	4	11	1, 1	25, 25	>99
7	–	12	4, 2	–	ND
8	1a	12	12, 19	300, 475	>99
9	2	12	6, 6	75, 75	>99
10	3a	12	36, 15	900, 375	>99
11	3b	12	37, 15	925, 375	>99
12	4	12	5, 4	125, 100	>99
13	–	13	1, 1[i]	–	ND
14	1a	13	6, 21[i]	10, 35	>99
15	2	13	5, 8[i]	4, 7	>99
16	3a	13	20, 12[i]	33, 20	>99
17	3b	13	25, 18[i]	42, 30	>99
18	4	13	2, 4[i]	3, 7	>99

[a] Reaction conditions: epoxide (5.0 mmol), Al complex (0.002 mmol; 0.04 mol%), Nu (0.010 mmol; 0.2 mol%), mesitylene (1.0 mmol), 10 bar, 2 h; Nu: PPNCl/TBAB. [b] Sub=substrate. [c] Determined by ^{1}H NMR (CDCl$_3$) using mesitylene as internal standard, first number refers to yield when using PPNCl; the average of two runs is reported. Selectivity towards the cyclic carbonates was >99%, [d] TONs observed per Al; complex **2** contains two Al centers. [e] Sel.= diastereoselectivity, that is, *cis/trans* ratio in the product, *trans* (**14** and **16**) or *cis* (**15**) ; ND stands for not determined. [f] P^0 = 15 bar with partial CO$_2$ pressure being 10 bar. [g] Chemoselectivity was 81%, 19% of diol product was formed. [h] Chemoselectivity was 91%, 9% of diol product was formed. [i] Epoxide (1.0 mmol), Al complex (0.006 mmol ; 0.6 mol %), Nu (0.030 mol; 3.0 mol%), MEK (0.5 mL), 2 h (for PPNCl) and 14 h (for TBAB).

The other two internal epoxides **12** (cyclopentene oxide) and **13** (*trans*-2,3-diphenyloxirane) gave rise to stereospecific conversions as expected as the cyclic

Chapter 2

carbonate products **15** and **16** are known to be exclusively formed with this preferred configuration. Previous studies by Darensbourgh have shown that the *trans*-conformer of cyclopentene carbonate (**15**) is thermodynamically not feasible due to high ring-strain, as such only the *cis*-carbonate is observed.[70] The opposite is true for carbonate **16**, in this case formation of the *cis*-carbonate is less favored and only *trans*-product is obtained.[71]

For the porphyrin-based binary catalysts based on **3a** and **3b**, higher turnovers are again attained in the presence of PPNCl as additive (entries 10, 11, 16, and 17). For the sterically most crowded substrate **13**, the use of a smaller nucleophile (Cl) is advantageous as much shorter time frames (PPNCl: 2 h versus TBAB: 14 h) are required for appreciable conversion. While chloride is a weaker nucleophile than bromide, its smaller size is beneficial in the ring-opening of sterically hindered substrates. Upon changing to bromide as nucleophile, the binary system **1a**/TBAB provides higher conversion and turnover with respect to the porphyrin-based catalysts **3a**/TBAB and **3b**/TBAB (cf., entries 14, 16, and 17). However, the overall reactivity found with **3a**/PPNCl and **3b**/PPNCl stands out for the conversion of this particular substrate, in line with the turnover data observed when using cyclopentene oxide (**12**).

2.3.4   Mechanistic considerations

The initial activities determined herein for all binary catalysts based on Al complexes **1–4** using terminal (**5**, **7** and **8**) and internal (**11–13**) epoxides demonstrate a number of interesting features. First, higher activities are generally achieved when aminotriphenolate Al complexes **1a–1c** and the North complex (**2**) are combined with TBAB; however, the binary catalysts based on **1a–1c** show significantly higher reactivities at relatively low complex loadings (0.01 mol% for the terminal epoxide conversions, 0.04–0.60 mol% in case of the internal epoxides).

At ambient temperature (25 °C), the conversion of 1,2-epoxyhexane mediated by **2**/TBAB works most efficiently and shows comparable turnover/Al center as observed for **1a–1c** in the presence of the same nucleophile. However, both types of catalyst systems show clear opposite temperature effects. The North catalyst shows decreased turnovers whereas the aminotriphenolate complexes perform better at higher reaction temperature with TONs of up to 3800. These results seem to be in line with the reported mechanisms for the aminotriphenolate complex **1a**[44] and North complex[68] in the conversion of epoxides and CO_2 into cyclic carbonates.

Chapter 2
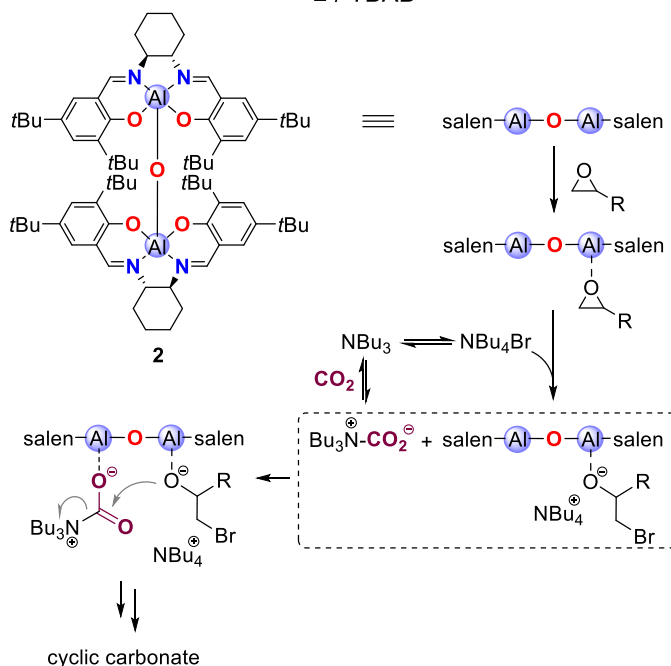
Scheme 8. Part of the mechanistic manifold reported for the binary catalyst **2**/TBAB.

The mechanism proposed by North *et al.* (Scheme 8)[68, 72] revealed a second order dependence on TBAB, meaning that catalysis mediated by the binary combination **2**/TBAB should be sensitive toward the loading of TBAB, and particularly slowed down at low concentration of the nucleophile. The loadings of complex **2** (0.01–0.04 mol%) and TBAB (0.05–0.20 mol%) were rather low (apart from those used for substrate **13**) throughout the studies performed here compared to the much higher loadings reported in the literature (typically 1.0–2.5 mol% for **2** and 2.5 mol% for TBAB).[68] Therefore, it is not surprising that initial catalytic turnover at these lower loadings was rather modest.

Another important aspect is that both Al centers in **2** are not exceptionally Lewis acidic and recent work[73] revealed that **2** itself in the absence of TBAB acts preferably as a Lewis base rather than a Lewis acid, activating CO_2 through the bridging oxygen atom to form an interesting carbonate-bridging [Al]$_2$-complex. This alternative pathway starts off with CO_2 insertion into the Al–O–Al bond, followed by epoxide activation through coordination to one of the metal centers (see Scheme 9). Subsequent intramolecular cyclization then affords the cyclic carbonate product. In both mechanisms, the activation of an epoxide by the [Al]$_2$-complex **2** is weak, and therefore

Chapter 2

reactions performed at higher reaction temperatures and at lower loading of **2** should increase the dynamics of this coordinative interaction. This results in a much lower population of the epoxide-activated intermediate, slowing down the catalytic transformation as was indeed observed experimentally.
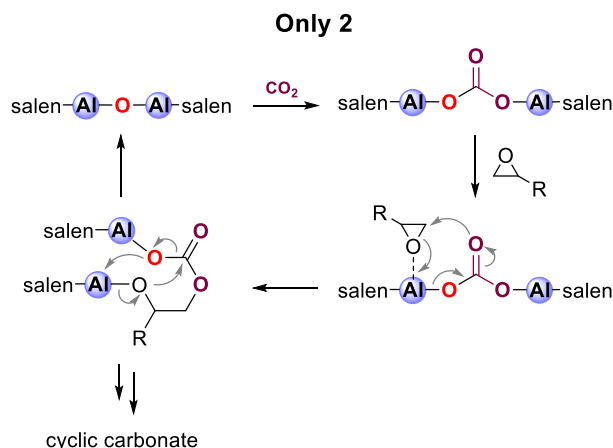
*Scheme 9. Mechanism for cyclic carbonate formation using only complex **2**.*

In contrast to **2**/TBAB, the activity for the binary couple **1a**/ TBAB increases at higher reaction temperatures. The mechanism operative for a similar binary couple (**1a**/TBAI; Scheme 10) was previously investigated in detail by DFT calculations and the initial ligand exchange was confirmed by X-ray analysis.[44] These studies revealed that the initial formation of an epoxide-ligated complex occurs with a free energy change of − 9.9 kcal·mol^{-1} (substrate was PO), thus demonstrating the favorable Lewis acidic character of the metal center. Compared to **2**, that forms a hexa-coordinated intermediate with the epoxide substrate, **1a** exchanges a THF molecule (see Figure 6, Scheme 10) for an epoxide and initially remains five-coordinate.

Chapter 2
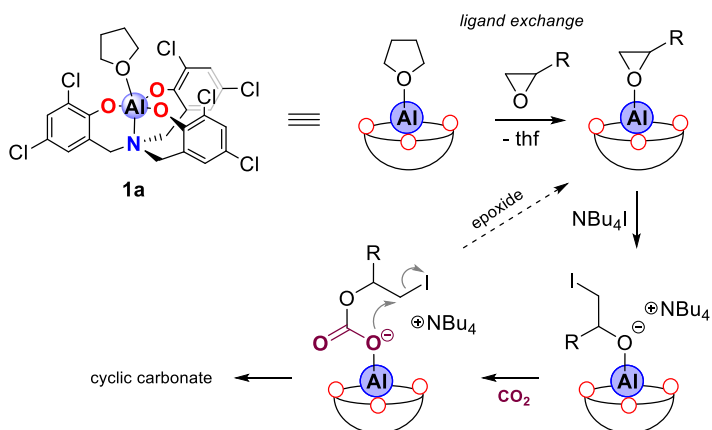
*Scheme 10. Part of the reported mechanism mediated by the binary catalyst **1a**/TBAI.*

At higher reaction temperatures the axial coordination site in the trigonal bipyramidal coordination sphere is expected to remain occupied by an epoxide substrate despite a faster rate of ligand exchange with bulk epoxide. Therefore, the observation of faster turnover for **1a**/TBAB (Table 3) at higher reaction temperatures is in line with this prediction, and the Lewis acidity for **1a** plays thus a dominant role in this mechanism. Beside the Lewis acidity, to create the most powerful binary combination, a bromide would be preferred over chloride nucleophile since bromide has a higher nucleophilic character and better leaving-group ability in the ring-opening and ring-closing step, respectively. This is indeed observed in the results of Table 1, 2 and 4 for all substrates; only in the case of a high degree of steric crowding in the epoxide (i.e., *trans*-2,3-diphenyloxirane **13**), chloride-based nucleophiles provide a better alternative as steric features at the epoxide ring-opening stage dominate.

The porphyrin-based binary catalysts derived from **3a** and **3b** show fairly similar results in terms of initial rates in the conversion of the six epoxide substrates that were analyzed in this chapter, and thus it seems that the porphyrin substitution does not play a decisive role. Moreover, these Al(porphyrins) show the highest activity when combined with PPNCl, and do not follow the typical reactivity trend observed for many binary catalysts comprising of halide nucleophiles. The fact that lower TONs are observed also for the porphyrins **3a** and **3b** combined with TBAB at high reaction temperature (105 °C, Table 3) seems to suggest the occurrence of a pre-equilibrium (Scheme 11).

Chapter 2
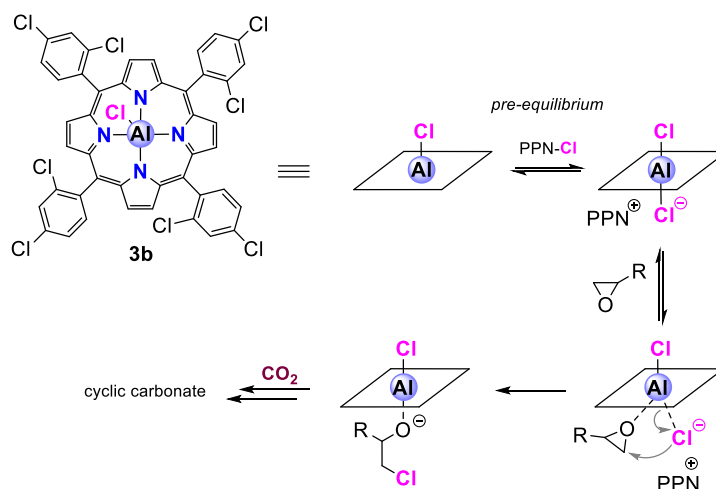
*Scheme 11. Proposed mechanism mediated by the binary catalyst **3b**/PPNCl based on literature data and experimental findings herein.*

Al(porphyrins) were previously shown to form hexa-coordinated species when combined with nucleophilic additives including 4-dimethylaminopyridine (DMAP), azides, and chloride salts.[74] Importantly, the copolymerization of PO and CO_2 can be mediated by an Al(porphyrin)/PPNCl combination. The reaction was found to be first order in [Al] and the nucleophilic ring opening of the coordinated epoxide was suggested to occur at the same face of the porphyrin scaffold. According to the Pearson acid/base concept,[75] a hard Lewis acid (the Al complex) binds more strongly with hard ligands such as chloride than with softer donors such as bromide or iodide. Such a behavior would therefore increase the probability for epoxide ring opening occurring at a di-chloro-Al(III)porphyrin anion, facilitating the formation of the cyclic carbonate. Therefore, the experimental findings reported in Table 1, 2 and 4 follow agreeably this trend. Also, at 105 °C and lower catalyst loading (0.02 mol% [Al]) the relative rate increase for epoxide conversion compared to **1a**/TBAB is attenuated (see Table 3), which may be caused by a more dynamic chloride coordination to **3b**.

Darensbourg and Billodeaux reported the use of Al(salen) complexes such as **4** (see reaction scheme in Figure 6) combined with NBu_4X as binary catalysts for the copolymerization of cyclohexene oxide (CHO) and CO_2.[76] Significantly higher copolymerization activities were obtained using salen ligands equipped with electron-withdrawing substituents that resulted in more electrophilic Al complexes. Thus, it is reasonable to assume that the bimetallic North catalysts (**2**) and Al(salen) complex (**4**) having peripheral electron-donating *tert*-butyl groups are not Lewis acidic enough to result in high relative activity for cyclic carbonate formation at comparatively low

Chapter 2

loadings of [Al]. This trend is essentially observed in the conversion of all terminal and internal epoxides, and complexes **2** and **4** give generally the lowest catalytic efficiencies among the binary combinations, apart from the reactions performed at 25 °C using 1,2-epoxyhexane (**5**) as substrate (Table 3).

*Table 5. Comparison of the reactivities of binary Al-catalysts **1a**/Nu and **3a**/Nu (Nu = TBAB, PPNCl) in the conversion of propylene oxide **8** into cyclic carbonate **10** at different metal-to-nucleophile ratios.[a]*

Entry	Cat	Nu	ratio [Al]/Nu	Yield [%][b]	TON[c]
1	—	PPNCl[d]	—	4	—
2	—	PPNCll[e]	—	5	—
3	—	TBABI[d]	—	3	—
4	—	TBABI[e]	—	4	—
5	**1a**	TBAB	1:5	32	16.1
6	**1a**	TBAB	1:120	14	7.0
7	**1a**	PPNCl	1:5	26	13.0
8	**1a**	PPNCl	1:120	7	3.5
9	**3b**	TBAB	1:5	38	19.1
10	**3b**	TBAB	1:120	33	16.6
11	**3b**	PPNCl	1:5	32	16.1
12	**3b**	PPNCl	1:120	41	20.6

[a] Propylene oxide (28.6 mmol), Al-complex (0.00057 mmol), nucleophile (Nu: 0.069 mmol or 0.0029 mmol), mesitylene (1.0 mmol), 15 bar, 90ºC; 1:5 [Al]/Nu ratios for 18 h, 1:120 [Al]/Nu ratios for 0.5 h. [b] Determined by ^{1}H NMR (CDCl$_3$) using mesitylene as internal standard; the average of two runs is reported. Selectivity towards propylene carbonate was >99%. [c] TON = total turnover number ($\times 10^3$) observed per Al center. [d] Blank reaction using 0.0029 mmol Nu, 18 h. [e] Blank reaction using 0.069 mmol Nu, 0.5 h.

The two most efficient catalyst systems at low loading of [Al] and nucleophile (i.e., **1a** and **3b**) were then evaluated for the synthesis of propylene carbonate (PC) using PO (**8**) as substrate (Table 5). The porphyrin catalyst **3b** previously displayed very high TONs of >100 000 in short time frames (0.5 h) for the coupling of PO and CO$_2$ at 120 °C/3.0

36

Chapter 2

MPa using PPNCl as nucleophilic additive.[48] Thus, we decided to benchmark the performance of **1a** and **3b** under similar conditions using this specific substrate and investigated the influence of the relative loading of the halide on the overall performance. Both **1a** and **3b** were combined with TBAB and PPNCl in different ratios (1:5 and 1:120) in standard autoclave reactors. The conversion was determined after a pre-set time interval, that is, 0.5 h for the reactions performed with a 1:120 [Al]/Nu ratio, and 18 h for those reactions performed with 1:5 combinations of [Al]/Nu. In all cases a clear positive effect of the addition of the Al complex on the total conversion of PO into PC was noted, as the blank experiments in the absence of the Al complexes gave much lower conversion (entries 1–4).

Under these more dilute conditions, the relative performance of complex **1a** is improved and high turnovers are achieved in the presence of 5 equiv of TBAB or PPNCl (entries 5 and 7; TON up to 16.1×10^3). When the relative loading of TBAB or PPNCl is increased (120 equiv, entries 6 and 8), activities are only slightly higher than the background reaction, which seems to suggest that a too large excess of halide additive may result in competition for coordination to the Al center and thus block turnover of the epoxide substrate. This seems to be in line with the reported mechanism for **1a**/TBAI,[44] where initial epoxide coordination to the metal center is a key step towards the formation of the cyclic carbonate.

The porphyrin binary catalysts based on **3b**, however, do not show this behavior, and at higher PPNCl loading (120 equiv) the catalytic performance is further improved (cf., entries 10 and 12) with a significantly higher TON (20.6×10^3). This result also aligns well with the mechanistic proposal that an initial equilibrium exists where the Al(porphyrin)Cl coordinates a chloride anion before it interacts with the epoxide substrate to facilitate its ring opening (Scheme 11). The data presented in Table 5 illustrates that both **1a** and **3b** provide highly active binary catalysts under dilute conditions, and result in high TONs for the conversion of PO into PC at different [Al]/Nu ratios.

2.3.5   Catalyst synthesis & cost

A comparison was made between the different catalysts concerning their synthetic protocol and price. The synthesis of ligands and complexes is displayed in section 2.5.3, showing that each metal complex can be prepared by a two-step procedure starting from commercially available starting materials. Almost quantitative yields are obtained for the salen ligands used in complexes **2** and **4**, much higher than in case of the

Chapter 2

porphyrin and aminotriphenolate syntheses. However this is offset by the expensive starting materials for the salen ligand, leading to higher catalyst prices (see Table 6). In general the use of catalysts **1a** and **3b** seems attractive both in terms of the low catalyst cost and high activity. From a sustainable point of view, the porphyrin catalyst **3b** is a good option due to its efficiency at room temperature reactions. However, catalyst **3b** requires a large excess of PPNCl to achieve high conversions, which is significantly more expensive than TBAB (10 vs < 1 €/g).

Table 6. Total catalyst cost.[a]

entry	catalyst	price per mmol (€)	price per gram (€)
1	$[Al]^{Cl}$ (**1a**)	0,93	1,65
2	$[Al]_2O$ (**2**)	6,66	5,75
3	$[Al]^{TPP}$ (**3a**)	1,06	1,57
4	$[Al]^{Cl-TPP}$ (**3b**)	1,58	1,67
5	$[Al]^{Salen}$ (**4**)	3,40	5,60

[a] Total calculated prices (including ligand and complex synthesis) based on their respective starting materials purchased from either Sigma-Aldrich or TCI (lowest prices taken, dd. 24-nov-2016), taking into account the typical reaction yield for both ligand and catalyst synthesis (see also Tables 7 and 8).

Table 7. Cost of ligand synthesis[a]

entry	catalyst	cost ligand (€) (mmol^{-1})	ligand yield	cost ligand (€) (yield corrected)
1	$[Al]^{Cl}$ (**1a**)	0,08	37	0,22
2	$[Al]_2O$ (**2**)	4,72	95	4,97
3	$[Al]^{TPP}$ (**3a**)	0,11	40	0,28
4	$[Al]^{Cl-TPP}$ (**3b**)	0,19	25	0,76
5	$[Al]^{Salen}$ (**4**)	2,36	95	2,48

[a] Ligand synthesis prices are based on the price of their respective starting materials purchased from either Sigma-Aldrich or TCI (lowest prices taken, dd. 24-nov-2016), taking into account the required equivalents of each reagent and a typical reaction yield.

Chapter 2

Table 8. Cost of complex synthesis[a]

entry	catalyst	cost catalyst (€) (mmol^{-1})	catalyst yield	cost catalyst (€) (yield corrected)
1	[Al]^{Cl} (**1a**)	0,56	60	0,93
2	[Al]$_2$O (**2**)	5,66	85	6,66
3	[Al]^{TPP} (**3a**)	1,01	95	1,06
4	[Al]$^{Cl-TPP}$ (**3b**)	1,50	95	1,58
5	[Al]^{Salen} (**4**)	3,23	95	3,40

[a] Complex synthesis prices are calculated based on the aluminum precursors purchased from Sigma-Aldrich (lowest prices taken, dd. 24-nov-2016) and the price of the ligand (see Table 7), taking into account the required equivalents of each reagent and a typical reaction yield.

2.4 Conclusion

Herein we have described a detailed comparison between a series of Al-based binary catalysts derived from complexes **1–4** and their (initial) efficiencies to mediate the coupling reaction between various terminal and internal epoxides, and CO$_2$ to produce their corresponding cyclic carbonates. Under more dilute catalysis conditions using low loadings of [Al] and Nu (Nu: nucleophile) while fixing their relative ratio (1:5), the binary catalysts **1a**/TBAB and **3b**/PPNCl display the highest reactivities among all combinations tested and this trend was observed for all substrates. In the conversion of the highly sterically crowded *trans*-2,3-diphenyloxirane, however, the use of a chloride-based nucleophile is more beneficial.

These studies also demonstrate that benchmarking studies are vital to provide insight into the relative reactivities of binary catalyst systems, and to determine the best operating window (temperature, metal-to-nucleophile ratio, solvent, scale) for each individual catalyst. The known mechanistic manifolds for epoxide conversion into cyclic carbonate can be used as directing blueprints to select the most appropriate catalyst system depending on the reaction temperature, the nature of the substrate (focusing on chemoselectivity, cf. conversion of substrate **11** in Table 4), and the accessibility of the catalyst structures. The latter feature can be of high importance in those cases where scale up of the catalytic process is desired and larger quantities of catalyst are thus required. Detailed benchmarking studies for similar type binary catalysts such as described in this chapter offer a way to compare performance metrics under identical reaction conditions and to unravel intrinsic and relative reactivities. These benchmarking approaches are essential to support general claims on catalyst performance in a wider context, thereby stimulating careful assessment of other

Chapter 2

features that are also important to select the most appropriate catalyst for CO_2 conversion.

2.5 Experimental

2.5.1 General comments

The ligands and catalysts (see below) were prepared according to previously reported procedures. References to all ligands and complexes are given in the next section along with the ^1H and ^{13}C NMR characterization data for the complexes. ^1H and ^{13}C NMR spectra were recorded on a Bruker AV-300, AV-400 or AV-500 spectrometer. Carbon dioxide was purchased from PRAXAIR and used without further purification. Solvents used in the synthesis of the complexes were dried using an Innovative Technology PURE SOLV solvent purification system. All epoxides are commercially available and were used as received.

2.5.2 Typical catalytic experiment

The respective epoxide, Al-complex, co-catalyst (PPNCl, TBAB or TBAI) and internal standard (mesitylene) were charged into a stainless steel autoclave. The autoclave was then sealed and heated to the required temperature while stirring. After reaching the selected reaction temperature, the autoclave was pressurized with CO_2 to the desired pressure and left stirring. At the end of the chosen time interval, the autoclave was cooled to rt and then carefully depressurized. An aliquot of the reaction mixture was taken for analysis and the conversion was determined by ^1H NMR spectroscopy in $CDCl_3$. The identities of the cyclic carbonate products were confirmed by comparison to literature data. For specific details on the used (parallel) reactor systems, their volumes and amount of substrates, Al complexes and additives, see the next sections.

HP-reactor

Typical example (Table 5, entry 5):

Al-complex **1a** (0.00057 mmol, 0.32 mg), TBAB (0.0029 mmol, 0.93 mg) and propylene oxide (28.6 mmol, 1.66 g) were added into the Teflon insert. This high pressure reactor was operated according to the general catalytic procedure described in section 2.5.2. The only difference is that the mesitylene is used as an external standard in this case,

Chapter 2

being added after the reaction had finished and the reactor had been cooled down and depressurized. All results from Table 5 have been obtained with this reactor system.

Figure 7. 35 mL stainless steel autoclave (left) with a 15 mL Teflon insert (right)

HEL-multireactor

Typical example (Table 3, entry 5):

Al-complex **2** (0.005 mmol, 5.8 mg), TBAB (0.025 mmol, 8.0 mg), mesitylene (0.5 mmol, 61 mg) and 1,2-epoxyhexane (5.0 mmol, 0.50 g) were added into a glass insert. This HEL multi-reactor system was operated according to the general catalytic procedure described in section 2.5.2. All results from Table 3 have been obtained with this system.

Figure 8. Multireactor system (left) with 3 mL glass inserts (right).

41

Chapter 2

AMTEC II

Typical example (Table 1, entry 5):

Al-complex **3b** (0.001 mmol, 0.95 mg), TBAB (0.005 mmol, 2.87 mg), mesitylene (1.0 mmol, 121 mg) and 1,2-epoxyhexane (10.0 mmol, 1.00 g) were added into a stainless steel insert. This parallel reactor system was operated according to the general catalytic procedure described in section 2.5.2. All results from Table 1, 2 and 4 have been obtained with this system.
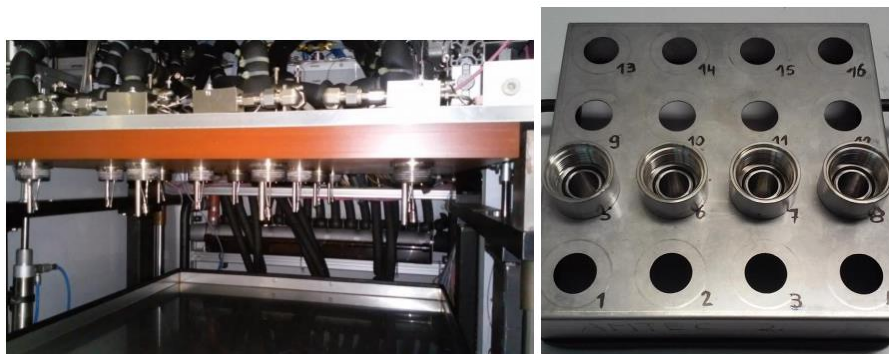
Figure 9. AMTEC II system (top) with 10 mL stainless steel inserts (bottom).

2.5.3   Catalyst synthesis

(Cl-triphenolate)Aluminum (**1a**)
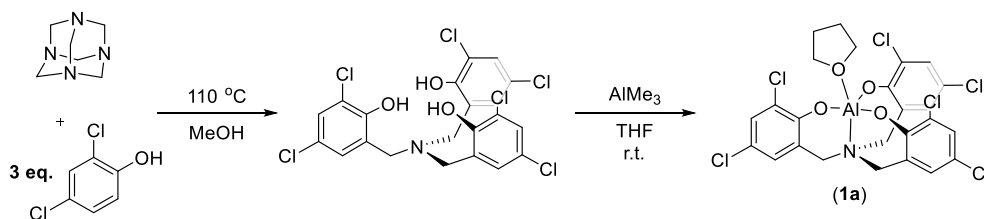
Both the ligand and complex were synthesized according to previously described procedures.[44] (**1a**): **^{1}H NMR** (500 MHz, CDCl$_3$) δ 7.33 (d, *J* = 2.6 Hz, 3H), 6.90 (d, *J* = 2.6 Hz, 3H), 4.75 – 4.64 (m, 4H), 4.18 (d, *J* = 13.8 Hz, 3H), 2.95 (d, *J* = 13.8 Hz, 3H), 2.28 – 2.17 (m, 4H). **^{13}C NMR** (101 MHz, CDCl$_3$) δ 152.46, 129.75, 127.13, 124.68, 123.08, 122.16, 72.38, 58.26, 25.48.

42

Chapter 2

(Me-triphenolate)Aluminum (**1b**)
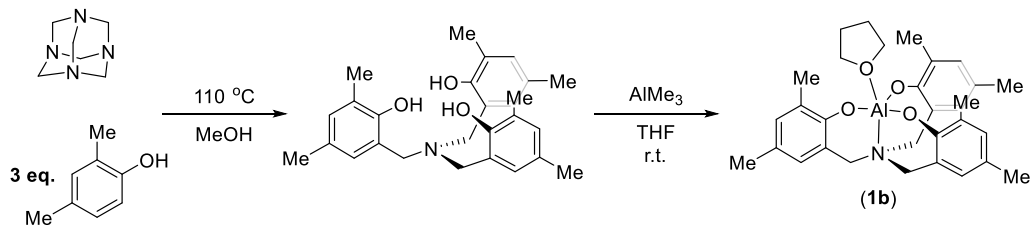
Both the ligand and complex were synthesized according to previously described procedures.[44, 56] (**1b**): **^{1}H NMR** (500 MHz, CDCl$_3$) δ 6.88 (d, *J* = 2.2 Hz, 3H), 6.61 (d, *J* = 2.2 Hz, 3H), 4.59 (s, 2H), 4.26 (d, *J* = 13.6 Hz, 3H), 2.84 (d, *J* = 13.8 Hz, 3H), 2.20 (m, 18H). **^{13}C NMR** (101 MHz, CDCl$_3$) δ 154.25, 131.01, 126.95, 126.89, 125.84, 120.63, 58.66, 25.60, 20.39, 16.94.

(*t*Bu-triphenolate)Aluminum (**1c**)
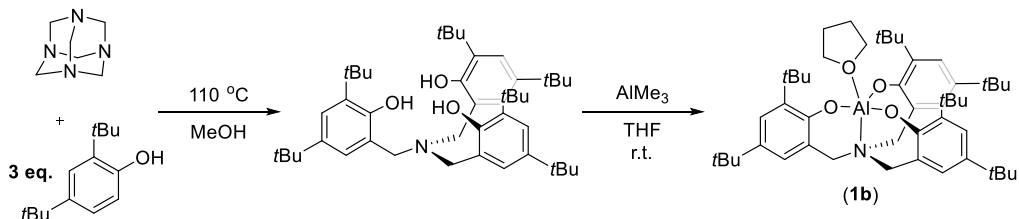
Both the ligand and complex were synthesized according to previously described procedures.[44, 77] (**1c**): **^{1}H NMR** (500 MHz, (CDCl$_3$) δ 7.23 (d, *J* = 2.5 Hz, 3H), 6.88 (d, *J* = 2.5 Hz, 3H), 4.30 (d, *J* = 13.4 Hz, 3H), 3.79 (s, 4H), 2.94 (d, *J* = 13.6 Hz, 3H), 1.89 (s, 4H), 1.42 (s, 27H), 1.28 (s, 27H). **^{13}C NMR** (126 MHz, CDCl$_3$) δ 154.89, 139.10, 137.08, 123.76, 123.57, 121.50, 70.61, 58.84, 34.90, 34.03, 31.73, 29.74, 25.40.

μ-Oxo-bis(salen)Aluminum (**2**)
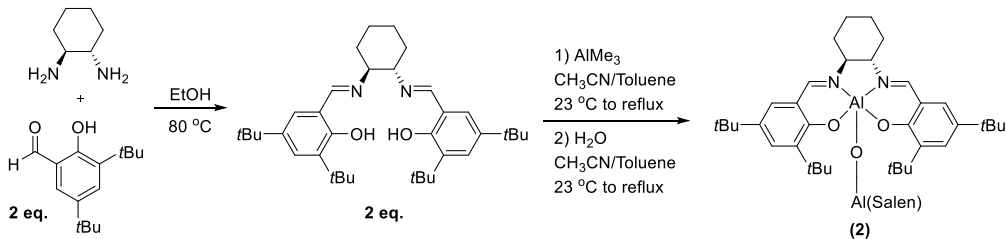
Chapter 2

Both the ligand[8] and complex[53a] were synthesized according to previously described procedures. (**2**): **¹H NMR** (400 MHz, Benzene-d_6) δ 7.89 (m, 1H), 7.79 (m, 1H), 7.68 (m, 4H), 7.47 (s, 2H), 7.13 (m, 2H), 7.07 (s, 2H), 3.40 (t, J = 11.2 Hz, 2H), 2.18 (t, J = 11.2 Hz, 2H), 1.63 (s, 18H), 1.59 (s, 18H), 1.55 (s, 18H), 1.54 (s, 18H), 1.26 (m, 2H), 1.11 − 1.01 (m, 4H), 0.82 (m, 2H), 0.61 (m, 8H). **¹³C NMR** (126 MHz, Benzene-d_6) δ 166.12, 165.20, 163.11, 159.65, 141.17, 141.04, 136.95, 135.97, 129.15, 128.54, 127.25, 126.31, 118.82, 118.76, 64.78, 61.65, 35.91, 35.57, 33.90, 33.88, 31.66, 31.59, 30.04, 29.71, 27.74, 26.33, 24.05, 23.46.

(Tetraphenylporphyrin)Aluminum Chloride (**3a**)
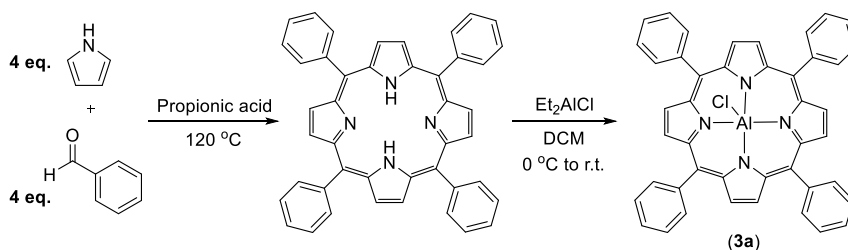
Both the ligand[78] and complex[48] were synthesized according to previously described procedures. (**3a**): **¹H NMR** (400 MHz, DMSO-d_6) δ 9.00 (s, 8H), 8.24 − 8.17 (m, 8H), 7.90 − 7.83 (m, 12H). **¹³C NMR** (126 MHz, DMSO-d_6) δ 147.04, 141.40, 134.51, 132.57, 128.71, 127.57, 120.65.

(5, 10, 15, 20-Tetrakis-2,4-dichlorophenylporphyrin)Aluminum Chloride (**3b**)
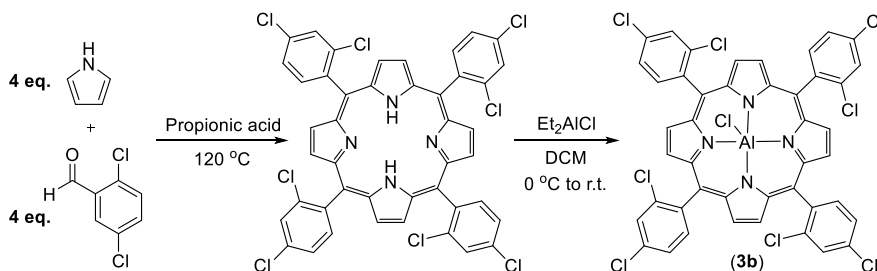
Both the ligand and complex were synthesized according to previously described procedures.[48] (**3b**): **¹H NMR** (300 MHz, DMSO-d_6) δ 8.95 (m, 8H), 8.40 − 8.13 (m, 8H), 7.97 − 7.87 (m, 4H). **¹³C NMR** (126 MHz, DMSO-d_6) δ 147.10, 138.63, 137.04, 136.91, 135.25, 132.51, 129.06, 126.91, 116.47.

Chapter 2

(Salen)Aluminum Chloride (**4**)
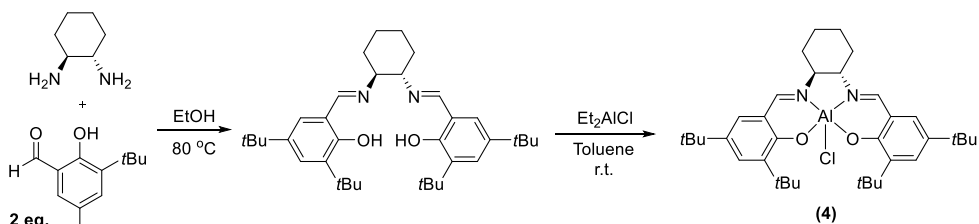
Both the ligand[8] and complex[53b] were synthesized according to previously described procedures. (**4**): **¹H NMR** (500 MHz, DMSO-d_6) δ 8.35 (s, 2H), 7.42 (d, J = 2.7 Hz, 2H), 7.36 (d, J = 2.6 Hz, 2H), 2.66 – 2.58 (m, 1H), 2.37 (m, 1H), 1.97 (m, 2H), 1.53 (s, 18H), 1.48 – 1.33 (m, 2H), 1.29 (s, 18H), 1.24 (m, 4H). **¹³C NMR** (126 MHz, DMSO-d_6) δ 164.50, 162.01, 139.36, 136.84, 129.61, 129.29, 119.38, 63.78, 35.63, 34.17, 31.86, 30.25, 27.41, 23.98.

Chapter 2

2.6 References

[8]   E. N. Jacobsen, W. Zhang, A. R. Muci, J. R. Ecker, L. Deng, *J. Am. Chem. Soc.* **1991**, *113*, 7063-7064.

[44]   C. J. Whiteoak, N. Kielland, V. Laserna, F. Castro-Gómez, E. Martin, E. C. Escudero-Adán, C. Bo, A. W. Kleij, *Chem. Eur. J.* **2014**, *20*, 2264-2275.

[48]   Y. Qin, H. Guo, X. Sheng, X. Wang, F. Wang, *Green Chem.* **2015**, *17*, 2853-2858.

[53]   a) M. S. Taylor, E. N. Jacobsen, *J. Am. Chem. Soc.* **2003**, *125*, 11204-11205; b) G. M. Sammis, H. Danjo, E. N. Jacobsen, *J. Am. Chem. Soc.* **2004**, *126*, 9928-9929.

[56]   A. Chandrasekaran, R. O. Day, R. R. Holmes, *J. Am. Chem. Soc.* **2000**, *122*, 1066-1072.

[59]   C. J. Whiteoak, N. Kielland, V. Laserna, E. C. Escudero-Adán, E. Martin, A. W. Kleij, *J. Am. Chem. Soc.* **2013**, *135*, 1228-1231.

[60]   a) B. Milani, G. Licini, E. Clot, M. Albrecht, *Dalton Trans.* **2016**, *45*, 14419-14420; b) W. Zhang, W. Lai, R. Cao, *Chem. Rev.* **2017**, *117*, 3717-3797.

[61]   a) J. Klankermayer, S. Wesselbaum, K. Beydoun, W. Leitner, *Angew. Chem. Int. Ed.* **2016**, *55*, 7296-7343; b) Q. Liu, L. Wu, R. Jackstell, M. Beller, *Nat. Commun.* **2015**, *6*, 5933.

[62]   a) A. Buonerba, A. De Nisi, A. Grassi, S. Milione, C. Capacchione, S. Vagin, B. Rieger, *Catal. Sci. Technol.* **2015**, *5*, 118-123; b) D. Alhashmialameer, J. Collins, K. Hattenhauer, F. M. Kerton, *Catal. Sci. Technol.* **2016**, *6*, 5364-5373.

[63]   a) M. A. Fuchs, C. Altesleben, S. C. Staudt, O. Walter, T. A. Zevaco, E. Dinjus, *Catal. Sci. Technol.* **2014**, *4*, 1658-1673; b) M. Adolph, T. A. Zevaco, C. Altesleben, S. Staudt, E. Dinjus, *J. Mol. Catal. A: Chem.* **2015**, *400*, 104-110.

[64]   a) Y. Xu, D. Yuan, Y. Wang, Y. Yao, *Dalton Trans.* **2017**, *46*, 5848-5855; b) M. North, S. C. Z. Quek, N. E. Pridmore, A. C. Whitwood, X. Wu, *ACS Catal.* **2015**, *5*, 3398-3402.

[65]   C. Maeda, T. Taniguchi, K. Ogawa, T. Ema, *Angew. Chem. Int. Ed.* **2015**, *54*, 134-138.

[66]   J. A. Castro-Osma, K. J. Lamb, M. North, *ACS Catal.* **2016**, *6*, 5012-5025.

[67]   M. Alves, B. Grignard, S. Gennen, R. Mereau, C. Detrembleur, C. Jerome, T. Tassaing, *Catal. Sci. Technol.* **2015**, *5*, 4636-4643.

[68]   W. Clegg, R. W. Harrington, M. North, R. Pasquale, *Chem. Eur. J.* **2010**, *16*, 6828-6843.

[69]   F. Castro-Gómez, G. Salassa, A. W. Kleij, C. Bo, *Chem. Eur. J.* **2013**, *19*, 6289-6298.

[70]   a) D. J. Darensbourg, A. D. Yeung, *Macromolecules* **2013**, *46*, 83-95; b) D. J. Darensbourg, A. D. Yeung, S.-H. Wei, *Green Chem.* **2013**, *15*, 1578-1583.

[71]   C. Beattie, M. North, P. Villuendas, C. Young, *J. Org. Chem.* **2013**, *78*, 419-426.

[72]   M. North, R. Pasquale, *Angew. Chem. Int. Ed.* **2009**, *48*, 2946-2948.

Chapter 2

[73]   J. A. Castro-Osma, M. North, W. K. Offermans, W. Leitner, T. E. Müller, *ChemSusChem* **2016**, *9*, 791-794.
[74]   C. Chatterjee, M. H. Chisholm, *Inorg. Chem.* **2011**, *50*, 4481-4492.
[75]   R. G. Pearson, *J. Am. Chem. Soc.* **1963**, *85*, 3533-3539.
[76]   D. J. Darensbourg, D. R. Billodeaux, *Inorg. Chem.* **2005**, *44*, 1433-1442.
[77]   M. Kol, M. Shamis, I. Goldberg, Z. Goldschmidt, S. Alfi, E. Hayut-Salant, *Inorg. Chem. Commun.* **2001**, *4*, 177-179.
[78]   L. Maqueira, A. Iribarren, A. C. Valdés, C. P. de Meloc, C. G. dos Santos, *J. Porphyr. Phthalocyanines* **2012**, *16*, 267-272.

UNIVERSITAT ROVIRA I VIRGILI
ALUMINUM-CATALYZED COUPLING OF CARBON DIOXIDE AND CYCLIC ETHERS
Jeroen Rintjema Tanger

Chapter 3.

Highly Chemoselective Catalytic Coupling of Substituted Oxetanes and Carbon dioxide
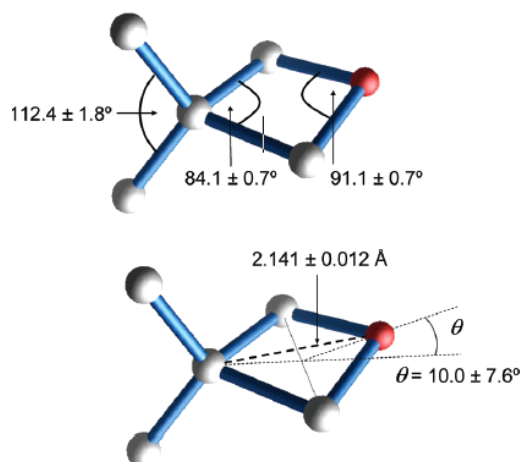
This work has been published in:

UNIVERSITAT ROVIRA I VIRGILI
ALUMINUM-CATALYZED COUPLING OF CARBON DIOXIDE AND CYCLIC ETHERS
Jeroen Rintjema Tanger

Chapter 3

3.1 Introduction

In the field of cyclic carbonate synthesis, focus lies mainly on the production of 5MCCs (see previous chapter), while formation of the related 6MCCs has received far less attention to date. Apart from the general applications of carbonates listed in the introduction to this thesis, the six-membered variants are often used in ring-opening polymerization (ROP) reactions.[79] Functional derivatives of the carbonate monomers have led to the development of biodegradable polymers[80] or compounds that are used in biomedical applications.[81] A series of interesting azide-functionalized carbonates were reported by Bowden *et al.*, which opened up possibilities for various post-modification reactions.[82]

Different methods for the formation of 6MCCs exist, including the coupling of diols with either tosyl chloride[83] or dialkylcarbonates.[84] These reactions however produce large amounts of waste or require harsh reaction conditions. Another approach relies on the use of halo-alcohols that can cyclize with CO_2 under basic conditions.[85] While this reaction operates under mild conditons, it uses stoichiometric amounts of base and has a rather limited scope. A much less explored option is the coupling of oxetanes with CO_2 catalyzed by a suitable binary catalytic system, similar as reported for the conversion of epoxides to 5MCCs. While oxetanes are a fairly common reagent in many chemical transformations,[86] its coupling with CO_2 is relatively unknown. The main challenges associated with the coupling of oxetanes and CO_2 are their lower reactivity compared to epoxides and competing polymerization reactions. The latter has been studied in great detail by the group of Darensbourg, who showed that there are two different reaction mechanisms towards polycarbonate formation.[87] One is the direct copolymerization of oxetanes with CO_2 while the second route proceeds via initial formation of the carbonate monomer following ROP.

The few succesful examples of 6MCC formation that have been reported either focused on the unsubstituted trimethylene carbonate (TMC)[88] or derivatives with some degree of substitution in the 6MCC scaffold albeit in low yield.[89] Very recently, an organocatalytic approach was also reported to produce TMC by initial formation of an oligocarbonate at high temperature (130 °C).[90] In order to explain the more challenging conversion of oxetanes compared to epoxides, a better understanding of the properties and reactivity are required. A common assumption is that the four-membered oxetane ring has less ring strain and is therefore less reactive compared to epoxides. Taking a closer look at some of their properties however, shows that while the bond angles in epoxides are significantly smaller, the amount of ring strain is

Chapter 3

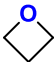comparable with only 2 kcal/mol difference between the two parent substrates (see Figure 10).[91]

	C-O-C Angle	Ring strain (kJ/mol)	pK_b
(oxirane)	60°	114	7.4
(oxetane)	90°	107	3.1

Figure 10. A comparison between several properties of oxirane and trimethylene oxide.

The smaller C–O–C angle in epoxides does have another effect; it increases the p-character of the nonbonding orbitals from the lone pairs.[92] This allows for electron delocalization within the epoxide which has two main effects: a reduced dipole moment and aromatic stabilization in the ring-opening transition state by orbital interaction through bonds (OITB).[93] The orbitals in oxetanes therefore retain more s-character leading to high electron density on the oxygen, in agreement with oxetanes having a higher dipole moment and basicity compared to epoxides. As a consequence, oxetanes are less susceptible towards nucleophilic attack, though they form more stable metal-substrate complexes. This effect has been demonstrated by Darensbourg *et al* , who reported a comparative study between initial coupling of oxetane or epoxide with CO_2 catalyed by chromium-salen complexes.[94] They showed that upon using a mixture of both substrates to displace a labile chloride ligand from the chromium center, the oxetane adduct is thermodynamically favored. On the other hand, when a nucleophile is added to ring-open the bound cyclic ethers, a much faster reaction was observed for the epoxide.

Taking this information into account, we envisioned that a highly Lewis acidic metal complex such as the dichloro-substituted Al-TPA complex (**1a**, Chapter 2) would form a very stable metal-substrate adduct as the oxetane is more basic than its epoxide counterpart. This may raise the activation energy associated to its conversion and slow down catalytic turnover. Thus, in these cases a less Lewic acidic Al complex might prove beneficial to reduce the stability of the oxetane-metal adduct. Ideally, the catalytic system should show high activity in cyclic carbonate formation while operating under mild conditions to prevent polymerization reactions (see Scheme 12).

Chapter 3
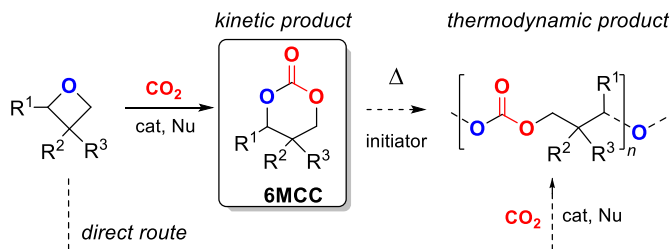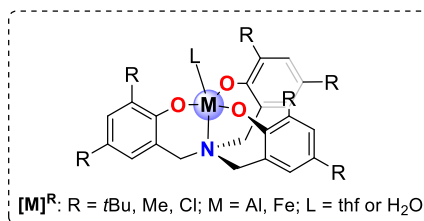
Scheme 12. Formation of 6MCCs and the challenges associated with their formation. Below the catalyst structures used in this work, which are based on aminotriphenolate complexes.

3.2 Objectives

Within this chapter we describe the quest for a catalyst and suitable reaction conditons to facilitate the formation of 6MCCs from substituted oxetanes and CO_2. Both iron and aluminum complexes derived from aminotriphenolate ligands have been tested in this type of transformation. The goal was to expand the current scope of 6MCCs and provide a general methodology for their synthesis, and allowing for different functionality in the 6MCC backbone.

Chapter 3

3.3 Results and discussion

Oxetane starting materials (Figure 11) used throughout this chapter were either commercialy available or synthesized according to existing protocols (see experimental section for details). There are three main methods for the synthesis of oxetanes,[95] being the intramolecular Williamson ether synthesis from diols[96] or halo-alcohols, the Paternó-Büchi [2+2] cycloaddition[97] and methylene insertion into ketones/epoxides using sulfoxonium ylides.[98] Very recently, a stereoselective synthesis of oxetanes via an intramolecular Michael addition was developed.[99]
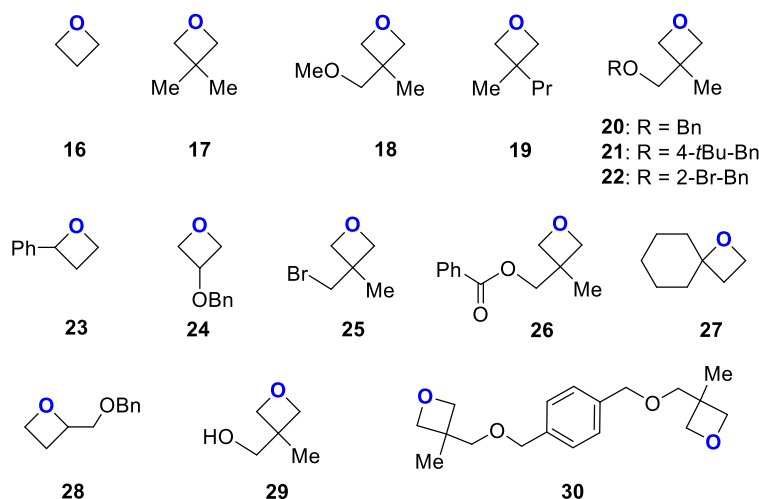
*Figure 11. Oxetane substrates **16**-**30** probed in the screening and substrate scope studies. Bn = benzyl, Ph = phenyl, Pr = propyl.*

3.3.1   Optimization of reaction conditions

To assess the suitability of aminotriphenolate complexes to selectively mediate the coupling between oxetanes and CO_2 towards 6MCCs, we first considered the use of various Fe^{III} and Al^{III} complexes, 3,3'-dimethyloxetane (**17**, Figure 11) as substrate and based on our previous experience with oxetane/CO_2 coupling reactions TBAX (TBA = tetrabutylammonium; X = Br, I) as a nucleophilic additive (Table 9).

Chapter 3

*Table 9. Results of the screening stage using 3,3´-dimethyloxetane **17** and CO_2 under various conditions.[a]*

Al^{Cl}: R = Cl; L = thf
Al^{Me}: R = Me; L = thf
Al^{tBu}: R = tBu; L = thf
Fe^{Me}: R = Me; L = thf
Fe^{tBu}: R = tBu; L = H_2O
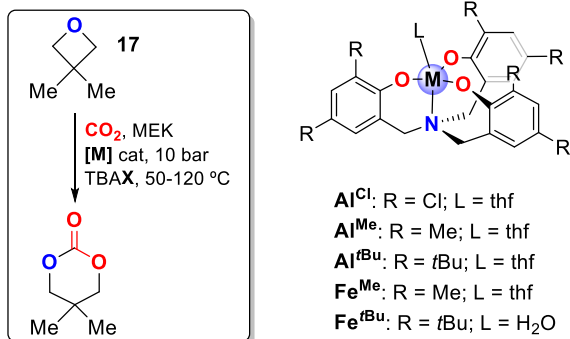
Entry	Cat. [mol%]	Co-cat [mol%]	T [ºC]	Yield [%][b,c]
1	–	TBAB (5.0)	75	<1
2	Al^{Cl} (2.5)	TBAB (5.0)	75	20
3	Al^{Me} (2.5)	TBAB (5.0)	75	37 (50)[d]
4	Al^{tBu} (2.5)	TBAB (5.0)	75	83 (94)[d]
5	Fe^{Me} (2.5)	TBAB (5.0)	75	25
6	Fe^{tBu} (2.5)	TBAB (5.0)	75	26
7	Al^{Cl} (2.5)	TBAI (5.0)	75	7 (10)[d]
8	Al^{Me} (2.5)	TBAI (5.0)	75	15 (34)[d]
9	Al^{tBu} (2.5)	TBAI (5.0)	75	51
10	Al^{tBu} (1.0)	TBAB (2.0)	75	27
11	Al^{tBu} (1.0)	TBAB (4.0)	75	38
12	Al^{tBu} (2.5)	TBAB (2.5)	75	71
13	Al^{tBu} (2.5)	TBAB (5.0)	50	<1
14	Al^{tBu} (2.5)	TBAB (5.0)	65	71
15	Al^{tBu} (2.5)	TBAB (5.0)	90	82
16	Al^{tBu} (2.5)	TBAB (5.0)	100	80
17	Al^{tBu} (2.5)	TBAB (5.0)	120	0[e]

[a] General conditions: 2 mmol substrate, $p(CO_2)$ = 10 bar, 18 h, MEK (1 mL) as solvent. [b] NMR yield based on the use of mesitylene as internal standard. [c] Selectivity for the cyclic carbonate in each case >98% as determined by ^{1}H NMR (CDCl$_3$). [d] In parenthesis the NMR yield after 60 h. [e] 70% conversion to polyether product was observed.

Chapter 3

Our first experiments were performed under relatively mild conditions (75 °C, 10 bar) using methylethyl ketone (MEK) as a solvent to favor the formation of the desired product (Table 9). MEK has a convenient boiling point and posseses the highest capacity to dissolve CO_2 in comparison to other hydroxy- and ketone-containing solvents.[100] Note that the sole use of TBAB (entry 1) gave only trace amounts of product, emphasizing the crucial role of the Lewis acid to obtain high yields. While the Al complexes bearing chloro or methyl substituents (**Al^{Cl}** and **Al^{Me}**) are excellent catalysts for the conversion of epoxides, they performed poorly in the coupling of oxetanes with CO_2. Interestingly, the complex containing bulky *tert*-butyl groups (**Al^{tBu}**) showed 83% yield under these conditions along with perfect selectivity towards the cyclic carbonate product. This result is ascribed to a lower stability of the oxetane-metal adduct due to a combination of increased steric hindrance and reduced Lewis acidic character, which ultimately leads to faster turnover.

Both Fe complexes (**Fe^{Me}** and **Fe^{tBu}**) showed inferior activity and gave much lower 6MCC yield under these conditions (Table 9, entries 5 and 6). Changing the anion in the ammonium salt (entries 7-9) from bromide to iodide had a pronounced negative effect on the observed yield, and the most optimal ratio between the best performing Al complex **Al^{tBu}** and the nucleophilic co-catalyst tetrabutylammonium bromide (TBAB) turned out to be 1 : 2 (entries 4 and 10-12).

Next, we turned our attention to the influence of the reaction temperature on the product distribution (cyclic versus polycarbonate) and the observed yield of the 6MCC target (entries 4 and 13-17). At 50 °C there is hardly any product formation, which is in line with the more difficult activation of oxetane substrates compared to oxiranes. Upon raising the temperature (entry 4), we found that 75 °C is optimal, with no further increase in yield observed beyond this temperature. At 120 °C, the only product that was observed was (presumably) a polyether as testified by the resonance observed around δ = 3.5 ppm in the ^{1}H NMR spectrum of the crude mixture. A longer reaction time improved the yield of the carbonate from 83 to 94%, while maintaining high chemoselectivity (entry 4). The optimal reaction conditions (75 °C, 10 bar, **Al^{tBu}** (2.5 mol%), TBAB (5 mol%), MEK as solvent) were then taken as starting point to investigate the scope of this catalytic process (Figure 12).

3.3.2 Scope of six-membered cyclic carbonates

We examined a series of oxetane substrates having different substitution patterns (Figure 12; R_1–R_3). As expected, the most simple 6MCC **31** (R_1 = R_2 = R_3 = H) could be

Chapter 3

easily produced in high yield (92 %). Oxetanes with various substitution patterns in the oxetane ring could also be conveniently converted into their 6MCCs.
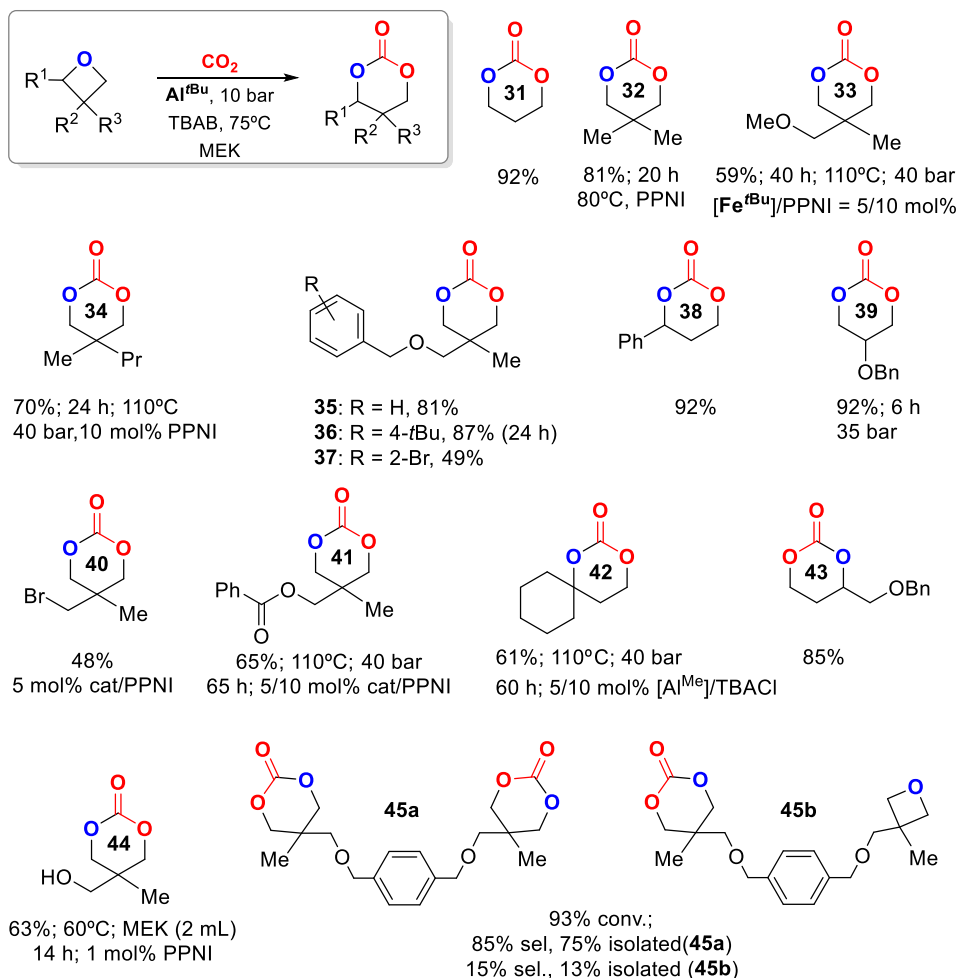

Figure 12. Scope of 6MCCs obtained through the coupling reactions of oxetanes with CO_2. Reaction conditions (unless stated otherwise): 75 ºC, 10 bar, 2.5 mol% Al^{tBu}, 5.0 mol% TBAB, 1 mL MEK, 18 h. TBACl=tetrabutylammonium chloride. In all cases the chemoselectivity for the 6MCC was >95% as determined by using ^1H NMR spectroscopy. Yields of the isolated product are reported.

Several (functional) groups were tolerated including ether (**33**, **35**-**37**, **39**, **43**, **45**), alkyl halide (**40**), aryl-bromide (**37**), and ester (**41**) groups. Of particular note are the syntheses of 6MCCs **38**, **42**, and **43** having the substitution in the 2-position of the oxetane ring: such 6MCCs have been seldom reported. Whereas **38** and **43** were isolated in high yield (92 and 85%) under mild conditions, for the sterically challenging

57

Chapter 3

substrate having a 2-cyclohexyl substituent (**27**), the catalytic protocol required sterically less demanding catalyst components (**Al^Me**, tetrabutylammonium chloride (TBACl) and harsher reaction conditions: 110 °C, 40 bar), which resulted in a reasonable yield for **42** (61 %). For some of the oxetane substrates, the use of PPNI as nucleophile in combination with higher reaction temperatures (80-110 °C) proved to be more productive. The formation of carbonate **33** could be best achieved with the Fe-based catalyst **Fe^tBu** giving 75% yield as determined by NMR spectroscopy (isolated in 59% yield) after 40 h.

Of further note is the formation of unprotected carbonate **44** (63%); previous literature describing this compound indicated the decomposition of this compound at elevated temperatures through intramolecular rearrangement.[101] We were pleased to find that the application of a moderate reaction temperature (60 °C) gave clean access to **44** in good selectivity (93% yield, as determined by NMR spectroscopy), with partial loss of product being ascribed to the isolation procedure. Significant diol formation can be observed in some cases during column chromatography in contrast to the 5-membered analogues that are more stable. Both bis- and monocarbonate products **45a** and **45b**, respectively, could be easily isolated, and under optimized conditions the yield for **45a** was 75%.
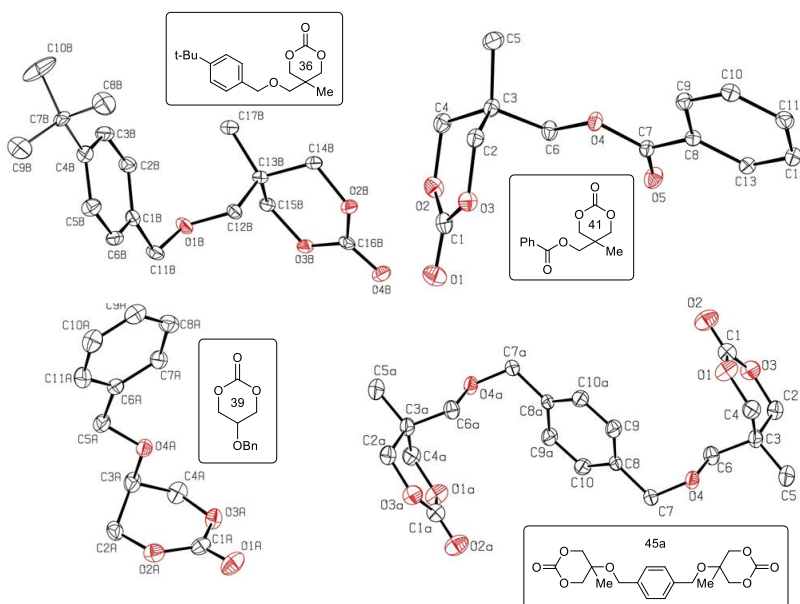
Figure 13. X-ray molecular structures determined for several 6MCCs.

Chapter 3

Biscarbonate **45a** is a potentially interesting candidate for ROP as two propagating polymer chains may be induced simultaneously having rigid interconnecting linkers. All 6MCCs were fully characterized (see Experimental) and the X-ray molecular structures for **36**, **39**, **41** and **45a** (Figure 13) have also been determined (see Experimental section for crystallographic details).

Particularly useful are the IR spectral features for the 6MCCs, because they provide diagnostic C=O absorption bands. Typically, the carbonyl stretching frequency is observed in the range 1720-1750 cm^{-1}, which is at much lower wavenumbers when compared to five-membered carbonates that usually show C=O stretching frequencies between 1770-1800 cm^{-1}.

3.3.3 Hydroxyl- and amino-substituted oxetanes

The use of oxetane precursors having pendent hydroxyl or amino substituents was then also studied in the context of 6MCC formation. First, we probed oxetane **46** (Figure 14) as a substrate and used the optimized conditions (75 °C, 10 bar, **Al^{tBu}**, TBAB, MEK, 18 h) from the previous substrate scope phase to study the formation of the 6MCC product **47**.
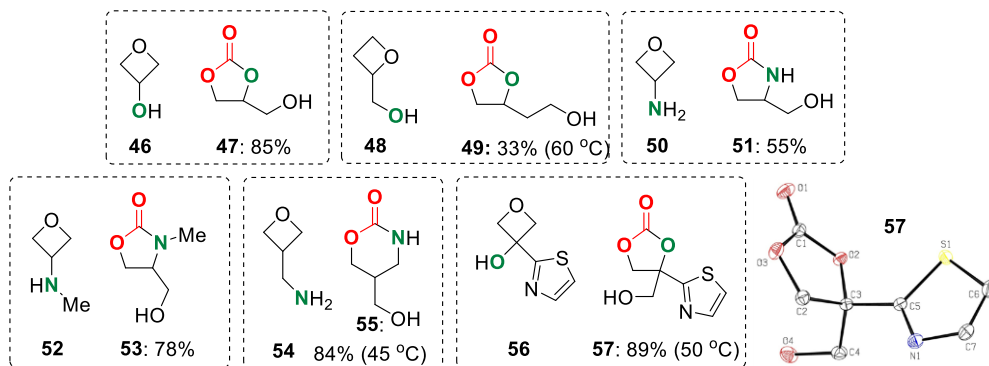
*Figure 14. Substrate scope using various amino- and hydroxy-substituted oxetanes in the coupling reactions with CO_2 affording organic carbonates/carbamates. Reaction conditions (unless stated otherwise): 25 °C, 10 bar, 2.5 mol% **Al^{tBu}**, 5.0 mol% TBAB, 1 mL MEK, 18 h. In all cases (except for **49**) the yield detected by NMR spectroscopy was >95%.*

Full conversion of **46** was observed in the ¹H NMR spectrum of the crude product, and the cyclic carbonate was isolated in 85% yield. Detailed NMR spectroscopic analysis, however, revealed that the five-membered carbonate **47** had been isolated and not the

Chapter 3

targeted 6MCC. Intrigued by this result, we then conducted a number of control experiments to explain this observation. Surprisingly, the reaction at 25 °C also proceeded smoothly with quantitative conversion (18 h) of **46** into **47**. Because the nucleophilic ring-opening of oxetanes in general takes place at somewhat elevated temperatures with a typical onset temperature of 50-60 °C, we then examined whether the addition of the bromide nucleophile was required for conversion of **46**. We found that formation of **47** takes place even in the absence of TBAB and under very mild conditions (25 °C, NMR yield 50 %, 18 h). Conversion does not occur in the absence of the complex **Al^{tBu}** however, stressing the imperative role of the Al complex. These results seem to indicate that the formation of the carbonate product **47** does not necessarily proceed through the established mechanism that involves nucleophilic ring-opening at the 2-position of the oxetane, but likely follows a different pathway. Instead, the formation of a carbonic acid intermediate was hypothesized through the activation of CO_2 by the alcohol group. A similar mechanism has been proposed by Minakata, who reported on the formation of highly functional organic carbonates and carbamates through the reaction of CO_2 with unsaturated alcohols[102] or amines[103] that were converted under very mild conditions using a stoichiometric amount of *t*BuOI as a reagent. These contributions nicely demonstrated that rather unstable and elusive carbonic acid intermediates can be conveniently trapped by the hypoiodite reagent mediating an intramolecular cyclization process that involves the unsaturated part of the substrate, and leading to five- or six-membered heterocycles.

Based on all observations we propose that five-membered carbonate **47** is formed through the formation of an intermediate carbonic acid that is stabilized/activated by the Al-complex **Al^{tBu}** acting thus as a bifunctional entity. The Al-center coordinates the linear carbonate fragment after initial reaction of **46** with CO_2, and the carbonic acid proton is abstracted by one of the phenolate anions of the aminotriphenolate ligand (Scheme 13). This allows for the linear carbonate to act as an internal nucleophile,[104] able to ring-open the oxetane after which the product (glycidol carbonate **47**) is formed. A similar mechanistic proposal has been reported by Murakami for the conversion of azetidinols to 5MCCs.[105]

Chapter 3
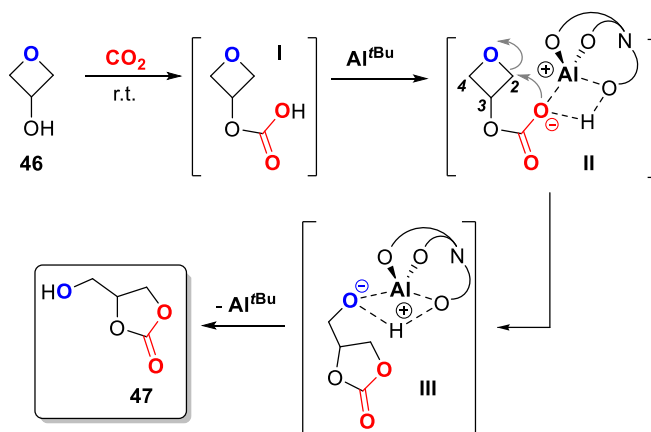
*Scheme 13. Proposed mechanism for the formation of carbonate **47** through intermediates I–III.*

Similar non-innocent ligand behavior in other Al^{III} complexes has been recently reviewed.[106] When the alcohol function in **46** is benzyl-protected (see the synthesis of **39**, Figure 12), a five-membered carbonate could not be detected, implying an important role for the unprotected alcohol function in the formation of **47** in line with the proposed mechanism in Scheme 13. Comparable observations were reported for benzyl-protected oxetane **28** in the synthesis of 6MCC **43**, see Figure 12. To further support the presence of a carbonic acid-derived intermediate, a series of hydroxyl/amino-terminated oxetanes (Figure 14) were then subjected to similar reaction conditions used to convert **46** into **47**. In all cases, the formation of the cyclic carbonate/carbamate products proceeded under very mild conditions (25-60 °C) with yields (as determined by NMR spectroscopy) exceeding 95% except for **48** (33%).

In the case where the intramolecular ring-closure first involved an attack on a tertiary carbon center (i.e., for the conversion of oxetane **48**) a slightly higher reaction temperature was required to obtain high conversion. Both amino- and hydroxy-terminated substrates showed similar behavior, giving rise to either cyclic carbonate or carbamate formation. The presence of a secondary amine function in oxetane **52** allowed for formation of the *N*-methyl oxazolidinone product at room temperature. The presence of another type of heteroatom in the oxetane structure allows for further differentiation between the proposed mechanism in Scheme 13 and the one that relates to conventional initial ring-opening of the oxetane followed by CO_2 insertion and ring-closing. Thus, the presence of the N-atom in the five- and six-membered ring systems of carbamates **51**, **53** and **55** is further testament that the hydroxyl- and amino-functionalized oxetanes first react with CO_2 to form intermediate carbonic or carbamic acid derivatives that activate the oxetane for ring-opening by an *in-situ* produced

Chapter 3

nucleophile. The structure for the five-membered, thiazole-based cyclic carbonate **57** (that would result from an intramolecular attack of a carbonic acid derivative) was confirmed by X-ray crystallography (Figure 14), in line with the proposed mechanism for the formation of these carbonates/carbamates.

A potential disadvantage of the presence of hydroxyl groups in the oxetane substrate is the formation of furan-based byproducts. This is for instance the case for **48** that upon combination with the binary catalyst and CO_2 gives as main product 3-hydroxy-trihydrofuran (**49***) instead of the desired cyclic carbonate (Scheme 14).
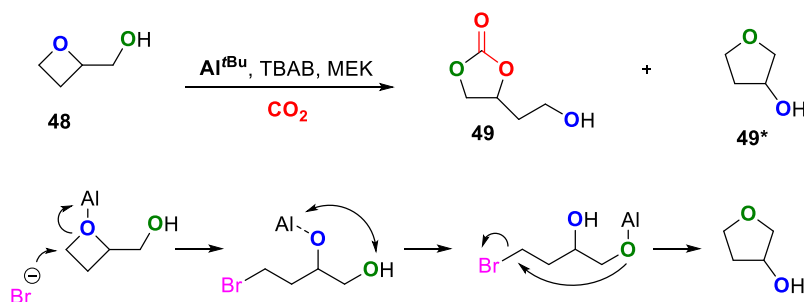
*Scheme 14. Proposed pathway for the formation of 3-hydroxy-trihydrofuran **49*** from oxetane **48**.*

After ring-opening of the oxetane and formation of an Al-alkoxide species, the aluminum complex can migrate to the adjacent alcohol group, which then may cyclize to a thermodynamically preferred five-membered furan without the involvement of CO_2. Theoretically, **49*** can also be formed from the cyclic carbonate **49** by an intramolecular attack of the pendant alcohol group followed by decarboxylation. However, control experiments showed that the product was quite stable under the reaction conditions with no conversion of **49** into **49*** at 60 °C and only 5% at 75 °C. To further support the mechanism shown in Scheme 14, the conversion of oxetane **48** was carried out in the absence of CO_2, which led to significant amounts of furan byproduct. These observations are in agreement with previous work from Loy *et al.* who reported the intramolecular opening of oxetanes containing hydroxy groups to form five- and six-membered hetereocycles.[104] A possible solution would be to lower the amount of co-catalyst used in the reaction, as the byproduct formation does not occur in the absence of nucleophile. However, the overall conversion is reduced drastically upon lowering the co-catalyst loading.

Chapter 3

3.3.4 One-pot oxetane to carbamate conversions

Further studies have led to the development of a one-pot three-component reaction (3CR) based on the oxetane-CO$_2$ coupling described in this chapter. This 3CR combines the coupling of oxetanes and CO$_2$ yielding 6MCCs with *in-situ* aminolysis of the latter, resulting in the formation of functionalized linear carbamates (Scheme 15).[107]
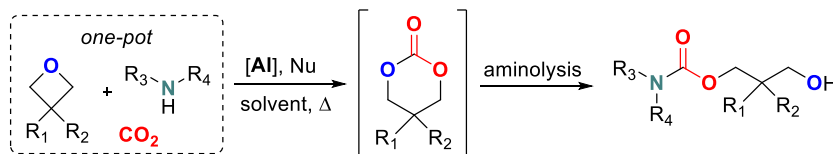
Scheme 15. Catalytic one-pot, modular approach towards oxetane-based carbamates.

By varying both the substituents on the oxetane and amine, a wide variety of linear carbamates could be obtained using this method. Good yields were obtained in most cases, however for some substrates a one-pot sequential approach was required (forming first in high conversion the carbonate intermediate before the aminolysis step). Catalyst inhibition may occur by coordination of the amine to the metal center or byproducts can be obtained by direct ring-opening of the oxetane by an amine as noted for some of the studied examples.

To expand the scope, the methodology was applied to the formal synthesis of two carbamate based drug percursors Carisoprodol and Felbatol. Both target molecules could be synthesized via a three step procedure starting from commercially available diols. Subsequent carbamate formation followed by treatment with trichloroacetyl isocyanate gives the final product Carisoprodol **58** in good yield (Scheme 16).
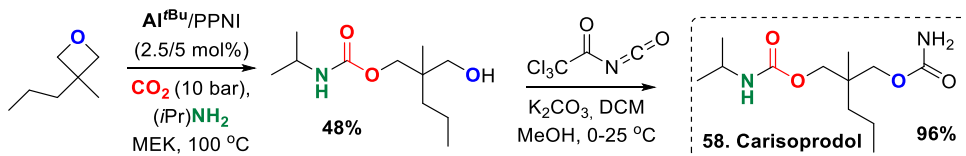
Scheme 16. Formal synthesis of Carisoprodol using in the key step the Al-catalyzed carbamate formation from an oxetane, amine and CO$_2$.

Chapter 3

3.4 Conclusion

We here present the first general and selective catalytic methodology for the efficient coupling of oxetanes and CO_2 giving a range of functional 6MCCs in fair to good yields. This method is further characterized by the use of catalysts based on cheap, abundant, and non-toxic metal complexes showing unparalleled reactivity with high potential in the preparation of 6MCCs that are of use in synthetic and polymer chemistry. The general methodology established in this chapter has been applied to the one-pot conversion of oxetanes to carbamates, leading to the formal synthesis of two drug molecules.

To further expand on the substrate scope and molecular complexity, it would be interesting to test the potential of the developed catalytic system in the conversion of tri- and tetra-substituted oxetanes. Highly subsituted substrates can, for instance, be obtained through the light induced Paternó-Büchi reaction or by intramolecular Michael addition of vinylogous urethane derivatives.

Furthermore, the first CO_2/oxetane couplings at ambient temperature conditions are reported herein with a crucial role for an intermediate carbonic acid derivative. A wide range of hydroxy-substituted oxetanes can be accessed through combination of Grignard reagents with 3-oxetanone, which is a common oxetane precursor. This alternative method for cyclic carbonate formation thus shows great potential in the synthesis of complex carbonate and carbamate products, as it proceeds readily under exceptionally mild conditions.

3.5 Experimental

3.5.1 General comments

Both the ligands[77] and metal catalysts[44] (Table 9) were prepared according to previously reported procedures. ^1H and ^{13}C NMR spectra were recorded on a Bruker AV-300, AV-400, or AV-500 spectrometer. Mass spectrometric analysis and X-ray diffraction studies were performed by the Research Support Group at the ICIQ. Carbon dioxide was purchased from PRAXAIR and used without further purification. Solvents used in the synthesis of the complexes were dried using an Innovative Technology PURE SOLV solvent purification system.

Chapter 3

3.5.2 Preparation of oxetanes

Oxetanes **16**, **17**, **29**, **46**, **48**, **50**, **52**, **54** and **56** are commercially available and were used as received. Oxetanes **18**[87b] and **19**[96] were prepared according to previously reported procedures.

Oxetanes **20**,[87b] **23**,[98] **27**,[98] and **25**[108] were prepared according to modified literature procedures. Oxetanes **21**, **22**, **24**, **28**, and **30** were prepared in a similar way as oxetane **20**.

3-Benzyloxymethyl-3-methyloxetane (20):
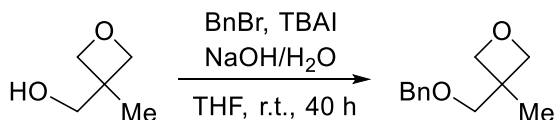
To a solution of 3-methyl-3-oxetane-methanol (1.020 g, 10.0 mmol) and benzyl bromide (2.050 g, 12.0 mmol, 1.2 equiv.) in THF (10 mL) was added tetrabutylammonium iodide (0.555 g, 1.5 mmol, 0.15 equiv.) and NaOH/H$_2$O (3.0 g NaOH in 3.0 g H$_2$O) and the mixture was stirred for 40 h at rt. The product was extracted with DCM and the organic layer was concentrated under vacuum. The product was obtained by column chromatography (EtOAc:Hexane 1:8) as a colorless liquid in 89% yield (1.710 g, 8.90 mmol). **^{1}H NMR** (500 MHz, CDCl$_3$) δ 7.37 (s, 5H), 4.61 (s, 2H), 4.56 (d, J = 5.8 Hz, 2H), 4.39 (d, J = 5.8 Hz, 2H), 3.55 (s, 2H), 1.37 (s, 3H). **^{13}C NMR** (75 MHz, CDCl$_3$) δ 138.30, 128.41, 127.65, 127.57, 80.20, 75.39, 73.37, 39.89, 21.43.

3-(4-*t*Bu-benzyl)oxymethyl-3-methyloxetane (21):
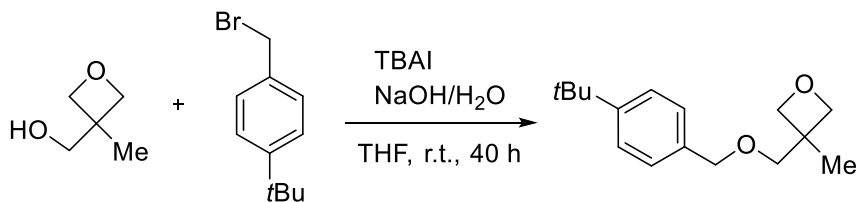
To a solution of 3-methyl-3-oxetane-methanol (0.408 g, 4.0 mmol) and 4-*tert*-butylbenzyl bromide (1.090 g, 4.8 mmol, 1.2 equiv.) in THF (5 mL) was added tetrabutylammonium iodide (222 mg, 0.6 mmol, 0.3 mmol) and NaOH/H$_2$O (1.2 g NaOH in 1.2 g H$_2$O) and stirred for 40 h at rt. The product was extracted with DCM and the organic layer was concentrated under vacuum. The product was obtained by column chromatography (EtOAc:Hexane 1:10) as a colorless liquid in 93% yield (0.924 g, 3.72

Chapter 3

mmol). **¹H NMR** (500 MHz, CDCl₃) δ 7.44 (d, J = 8.3 Hz, 2H), 7.34 (d, J = 8.3 Hz, 2H), 4.61 (s, 2H), 4.59 (d, J = 5.7 Hz, 2H), 4.42 (d, J = 5.7 Hz, 2H), 3.59 (s, 2H), 1.40 (s, 3H), 1.40 (s, 9H). **¹³C NMR** (126 MHz, CDCl₃) δ 150.58, 135.34, 127.45, 125.34, 80.20, 75.43, 73.23, 39.94, 34.58, 31.45, 21.50. **HRMS** (ESI+): calcd. m/z 271.1669 [M+Na]⁺; found: 271.1665.

3-(2-bromobenzyl)oxymethyl-3-methyloxetane (22):
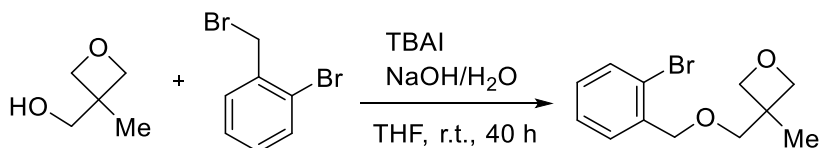
To a solution of 3-methyl-3-oxetane-methanol (0.408 g, 4.0 mmol) and 2-bromobenzyl bromide (1.200 g, 4.8 mmol, 1.2 equiv.) in THF (5 mL) was added tetrabutylammonium iodide (0.222 g, 0.6 mmol, 0.3 mmol) and NaOH/H₂O (1.2 g NaOH in 1.2 g H₂O) and stirred for 40 h at rt. The product was extracted with DCM and the organic layer was concentrated under vacuum. The product was obtained by column chromatography (EtOAc:Hexane 1:8) as a colorless liquid in 81% yield (0.877 g, 3.23 mmol). **¹H NMR** (500 MHz, CDCl₃) δ 7.57 (m, 1H), 7.50 (m, 1H), 7.35 (m, 1H), 7.18 (m, 1H), 4.65 (s, 2H), 4.60 (d, J = 5.8 Hz, 2H), 4.42 (d, J = 5.8 Hz, 2H), 3.65 (s, 2H), 1.39 (s, 3H). **¹³C NMR** (126 MHz, CDCl₃) δ 137.58, 132.54, 129.03, 128.95, 127.39, 122.68, 80.14, 75.96, 72.66, 39.98, 21.47. **HRMS** (ESI+): calcd. m/z 293.0148 [M+Na]⁺; found: 293.0154.

2-phenyloxetane (23):
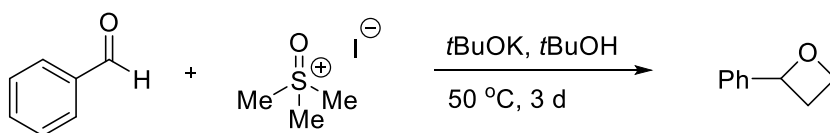
To a stirred solution of trimethylsulfoxonium iodide (8.800 g, 40.0 mmol, 4 equiv.) in *tert*-butanol (65 mL) at 50 °C, was added potassium *tert*-butoxide (4.480 g, 40.0 mmol, 4 equiv.). After 30 minutes, a solution of benzaldehyde (1.060 g, 10.0 mmol) in *tert*-butanol (10 mL) was added and the reaction was further stirred at 50 °C for 3 days. The solvent was then evaporated and water was added to the residue, the crude product was extracted with hexane. The product was purified by column chromatography (Et₂O:Hexane 1:10) as a colorless liquid in 54% yield (0.730 g, 5.4 mmol). **¹H NMR** (400 MHz, CDCl₃) δ 7.51 – 7.28 (m, 5H), 5.84 (t, J = 7.5 Hz, 1H), 4.86 (m, 1H), 4.69 (m, 1H), 3.13 – 2.97 (m, 1H), 2.70 (m, 1H). **¹³C NMR** (126 MHz, CDCl₃) δ 143.54, 128.48, 127.80, 125.21, 82.92, 68.24, 30.71.

Chapter 3

3-(benzyloxy)oxetane (24):
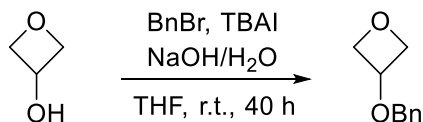
To a solution of 3-hydroxyoxetane (0.592 g, 8.0 mmol) and benzyl bromide (1.640 g, 9.6 mmol, 1.2 equiv.) in THF (10 mL) was added tetrabutylammonium iodide (0.444 g, 1.2 mmol, 0.15 equiv.) and NaOH/H_2O (2.4 g NaOH in 2.4 g H_2O) and stirred for 40 h at rt. The product was extracted with DCM and the organic layer was concentrated under vacuum. The product was obtained by column chromatography (EtOAc:Hexane 1:8) as a colorless liquid in 99% yield (1.310 g, 7.98 mmol). **^{1}H NMR** (500 MHz, Acetone-d_6) δ 7.51 − 7.20 (m, 5H), 4.67 (m, 3H), 4.48 (m, 4H). **^{13}C NMR** (126 MHz, Acetone-d_6) δ 138.23, 128.26, 127.82, 127.60, 77.97, 72.02, 70.48.

3-Methyl-3-(bromomethyl)oxetane (25):
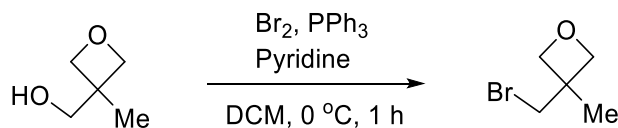
To a stirred solution of 3-methyl-3-oxetane-methanol (1.020 g, 10.0 mmol), triphenylphosphine (3.15 g, 12.0 mmol, 1.2 equiv.) and pyridine (1.90 g, 1.94 mL, 24.0 mmol, 2.4 equiv.) in DCM (20 mL) at 0 °C was added bromine (1.60 g, 0.52 mL,10.0 mmol, 1 equiv.) in DCM (5.0 mL). The ice bath was removed after addition of the bromine and the resulting solution was stirred for 1 h at rt. The solvent was then evaporated, followed by addition of diethyl ether (30 mL) and filtration through Celite. An additional filtration over silica with ether/hexane (1:1) was performed to remove traces of triphenylphosphine oxide. The product was obtained as a colorless liquid in 55% yield (0.900 g, 5.5 mmol). **^{1}H NMR** (500 MHz, CDCl$_3$) δ 4.48 (d, J = 6.1 Hz, 2H), 4.43 (d, J = 6.1 Hz, 2H), 3.67 (s, 2H), 1.46 (s, 3H). **^{13}C NMR** (126 MHz, CDCl$_3$) δ 80.64, 41.39, 40.64, 22.45.

Chapter 3

(3-methyloxetan-3-yl)methyl benzoate (26):
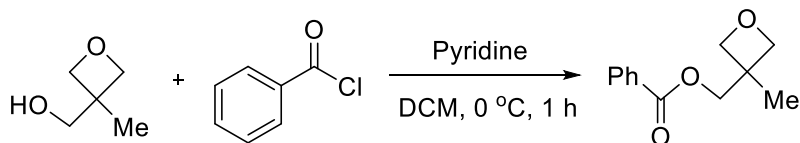
To a stirred solution of 3-methyl-3-oxetane-methanol (1.02 g, 10.0 mmol) and pyridine (0.79 g, 0.81 mL, 10.0 mmol, 1 equiv.) in anhydrous DCM at 0 °C was added benzoyl chloride (1.41 g, 1.16 mL, 10.0 mmol, 1 equiv.). The ice bath was removed after the addition of benzoyl chloride and the reaction mixture was stirred for 1 h at rt. The solvent was removed under vacuum to obtain the crude product which was purified by column chromatography (EtOAc:Hexane 1:16-1:8) to give the product as a colorless liquid in 78% yield (1.60 g, 7.8 mmol). **^{1}H NMR** (500 MHz, CDCl$_3$) δ 8.12 – 8.06 (m, 2H), 7.63 – 7.57 (m, 1H), 7.48 (m, 2H), 4.67 (d, J = 6.0 Hz, 2H), 4.49 (d, J = 6.0 Hz, 2H), 4.42 (s, 2H), 1.46 (s, 3H). **^{13}C NMR** (126 MHz, CDCl$_3$) δ 166.54, 133.18, 129.90, 129.63, 128.47, 79.63, 69.02, 39.34, 21.30. **HRMS** (ESI+): calcd. m/z 229.0835 [M+Na]$^+$; found: 229.0825.

2-cyclohexyl oxetane (27):
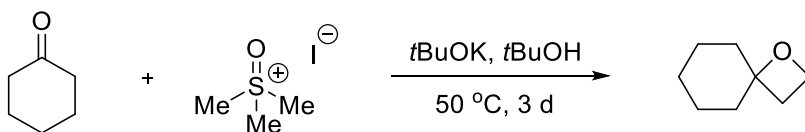
To a stirred solution of trimethylsulfoxonium iodide (8.80 g, 40.0 mmol, 4 equiv.) in *tert*-butanol (65 mL) at 50 °C, was added potassium *tert*-butoxide (4.48 g, 40.0 mmol, 4 equiv.). After 30 minutes a solution of cyclohexanone (0.980 g, 10.0 mmol) in *tert*-butanol (10 mL) was added and the reaction mixture was further stirred at 50 °C for 3 days. The solvent was evaporated after the reaction and water was added to the residue, the product was extracted with hexane. After concentration of the organic phase, the product was obtained as a slightly yellow liquid in 76% yield (0.730 g, 5.4 mmol). **^{1}H NMR** (500 MHz, CDCl$_3$) δ 4.51 (t, J = 7.8 Hz, 2H), 2.34 (t, J = 7.8 Hz, 2H), 1.90 – 1.81 (m, 2H), 1.76 – 1.61 (m, 4H), 1.36 (m, 4H). **^{13}C NMR** (126 MHz, CDCl$_3$) δ 86.53, 64.74, 38.63, 32.39, 25.08, 22.46.

Chapter 3

2-((benzyloxy)methyl)oxetane (28):
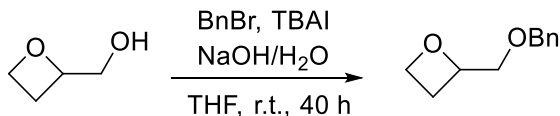
To a solution of 2-oxetane-methanol (0.352 g, 4.0 mmol) and benzyl bromide (821 mg, 4.8 mmol, 1.2 equiv.) in THF (10 mL) was added tetrabutylammonium iodide (0.222 g, 0.6 mmol, 0.15 equiv.) and NaOH/H_2O (1.2 g NaOH in 1.2 g H_2O) and the mixture stirred for 40 h at rt. The crude product was extracted with DCM and the organic layer was concentrated under vacuum. The pure product was obtained by column chromatography (EtOAc:Hexane 1:8-1:2) as a colorless liquid in 97% yield (0.688 g, 3.86 mmol). **¹H NMR** (400 MHz, Acetone-d_6) δ 7.45 – 7.22 (m, 5H), 4.94 – 4.85 (m, 1H), 4.61 (m, 2H), 4.58 – 4.44 (m, 2H), 3.70 – 3.56 (m, 2H), 2.71 – 2.47 (m, 2H). **¹³C NMR** (75 MHz, Acetone-d_6) δ 138.96, 128.16, 127.39, 127.27, 80.74, 73.72, 72.83, 67.80, 23.56. **HRMS** (ESI+): calcd. *m/z* 201.0886 [M+Na]⁺; found: 201.0893.

1,4-bis(((3-methyloxetan-3-yl)methoxy)methyl)benzene (30):
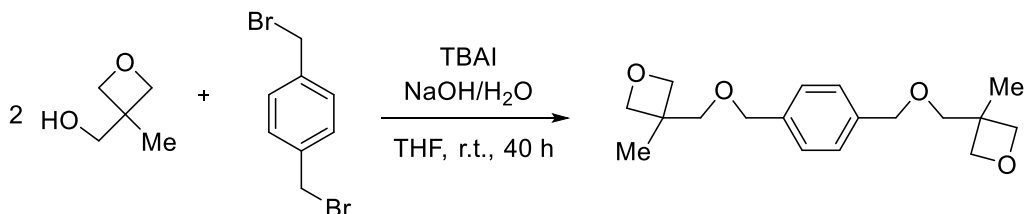
To a solution of 3-methyl-3-oxetane-methanol (2.150 g, 21.0 mmol, 1.05 equiv) and 1,4-bis(bromomethyl)benzene (2.64 g, 10.0 mmol) in THF (5 mL) was added tetrabutylammonium iodide (0.555 g, 1.5 mmol, 0.3 mmol) and NaOH/H_2O (6.0 g NaOH in 6.0 g H_2O) and the mixture stirred for 40 h at rt. The product was extracted with DCM and the organic layer was concentrated under vacuum. The product was obtained by column chromatography (Acetone:Hexane 1:5) as a slightly yellow liquid in 83% yield (2.65 g, 8.35 mmol). **¹H NMR** (400 MHz, CDCl₃) δ 7.33 (s, 4H), 4.57 (s, 4H), 4.53 (d, *J* = 5.8 Hz, 4H), 4.36 (d, *J* = 5.8 Hz, 4H), 3.52 (s, 4H), 1.33 (s, 6H). **¹³C NMR** (101 MHz, CDCl₃) δ 137.74, 127.63, 80.10, 75.39, 73.10, 39.87, 21.42. **HRMS** (ESI+): calcd. *m/z* 329.1723 [M+Na]⁺; found: 329.1726.

Chapter 3

3.5.3   Typical catalytic coupling between substituted oxetanes and CO_2

The respective oxetane, Al-complex, co-catalyst, and MEK (1 mL) were charged into a 30 mL stainless steel autoclave. The autoclave was then subjected to three cycles of pressurization and depressurization with carbon dioxide (5 bar), before final stabilization of the pressure to 10 bar. The autoclave was sealed and heated to the required temperature and left stirring. At the end of the reaction an aliquot of the resulting mixture was taken and the conversion/yield determined by means of ^{1}H NMR spectroscopy using $CDCl_3$ as the solvent and mesitylene as internal standard. The pure cyclic carbonate product was then isolated by column chromatography and the solvent removed under vacuum. The identities of the cyclic carbonate products were confirmed by comparison to literature data or where unavailable, characterized by ^{1}H/^{13}C NMR spectroscopy, IR, and HRMS. In the case of the carbonates **36**, **39**, **41**, **45a**, and **57**, the molecular structures were further supported by X-ray diffraction studies.

3.5.4   Catalytic and analytical details for the cyclic carbonate structures

1,3-Dioxan-2-one (31):
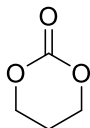
Conditions: **Al^{tBu}** (2.5 mol%), TBAB (5 mol %), 75 °C, 10 bar, 18 h; conversion: 99%. Isolated by column chromatography (EtOAc/hexane 1:8 to 1:1 v/v) in 92% yield. **^{1}H NMR** (300 MHz, $CDCl_3$): δ = 4.40 (t, J = 5.7 Hz, 4H), 2.02–2.19 (m, 2H); **^{13}C NMR** (75 MHz, $CDCl_3$): δ = 148.60, 68.07, 21.65; **IR** (neat): 1725 cm^{-1} (C=O).

5,5-dimethyl-1,3-dioxan-2-one (32):
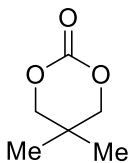
Conditions: **Al^{tBu}** (2.5 mol%), PPNI (2.5 mol%), 75 °C, 10 bar, 20 h; conversion: 96%. Isolated by column chromatography (EtOAc:hexane 1:2 to 1:1 v/v) in 81% yield. **^{1}H NMR** (400 MHz, $CDCl_3$): δ = 4.09 (s, 4H), 1.14 (s, 6H); **^{13}C NMR** (75 MHz, $CDCl_3$): δ = 148.11, 77.49, 28.45, 21.12; **IR** (neat): 1736 cm^{-1} (C=O).

Chapter 3

**5-(methoxymethyl)-5-methyl-1,3-dioxan-2-one (33):**
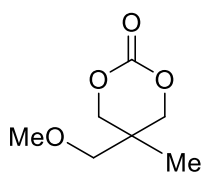
Conditions: **Fe^{tBu}** (5 mol%), PPNI (10 mol%), 110 °C, 40 bar, 40 h; conversion: 75%. Isolated by column chromatography (EtOAc:hexane 1:4 v/v) in 59% yield. **^{1}H NMR** (400 MHz, Acetone-d_6): δ = 4.32 (d, J = 10.6 Hz, 2H), 4.18 (d, J = 10.6 Hz, 2H), 3.39 (s, 2H), 3.36 (s, 3H), 1.08 (s, 3H); **^{13}C NMR** (126 MHz, Acetone-d_6): δ = 147.41, 73.63, 73.43, 58.62, 32.65, 16.23; **IR** (neat): 1742 cm^{-1} (C=O).

5-methyl-5-propyl-1,3-dioxan-2-one (34):
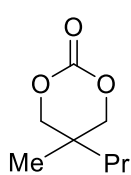
Conditions: **Al^{tBu}** (2.5 mol%), PPNI (10 mol%), 110 °C, 40 bar, 24 h; conversion: 73%. Isolated by column chromatography (EtOAc:hexane 1:1 v/v) in 70% yield. **^{1}H NMR** (400 MHz, CDCl$_3$): δ = 4.15 (d, J = 10.6 Hz, 2H), 4.07 (d, J = 10.6 Hz, 2H), 1.31-1.47 (m, 4H), 1.09 (s, 3H), 0.97 (t, J = 6.9 Hz, 3H); **^{13}C NMR** (75 MHz, CDCl$_3$): δ = 148.34, 77.46, 77.03, 76.61, 76.47, 36.40, 31.13, 18.33, 16.49, 14.54; **IR** (neat): 1743 cm^{-1} (C=O).

5-((benzyloxy)methyl)-5-methyl-1,3-dioxan-2-one (35):
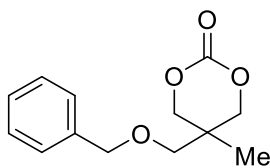
Conditions: **Al^{tBu}** (2.5 mol%), TBAB (5 mol%), 75 °C, 10 bar, 24 h; conversion: 99%. Isolated by column chromatography (EtOAc:hexane 1:8 to 1:1 v/v) in 92% yield. **^{1}H NMR** (400 MHz, CDCl$_3$): δ = 7.29-7.42 (m, 5H), 4.55 (s, 2H), 4.38 (d, J = 10.8 Hz, 2H), 4.10 (d, J = 10.8 Hz, 2H), 3.43 (s, 2H), 1.12 (s, 3H); **^{13}C NMR** (101 MHz, CDCl$_3$): δ = 148.25, 137.46, 128.53, 127.96, 127.59, 73.95, 73.59, 71.10, 33.03, 17.43; **IR** (neat): 1743 cm^{-1} (C=O); **HRMS** (ESI+): calcd. for C$_{13}$H$_{16}$O$_4$: m/z 259.0946 [M+Na]$^+$; found: 259.0932.

5-(((4-(*tert*-butyl)benzyl)oxy)methyl)-5-methyl-1,3-dioxan-2-one (36):
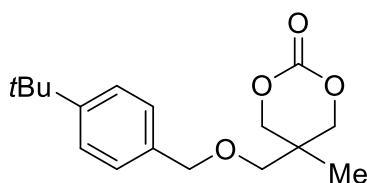
Conditions: **Al^{tBu}** (2.5 mol%), TBAB (5 mol%), 75 °C, 10 bar, 24 h; conversion: 93%. Isolated by column chromatography (EtOAc:hexane 1:4 to 1:1 v/v) in 87% yield. **^{1}H NMR** (500 MHz, CDCl$_3$): δ = 7.41 (d, J = 8.3 Hz, 2H), 7.26 (d, J = 8.3 Hz, 2H), 4.52 (s, 2H), 4.38 (d, J = 10.9 Hz, 2H), 4.10 (d, J = 10.8 Hz, 2H), 3.43 (s, 2H), 1.35 (s, 9H), 1.13 (s, 3H); **^{13}C NMR** (126 MHz, CDCl$_3$): δ = 150.91, 148.32, 134.52, 127.41,

Chapter 3

125.42, 74.01, 73.41, 71.16, 34.58, 33.03, 31.38, 17.43; **IR** (neat): 1771 cm^{-1} (C=O); **HRMS** (ESI+): calcd. for $C_{17}H_{24}O_4$: *m/z* 315.1572 [M+Na]$^+$; found: 315.1561.
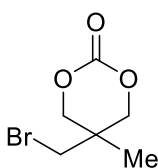
5-(((2-bromobenzyl)oxy)methyl)-5-methyl-1,3-dioxan-2-one (37):
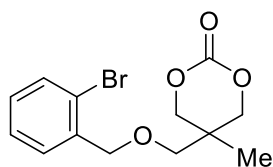
Conditions: **Al^{tBu}** (2.5 mol%), TBAB (5 mol%), 75 °C, 10 bar, 24 h; conversion: 53%. Isolated by column chromatography (EtOAc:hexane 1:4 to 1:2 v/v) in 49% yield. **^{1}H NMR** (400 MHz, CDCl$_3$): δ = 7.58 (m, 1H), 7.41 (m, 1H), 7.35 (m, 1H), 7.20 (m, 1H), 4.61 (s, 2H), 4.42 (d, *J* = 10.9 Hz, 2H), 4.13 (d, *J* = 10.9 Hz, 2H), 3.53 (s, 2H), 1.16 (s, 3H); **^{13}C NMR** (101 MHz, CDCl$_3$): δ = 148.16, 136.67, 132.77, 129.40, 129.27, 127.48, 123.06, 73.92, 72.98, 71.61, 33.13, 17.50; **IR** (neat): 1740 cm^{-1} (C=O); **HRMS** (ESI+): calcd. for $C_{13}H_{15}BrO_4$: *m/z* 337.0051 [M+Na]$^+$; found: 337.0049.

4-phenyl-1,3-dioxan-2-one (38):
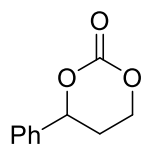
Conditions: **Al^{tBu}** (2.5 mol%), TBAB (5 mol%), 75 °C, 10 bar, 18 h; conversion: 96%. Isolated by column chromatography (EtOAc:hexane 1:2 to 1:1 v/v) in 92% yield. **^{1}H NMR** (500 MHz, Acetone-d_6): δ = 7.38-7.50 (m, 5H), 5.69 (m, 1H), 4.63 (m, 1H), 4.49 (m, 1H), 2.45 (m, 1H), 2.26-2.36 (m, 1H); **^{13}C NMR** (126 MHz, Acetone-d_6): δ = 148.42, 139.59, 129.06, 128.95, 126.30, 80.36, 67.49; **IR** (neat): 1742 cm^{-1} (C=O); **HRMS** (ESI+): calcd. for $C_{10}H_{10}O_3$: *m/z* 201.0528 [M+Na]$^+$; found: 201.0522.

5-(benzyloxy)-1,3-dioxan-2-one (39):
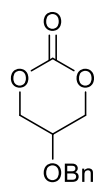
Conditions: **Al^{tBu}** (2.5 mol%), TBAB (5 mol%), 75 °C, 35 bar, 6 h; conversion: 99%. Isolated by column chromatography (EtOAc:hexane 1:4 to 1:1) in 92% yield. **^{1}H NMR** (400 MHz, Acetone-d_6): δ = 7.29-7.46 (m, 5H), 4.74 (s, 2H), 4.65 (d, *J* = 11.2 Hz, 2H), 4.55 (d, *J* = 11.4 Hz, 2H), 4.12 (m, 1H); **^{13}C NMR** (101 MHz, Acetone-d_6): δ = 147.21, 137.98, 128.31, 127.64, 70.02, 69.66, 66.79; **IR** (neat): 1731 cm^{-1} (C=O); **HRMS** (ESI+): calcd. for $C_{11}H_{12}O_4$: *m/z* 231.0633 [M+Na]$^+$; found: 231.0633.

Chapter 3

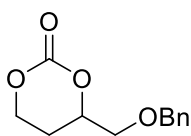**5-(bromomethyl)-5-methyl-1,3-dioxan-2-one (40):**

Conditions: **Al^{tBu}** (5 mol%), PPNI (5 mol%), 75 °C, 10 bar, 18 h; conversion: 55%. Isolated by column chromatography (EtOAc:hexane 1:2 to 1:1 v/v) in 48% yield. **^{1}H NMR** (500 MHz, CDCl$_3$): δ = 4.37 (d, J = 11.0 Hz, 2H), 4.24 (d, J = 11.0 Hz, 2H), 3.48 (s, 2H), 1.23 (s, 3H); **^{13}C NMR** (126 MHz, CDCl$_3$): δ = 147.42, 74.22, 35.48, 32.72, 18.56; **IR** (neat): 1722 cm^{-1} (C=O); **HRMS** (ESI+): calcd. for C$_6$H$_9$BrO$_3$: m/z 230.9633 [M+Na]$^+$; found: 230.9628.

5-Methyl-5-benzoyloxymethyl-1,3-dioxan-2-one (41):
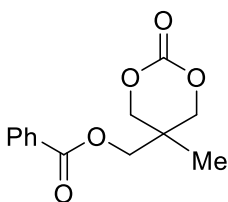
Conditions: **Al^{tBu}** (5 mol%), PPNI (10 mol%), 110 °C, 40 bar, 65 h; conversion: 80%. Isolated by column chromatography (EtOAc:hexane 1:2 to 1:1 v/v) in 65% yield. **^{1}H NMR** (400 MHz, CDCl$_3$): δ = 8.04 (m, 2H), 7.63 (m, 1H), 7.50 (m, 2H), 4.45 (d, J = 11.1 Hz, 2H), 4.37 (s, 2H), 4.25 (d, J = 11.0 Hz, 2H), 1.25 (s, 3H); **^{13}C NMR** (101 MHz, CDCl$_3$): δ = 165.96, 147.65, 133.61, 129.62, 129.12, 128.64, 73.68, 65.52, 32.60, 17.41; **IR** (neat): 1727, 1718 cm^{-1} (C=O); **HRMS** (ESI+): calcd. for C$_{13}$H$_{14}$O$_5$: m/z 273.0739 [M+Na]$^+$; found: 273.0739.

1,3-Dioxaspiro[5.5]undecan-2-one (42):
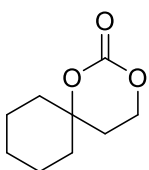
Conditions: **Al^{Me}** (5 mol%), TBACl (10 mol%), 110 °C, 40 bar, 60 h; conversion: 72%. Isolated by column chromatography (EtOAc:hexane 1:3) in 61% yield. **^{1}H NMR** (500 MHz, CDCl$_3$): δ = 4.39-4.44 (t, J = 6.0 Hz, 2H), 2.00 (t, J = 6.0 Hz, 2H), 1.88-1.96 (m, 2H), 1.76-1.86 (m, 2H), 1.61 (m, 2H), 1.52 (m, 2H), 1.24-1.46 (m, 2H); **^{13}C NMR** (126 MHz, CDCl$_3$): δ = 149.27, 82.52, 64.11, 36.59, 31.53, 25.09, 21.54; **IR** (neat): 1731 cm^{-1} (C=O); **HRMS** (ESI+): calcd. for C$_9$H$_{14}$O$_3$: m/z 193.0841 [M+Na]$^+$; found: 193.0833.

**4-((benzyloxy)methyl)-1,3-dioxan-2-one (43):**

Conditions: **Al^{tBu}** (2.5 mol%), TBAB (5 mol%), 75 °C, 10 bar, 18 h; conversion: 99%. Isolated by column chromatography (EtOAc:hexane 1:2 to 1:1 v/v) in 85% yield. **^{1}H NMR** (300 MHz, Acetone-d_6): δ = 7.27-7.42 (m, 5H), 4.71-4.82 (m, 1H), 4.61 (s, 2H), 4.46 (m, 2H), 3.70 (d, J = 4.6 Hz, 2H), 2.09-2.23 (m, 2H); **^{13}C NMR** (75 MHz, Acetone-d_6): δ = 148.02, 138.36, 128.24, 127.51, 127.49, 77.82, 72.91, 71.20, 66.61, 23.58; **IR** (neat):

Chapter 3

1737 cm^{-1} (C=O); **HRMS** (ESI+): calcd. for $C_{12}H_{14}O_4$: *m/z* 245.0790 [M+Na]$^+$; found: 245.0793.

**5-(hydroxymethyl)-5-methyl-1,3-dioxan-2-one (44):**
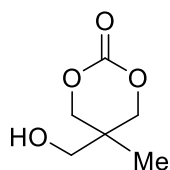
Conditions: **Al^{tBu}** (2.5 mol%), PPNI (1 mol%), 60 °C, 10 bar, 2 mL MEK, 18 h; conversion: 87%. Isolated by column chromatography using neutral alumina (EtOAc:hexane 1:1) in 63% yield. **^{1}H NMR** (400 MHz, CDCl$_3$): δ = 4.37 (d, *J* = 10.9 Hz, 2H), 4.13 (d, *J* = 10.8 Hz, 2H), 3.65 (d, *J* = 4.9 Hz, 2H), 2.89 (t, *J* = 5.1 Hz, 1H), 1.08 (s, 3H); **^{13}C NMR** (101 MHz, CDCl$_3$): δ = 148.94, 73.83, 63.61, 33.54, 16.72; **IR** (neat): 1721 cm^{-1} (C=O).

5,5'-(((1,4-phenylenebis(methylene))-bis(oxy))bis(methylene))-bis(5-methyl-1,3-dioxan-2-one) (45a):
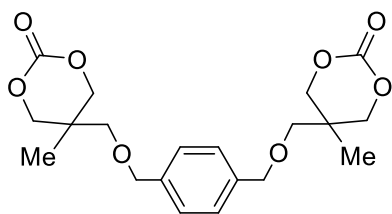
Conditions: **Al^{tBu}** (2.5 mol%), TBAB (5 mol%), 75 °C, 10 bar, 24 h; conversion: 93%, selectivity towards dicarbonate: 85%. Isolated by column chromatography (EtOAc:hexane 1:2 to 1:1 v/v) in 75% yield. **^{1}H NMR** (400 MHz, CDCl$_3$): δ = 7.31 (s, 4H), 4.55 (s, 4H), 4.37 (d, *J* = 10.8 Hz, 4H), 4.11 (d, *J* = 10.8 Hz, 4H), 3.43 (s, 4H), 1.13 (s, 6H); **^{13}C NMR** (126 MHz, CDCl$_3$): δ = 148.17, 137.23, 127.79, 73.89, 73.25, 71.02, 33.02, 17.40; **IR** (neat): 1755 cm^{-1} (C=O); **HRMS** (ESI+): calcd. for $C_{20}H_{26}O_8$: *m/z* 417.1525 [M+Na]$^+$; found: 417.1504.

5-methyl-5-(((4-(((3-methyloxetan-3-yl)methoxy)methyl)benzyl)-oxy)methyl)-1,3-dioxan-2-one (45b):
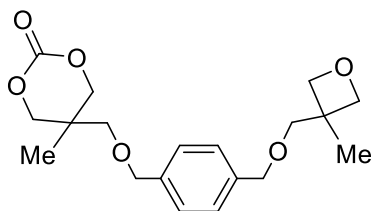
Conditions: **Al^{tBu}** (2.5 mol%), TBAB (5 mol%), 75 °C, 10 bar, 24 h; conversion: 93%, selectivity towards monocarbonate: 15%. Isolated by column chromatography (EtOAc:Hexane 1:2 to 1:1 v/v) in 13% yield. **^{1}H NMR** (500 MHz, CDCl$_3$): δ = 7.34-7.36 (m, 2H), 7.27-7.31 (m, 2H), 4.58 (s, 2H), 4.53 (m, 4H), 4.34-4.39 (m, 4H), 4.09 (m, 2H), 3.54 (s, 2H), 3.42 (s, 2H), 1.35 (s, 3H), 1.11 (s, 3H); **^{13}C NMR** (126 MHz, CDCl$_3$): δ = 148.21, 138.14, 136.85, 127.73, 127.69, 80.17, 75.50, 73.93, 73.38, 73.06, 71.12, 39.90, 33.04, 21.42, 17.45; **IR** (neat): 1747 cm^{-1} (C=O); **HRMS** (ESI+): calcd. for $C_{19}H_{26}O_6$: *m/z* 373.1626 [M+Na]$^+$; found: 373.1625.
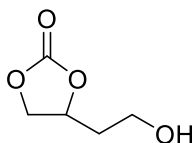
Chapter 3

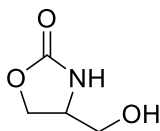### 4-(hydroxymethyl)-1,3-dioxolan-2-one (47):
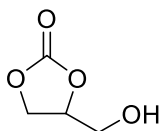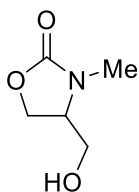
Conditions: **Al^{tBu}** (2.5 mol%), TBAB (5 mol%), 25 °C, 10 bar, 18 h; conversion: 99%. Isolated by column chromatography (EtOAc:hexane 3:1) in 85% yield. **^{1}H NMR** (500 MHz, Acetone-d_6): δ = 4.88 (m, 1H), 4.53-4.61 (m, 2H), 4.42 (m, 1H), 3.88 (m, 1H), 3.71 (m, 1H); **^{13}C NMR** (75 MHz, Acetone-d_6): δ = 155.24, 76.99, 65.79, 61.21; **IR** (neat): 1763 cm^{-1} (C=O).

4-(2-hydroxyethyl)-1,3-dioxolan-2-one (49):

Conditions: **Al^{tBu}** (2.5 mol%), TBAB (5 mol%), 60 °C, 10 bar, 18 h; conversion: 99%, chemo-selectivity 38%. Isolated by column chromatography (EtOAc:hexane 1:2 to 1:1 v/v) in 33% yield. **^{1}H NMR** (400 MHz, Acetone-d_6): δ = 4.95-4.99 (m, 1H), 4.65 (m, 1H), 4.26 (m, 1H), 3.85 (m, 1H), 3.71-3.77 (m, 2H), 1.97-2.02 (m, 2H); **^{13}C NMR** (126 MHz, Acetone-d_6): δ = 154.73, 75.12, 69.61, 57.20, 36.29; **IR** (neat): 1774 cm^{-1} (C=O).

4-(hydroxymethyl)oxazolidin-2-one (51):

Conditions: **Al^{tBu}** (2.5 mol%), TBAB (5 mol%), 25 °C, 10 bar, 18 h; conversion: 99%. Isolated by column chromatography using neutral alumina (EtOAc:MeOH 1:0 to 10:1 v/v) in 55% yield. **^{1}H NMR** (500 MHz, Acetone-d_6): δ = 6.71 (s, 1H), 4.42 (t, J = 8.6 Hz, 1H), 4.29 (t, J = 5.5 Hz, 1H), 4.19 (m, 1H), 3.89-3.99 (m, 1H), 3.60 (m, 2H); **^{13}C NMR** (126 MHz, Acetone-d_6): δ = 159.23, 66.59, 63.33, 53.61; **IR** (neat): 1716 cm^{-1} (C=O).

4-(hydroxymethyl)-3-methyloxazolidin-2-one (53):

Conditions: **Al^{tBu}** (2.5 mol%), TBAB (5 mol%), 25 °C, 10 bar, 18 h; conversion: 99%. Isolated by column chromatography using neutral alumina (EtOAc:Hexane 1:1 to 1:0 v/v) in 78% yield. **^{1}H NMR** (400 MHz, Acetone-d_6): δ = 4.28-4.36 (m, 1H), 4.13 (m, 2H), 3.78-3.86 (m, 2H), 3.59-3.68 (m, 1H), 2.83 (s, 3H); **^{13}C NMR** (126 MHz, Acetone-d_6): δ = 158.20, 99.99, 63.79, 60.15, 58.17; **IR** (neat): 1734 cm^{-1} (C=O); **HRMS** (ESI+): calcd. for C$_5$H$_9$NO$_3$: m/z 154.0480 [M+Na]$^+$; found: 154.0481.

Chapter 3

5-(hydroxymethyl)-1,3-oxazinan-2-one (55):
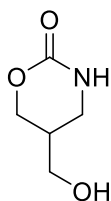
Conditions: **Al^{tBu}** (2.5 mol%), TBAB (5 mol%), 45 °C, 10 bar, 18 h; conversion: 99%. Isolated by washing the product with DCM followed by decantation of the liquid (the product is not soluble in DCM). The product was isolated in 84% yield. **^{1}H NMR** (400 MHz, Acetone-d_6): δ = 7.11 (s, 1H), 4.79 (t, J = 5.3 Hz, 1H), 4.19 (m, 1H), 3.99 (m, 1H), 3.40 (m, 2H), 3.20 (m, 1H), 2.91-3.03 (m, 1H), 1.95-2.08 (m, 1H); **^{13}C NMR** (126 MHz, Acetone-d_6): δ = 153.25, 68.06, 59.57, 41.40, 33.86; **IR** (neat): 1672 cm^{-1} (C=O); **HRMS** (ESI+): calcd. for C$_5$H$_9$NO$_3$: m/z 154.0480 [M+Na]$^+$; found: 154.0479.

4-hydroxy-4-(thiazol-2-yl)-1,3-dioxolan-2-one (57):
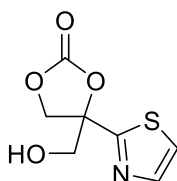
Conditions: **Al^{tBu}** (2.5 mol%), TBAB (5 mol%), 50 °C, 10 bar, 18 h; conversion: 95%. Isolated by column chromatography (EtOAc:hexane 1:2 to 1:1 v/v) in 89% yield. **^{1}H NMR** (500 MHz, Acetone-d_6): δ = 7.91 (d, J = 3.2 Hz, 1H), 7.79 (d, J = 3.2 Hz, 1H), 5.08-5.14 (m, 1H), 4.92 (s, 2H), 4.03-4.15 (m, 2H); **^{13}C NMR** (126 MHz, Acetone-d_6): δ = 166.89, 153.41, 143.24, 121.29, 85.11, 70.40, 65.19; **IR** (neat): 1785 cm^{-1} (C=O); **HRMS** (ESI+): calcd. for C$_7$H$_7$NO$_4$S: m/z 223.9993 [M+Na]$^+$; found: 223.9995.

3.5.6 Crystallographic studies

The measured crystals were stable under atmospheric conditions; nevertheless they were treated under inert conditions immersed in perfluoro-polyether as protecting oil for manipulation. Data Collection: measurements were made on a Bruker-Nonius diffractometer equipped with an APPEX II 4K CCD area detector, a FR591 rotating anode with Mo Kα radiation, Montel mirrors and a Kryoflex low temperature device (T = −173 °C). Full-sphere data collection was used with ω and ϕ scans. Programs used: Data collection Apex2 V2011.3 (Bruker-Nonius 2008), data reduction Saint+Version 7.60A (Bruker AXS 2008) and absorption correction SADABS V. 2008−1 (2008). Structure Solution: SHELXTL Version 6.10 (Sheldrick, 2000) was used. Structure Refinement: SHELXTL-97-UNIX VERSION. CCDC-1056843 (**36**), CCDC-1056845 (**39**), CCDC-1056846 (**41**), CCDC-1056844 (**45a**), and CCDC-1056847 (**57**), contain the supplementary crystallographic data for this paper. These data can be obtained free of charge from The Cambridge Crystallographic Data Centre via www.ccdc.cam.ac.uk/data_request/cif

Chapter 3

Crystallographic Data for Compound 36:

$C_{17}H_{24}O_4$, M_r = 292.36, triclinic, P-1, a = 6.4725(3) Å, b = 10.9994(5) Å, c = 45.127(2) Å, α = 83.0090(13)°, β = 87.280(2)°, γ = 85.6901(14)°, V = 3177.5(3) Å³, Z = 8, ρ = 1.222 mg·M⁻³, μ = 0.086 mm⁻¹, λ = 0.71073 Å, T = 100(2) K, $F(000)$ = 1264, crystal size = 0.04 × 0.01 × 0.002 mm, θ(min) = 0.91°, θ(max) = 27.93°, 57847 reflections collected, 13322 reflections unique (R_{int} = 0.0512), GoF = 1.051, R_1 = 0.0530 and wR_2 = 0.1194 [$I > 2\sigma(I)$], R_1 = 0.1012 and wR_2 = 0.1399 (all indices), min/max residual density = −0.386/0.330 [e·Å⁻³]. Completeness to θ(27.93°) = 87.1%.

Crystallographic Data for Compound 39:

$C_{11}H_{12}O_4$, M_r = 208.21, monoclinic, $P2(1)$, a = 10.9303(14) Å, b = 17.646(3) Å, c = 11.1951(14) Å, $\alpha = \gamma$ = 90°, β = 114.658(4)°, V = 1962.3(5) Å³, Z = 8, ρ = 1.409 mg·M⁻³, μ = 0.108 mm⁻¹, λ = 0.71073 Å, T = 100(2) K, $F(000)$ = 880, crystal size = 0.30 × 0.15 × 0.04 mm, θ(min) = 2.00°, θ(max) = 28.28°, 8911 reflections collected, 8911 reflections unique, GoF = 1.040, R_1 = 0.0633 and wR_2 = 0.1642 [$I > 2\sigma(I)$], R_1 = 0.0771 and wR_2 = 0.1752 (all indices), min/max residual density = −0.438/0.311 [e·Å⁻³]. Completeness to θ(28.28°) = 98.1%. Flack parameter x = 0.2 (7). The measured sample contained two single crystals domains and for its absorption correction the program TWINABS was used.[109] The asymmetric unit is made up of four molecules of the compound.

Crystallographic Data for Compound 41:

$C_{13}H_{14}O_5$, M_r = 250.24, monoclinic, $P2(1)/c$, a = 15.8444(10) Å, b = 5.8331(3) Å, c = 13.8570(8) Å, $\alpha = \gamma$ = 90°, β = 113.1386(17)°, V = 1177.67(12) Å³, Z = 4, ρ = 1.411 mg·M⁻³, μ = 0.109 mm⁻¹, λ = 0.71073 Å, T = 100(2) K, $F(000)$ = 528, crystal size = 0.60 × 0.10 × 0.10 mm, θ(min) = 2.80°, θ(max) = 30.62°, 6893 reflections collected, 6893 reflections unique, GoF = 1.075, R_1 = 0.0461 and wR_2 = 0.1238 [$I > 2\sigma(I)$], R_1 = 0.0534 and wR_2 = 0.1288 (all indices), min/max residual density = −0.271/0.366 [e·Å⁻³]. Completeness to θ(30.62°) = 99.8%.

Crystallographic Data for Compound 45a:

$C_{20}H_{26}O_8$, M_r = 394.41, orthorhombic, $Pbca$, a = 10.4970(8) Å, b = 11.6862(8) Å, c = 15.6413(12) Å, $\alpha = \beta = \gamma$ = 90°, V = 1918.7(2) Å³, Z = 4, ρ = 1.365 mg·M⁻³, μ = 0.106 mm⁻¹, λ = 0.71073 Å, T = 100(2) K, $F(000)$ = 840, crystal size = 0.55 × 0.04 × 0.03 mm, θ(min) = 2.60°, θ(max) = 25.63°, 13409 reflections collected, 1805 reflections unique (R_{int} = 0.0546), GoF = 1.045, R_1 = 0.0420 and wR_2 = 0.1022 [$I > 2\sigma(I)$], R_1 = 0.0703 and wR_2 =

Chapter 3

0.1148 (all indices), min/max residual density = −0.223/0.199 [e·Å^{-3}]. Completeness to θ(25.63°) = 99.7%.

Crystallographic Data for Compound 57:

$C_7H_7NO_4S$, M_r = 201.20, monoclinic, $P2(1)/c$, a = 9.4979(14) Å, b = 6.2542(10) Å, c = 14.097(2) Å, $\alpha = \gamma$ = 90°, β = 103.947(3)°, V = 812.7(2) Å^3, Z = 4, ρ = 1.644 mg·M^{-3}, μ = 0.377 mm^{-1}, λ = 0.71073 Å, T = 100(2) K, F(000) = 416, crystal size = 0.40 × 0.20 × 0.04 mm, θ(min) = 2.21°, θ(max) = 35.10°, 16993 reflections collected, 3443 reflections unique (R_{int} = 0.0365), GoF = 1.042, R_1 = 0.0298 and wR_2 = 0.0841 [$I > 2\sigma(I)$], R_1 = 0.0321 and wR_2 = 0.0864 (all indices), min/max residual density = −0.445/0.496 [e·Å^{-3}]. Completeness to θ(35.10°) = 95.3%.

3.6 References

[44]   C. J. Whiteoak, N. Kielland, V. Laserna, F. Castro-Gómez, E. Martin, E. C. Escudero-Adán, C. Bo, A. W. Kleij, *Chem. Eur. J.* **2014**, *20*, 2264-2275.

[77]   M. Kol, M. Shamis, I. Goldberg, Z. Goldschmidt, S. Alfi, E. Hayut-Salant, *Inorg. Chem. Commun.* **2001**, *4*, 177-179.

[79]   S. M. Guillaume, J.-F. Carpentier, *Catal. Sci. Technol.* **2012**, *2*, 898-906.

[80]   M. Helou, O. Miserque, J.-M. Brusson, J.-F. Carpentier, S. M. Guillaume, *Chem. Eur. J.* **2010**, *16*, 13805-13813.

[81]   J. Feng, R.-X. Zhuo, X.-Z. Zhang, *Prog. Polym. Sci.* **2012**, *37*, 211-236.

[82]   J. Mindemark, T. Bowden, *Polym. Chem.* **2012**, *3*, 1399-1401.

[83]   G. L. Gregory, M. Ulmann, A. Buchard, *RSC Adv.* **2015**, *5*, 39404-39408.

[84]   H. Matsukizono, T. Endo, *J. Appl. Polym. Sci.* **2015**, *132*, 41956-41966.

[85]   M. R. Reithofer, Y. N. Sum, Y. Zhang, *Green Chem.* **2013**, *15*, 2086-2090.

[86]   a) J. A. Burkhard, G. Wuitschik, M. Rogers-Evans, K. Müller, E. M. Carreira, *Angew. Chem. Int. Ed.* **2010**, *49*, 9052-9067; b) G. Wuitschik, E. M. Carreira, B. Wagner, H. Fischer, I. Parrilla, F. Schuler, M. Rogers-Evans, K. Müller, *J. Med. Chem.* **2010**, *53*, 3227-3246.

[87]   a) D. J. Darensbourg, A. I. Moncada, *Macromolecules* **2010**, *43*, 5996-6003; b) D. J. Darensbourg, A. I. Moncada, S.-H. Wei, *Macromolecules* **2011**, *44*, 2568-2576; c) D. J. Darensbourg, A. I. Moncada, W. Choi, J. H. Reibenspies, *J. Am. Chem. Soc.* **2008**, *130*, 6523-6533.

[88]   a) B. R. Buckley, A. P. Patel, K. G. U. Wijayantha, *Eur. J. Org. Chem.* **2015**, 474-478; b) D. J. Darensbourg, A. Horn Jr, A. I. Moncada, *Green Chem.* **2010**, *12*, 1376-1379.

[89]   C. J. Whiteoak, E. Martin, M. M. Belmonte, J. Benet-Buchholz, A. W. Kleij, *Adv. Synth. Catal.* **2012**, *354*, 469-476.

[90]   M. Alves, B. Grignard, A. Boyaval, R. Méreau, J. De Winter, P. Gerbaux, C. Detrembleur, T. Tassaing, C. Jérôme, *ChemSusChem* **2017**, *10*, 1128-1138.

[91]   H. Sasaki, J. M. Rudzinński, T. Kakuchi, *J. Polym. Sci., Part A: Polym. Chem.* **1995**, *33*, 1807-1816.

[92]   S. Searles, M. Tamres, E. R. Lippincott, *J. Am. Chem. Soc.* **1953**, *75*, 2775-2777.

[93]   D. Sawicka, S. Wilsey, K. N. Houk, *J. Am. Chem. Soc.* **1999**, *121*, 864-865.

[94]   D. J. Darensbourg, A. I. Moncada, *Inorg. Chem.* **2008**, *47*, 10000-10008.

[95]   J. A. Bull, R. A. Croft, O. A. Davis, R. Doran, K. F. Morgan, *Chem. Rev.* **2016**, *116*, 12150-12233.

[96]   P. Picard, D. Leclercq, J. P. Bats, J. Moulines, *Synthesis* **1981**, *1981*, 550-551.

[97]   M. Auria, R. Racioppi, *Molecules* **2013**, *18*, 11384.

[98]   K. Okuma, Y. Tanaka, S. Kaji, H. Ohta, *J. Org. Chem.* **1983**, *48*, 5133-5134.

[99]   G.-M. Ho, Y.-J. Li, *Chem. Commun.* **2016**, *52*, 12108-12111.

[100]   X. Gui, Z. Tang, W. Fei, *J. Chem. Eng. Data* **2011**, *56*, 2420-2429.

Chapter 3

[101]   K. M. Tomczyk, P. A. Gunka, P. G. Parzuchowski, J. Zachara, G. Rokicki, *Green Chem.* **2012**, *14*, 1749-1758.
[102]   S. Minakata, I. Sasaki, T. Ide, *Angew. Chem. Int. Ed.* **2010**, *49*, 1309-1311.
[103]   Y. Takeda, S. Okumura, S. Tone, I. Sasaki, S. Minakata, *Org. Lett.* **2012**, *14*, 4874-4877.
[104]   R. N. Loy, E. N. Jacobsen, *J. Am. Chem. Soc.* **2009**, *131*, 2786-2787.
[105]   N. Ishida, Y. Shimamoto, M. Murakami, *Angew. Chem. Int. Ed.* **2012**, *51*, 11750-11752.
[106]   L. A. Berben, *Chem. Eur. J.* **2015**, *21*, 2734-2742.
[107]   W. Guo, V. Laserna, J. Rintjema, A. W. Kleij, *Adv. Synth. Catal.* **2016**, *358*, 1602-1607.
[108]   M. A. Blaskovich, G. Evindar, N. G. W. Rose, S. Wilkinson, Y. Luo, G. A. Lajoie, *J. Org. Chem.* **1998**, *63*, 3631-3646.
[109]   R. Blessing, *Acta Crystallogr. Sect. A* **1995**, *51*, 33-38.

Chapter 4.

Substrate-Controlled Product Divergence:
Conversion of CO_2 into Heterocyclic Products
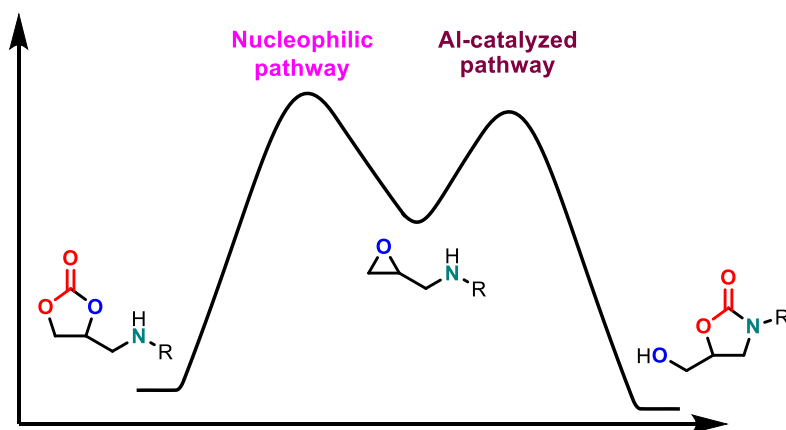
This work has been published in:

ALUMINUM-CATALYZED COUPLING OF CARBON DIOXIDE AND CYCLIC ETHERS

Jeroen Rintjema Tanger

Chapter 4

4.1 Introduction

Depletion of fossil fuels has triggered a growing interest within the chemical community to use alternative carbon feedstocks for the production of basic and fine-chemicals. Among the potential candidates, carbon dioxide is considered a valuable C1 building block due to its virtually unlimited supply.[61b, 110] Owing to the inert nature of CO_2, catalysis is essential to facilitate its coupling with a suitable substrate.[111] While the use of a catalyst enables the transformation of CO_2, it typically does so by activating a reactive coupling partner rather than CO_2 itself. Direct activation of CO_2 can, however, be performed by the substrate for instance in the case of propargylic alcohols. These substrates can be easily transformed into α-alkylidene cyclic carbonates, where the alcohol group of the substrate serves to activate CO_2. In addition, a coinage metal (Ag, Cu) is typically used to activate the alkyne moiety of the substrate. This double role of the substate to provide both activation of CO_2 (via the hydroxy group) and a reactive coupling partner (alkyne) has led to the synthesis of alkylidene cyclic carbonates under very mild conditions.[112]

Another example of substrate involvement in the activation of CO_2 is described in the previous chapter, where oxetanes containing alcohol or amine functional groups are transformed into five- or six-membered cyclic carbonates, and carbamates respectively.[113] The main disadvantage of both propargylic alcohols and oxetanes is their availability, as only a few examples are readily available thereby limiting the scope and applicability of these methodogies. An ideal substrate class for substrate-controlled activation are allylic alcohols, which have been used by the group of Minakata to form cyclic carbonates under very mild conditions.[102] Stoichiometric iodine (*tert*-butyl hypoiodite) is however required in this case to activate the double bond (see Scheme 17).
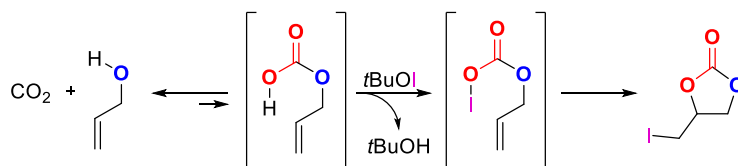

Scheme 17. Proposed mechanism of trapping of a carbonic acid monoester with tBuOI.

Recently, an enantioselective version of this reaction was developed by Johnston *et al.* using N-iodo succinimide (NIS) to synthesize a range of iodocarbonates.[114] A recent review highlights the synthesis of various heterocycles through substrate assisted CO_2

Chapter 4

activation.[115] An interesting alternative for the above-mentioned methods is the use of epoxy alcohols, which do not require any stoichiometric additives and can be easily accessed from allylic alcohols. Simple epoxidation of (homo)allylic alcohols gives access to a wide variety of substituted epoxy alcohols.[116] Although a few isolated examples of epoxy-alcohol/CO_2 couplings have been reported, this class of substrates has remained virtually unexplored.[117] Utilizing epoxides with pendant hydroxy or amine groups may give access to five-membered cyclic carbonates and carbamates, respectively, using substrate-induced CO_2 activation. Cyclic carbamates are also called oxazolidinones, a versatile type of scaffold that can be used as chiral auxiliaries,[30] antimicrobial drugs,[33] antidepressants[32] or building blocks for organic synthesis.[31]

We envisioned that through a substrate-assisted catalytic approach we would be able to access highly subsituted cyclic carbonates that would be difficult to synthesize via conventional epoxide/CO_2 coupling reactions. Apart from the copolymerization of limonene oxide,[118] the challenging coupling of tri-substituted epoxides with CO_2 is limited to a few examples.[119] This new catalytic approach towards epoxide CO_2 coupling would trigger an alternative mechanism following an intramolecular nucleophilic attack (see Scheme 18, right). Since the conventional mechanism (Scheme 18, left) is initiated by an external nucleophile and requires different reaction conditions, both mechanistic routes would be accessible and provide a conceptually new approach towards product diversity from a single epoxy alcohol or amine substrate.
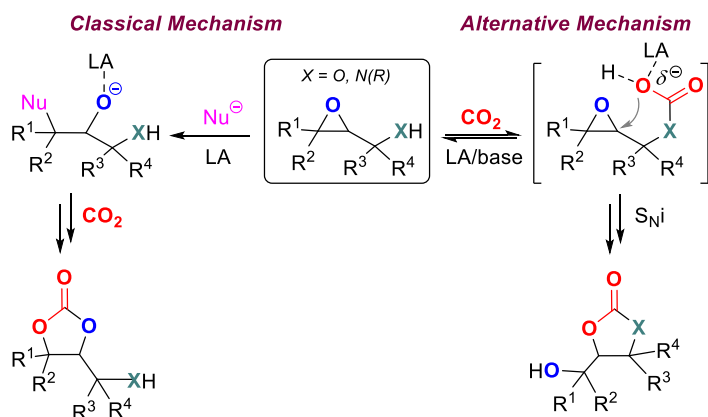
Scheme 18. Mechanistic divergence in the coupling between CO_2 and epoxy alcohols or amines leading to product diversity. LA = Lewis acid, Nu = nucleophile.

Chapter 4

4.2 Objectives

The aim of this chapter is to explore an alternative route for epoxide/CO_2 coupling using epoxides containing pendant hydroxyl or amine groups that have potential to form a nucleophilic species *in-situ* upon combination with CO_2. Utilizing this new approach may offer an effective way to access di- and tri-subtituted cyclic carbonates, that are difficult to synthesize via conventional epoxide/CO_2 conversions. The classical approach towards cyclic carbonate formation using an external nucleophile operates under different conditions, and consequently both mechanistic pathways (Scheme 18) would be selectively accessible, allowing for product divergence from a single epoxy alcohol or amine substrate.

4.3 Results and discussion

Epoxy alcohol and amine starting materials (Figure 15) used throughout this chapter were either commercialy available or synthesized according to existing protocols. A wide range of allylic alcohols is commercially available, others were easily synthesized by Grignard addition to ketones followed by epoxidation to yield the epoxy alcohol. Epoxy amines can be obtained through coupling of amines with epichlorohydrin.
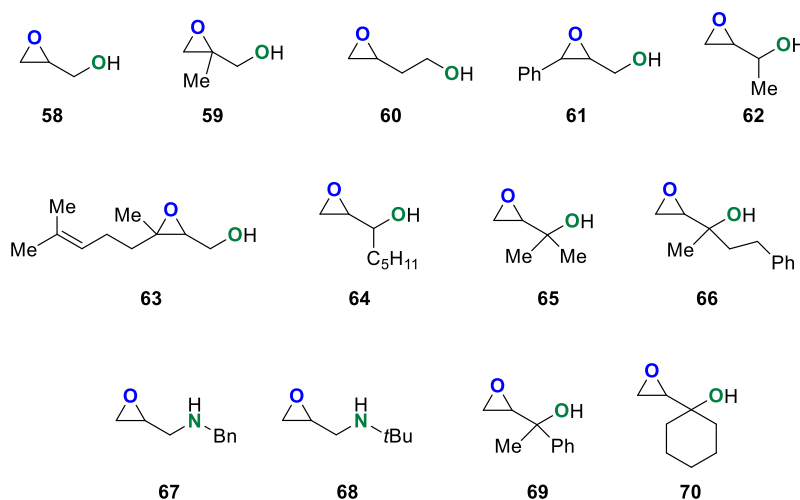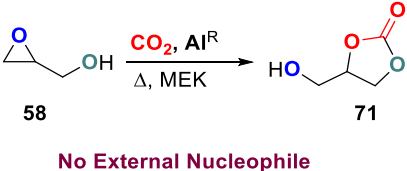

Figure 15. Epoxides containing pendant hydroxyl or amine groups that were probed in the synthesis of functionalized carbonates and carbamates.
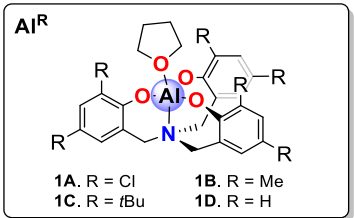
Chapter 4

4.3.1   Optimization of reaction conditions

We first established general reaction conditions using the simplest epoxy alcohol (i.e., glycidol) and a Lewis acid based on aluminium(III)-centered aminotriphenolate complexes **1A–D** (see Table 10) in the absence of an external nucleophile: these reactions conditions are related to the hydroxy oxetane conversions reported in the previous chapter. At 50 °C after 14 h we found that the Al catalyst **1C** (Table 10, entry 3) gives the highest conversion (89%) and selectivity (>99%). Whereas the catalyst **1D** shows higher reactivity (entry 4; >99% conversion), the reaction mixture was more complex likely resulting from polyether formation.

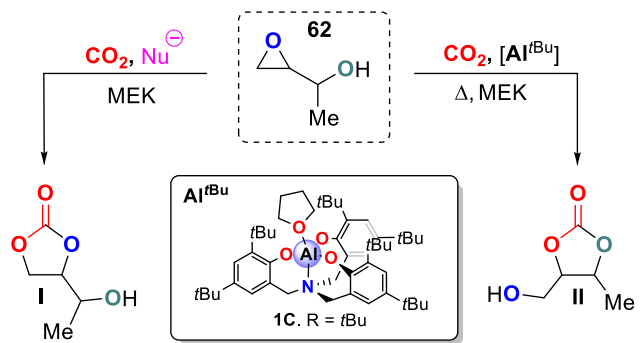*Table 10. Screening of suitable conditions to form glycidol carbonate using glycidol and CO_2.[a]*

entry	Cat.	Amount (mol%)	T (ºC)	t (h)	Yield (%)[b]
1	Al^H	1.0	50	14	20
2	Al^{Me}	1.0	50	14	78
3	Al^{tBu}	1.0	50	14	89
4	Al^{Cl}	1.0	50	14	<10[c]
5	Al^{tBu}	1.0	25	14	12
6	Al^{tBu}	1.0	50	14	0[d]
7	Al^{tBu}	1.0	75	1	96
8	Al^{tBu}	1.0	75	2	>99
9	–	–	75	14	59
10	–	–	75	1	10

[a] Conditions: glycidol (1.0 mmol), $p(CO_2)^o$ = 10 bar, 1.0 mL MEK (methyl ethyl ketone). [b] Determined by ^{1}H NMR. Selectivity for the carbonate >99%. [c] >99% conv.; Multiple products (polyether). [d] Benzyl protected glycidol as substrate.

Chapter 4

The formation of the carbonate **71** is sluggish at 25 °C (entry 5) but is virtually complete in 1 hour when raising the reaction temperature to 75 °C (entry 7). Benzyl protection of the alcohol unit in glycidol (entry 6) shuts down catalysis, thus hinting at a key role for the free alcohol to mediate an alternative pathway towards the carbonate. Surprisingly, the formation of **71** also proceeds without any Lewis acid present (entries 9 and 10) but with significantly slower kinetics than in the presence of **1C**. Next we examined reaction conditions to trigger the alternative mechanism using 1-(oxiran-2-yl)ethanol (Figure 15, **62**): if successful this would give direct evidence for an alternative pathway leading to structurally divergent organic carbonates as depicted in Scheme 18. The use of a nucleophile only (TBAB) at low temperature favors the conventional product **I** (Table 11, entry 1). A combination of both **1C** and TBAB gives improved reactivity, but a mixture of products of the types **I** and **II** (entry 2) was observed. Delightedly, complete selectivity towards the alternative carbonate product (**II**) is achieved at 50 °C in the absence of an external nucleophile (entry 3).

*Table 11. Screening of suitable reaction conditions to trigger an alternative mechanism leading to formation of carbonate type **II**.[a]*

entry	Cat. [mol%]	Co-cat [mol%]	T [ºC]	t [h]	Conv. [%][b]	Ratio I:II[b]
1	–	TBAB (5.0)	25	40	55	81:19
2	**1C** (1.0)	TBAB (5.0)	25	14	>99	22:78
3	**1C** (1.0)	–	50	14	>99	0:100

[a] Conditions: 1-(oxiran-2-yl)ethanol (1.0 mmol), $p(CO_2)$ = 10 bar, 1.0 mL MEK (methyl ethyl ketone). [b] Determined by ^{1}H NMR (CDCl$_3$).

Chapter 4

4.3.2 Scope of carbonate and carbamate products

The results presented in Table 10 and Table 11 suggest that organic carbonates may indeed be accessed through an alternative mechanism based on *in-situ* formation of CO_2-derived nucleophiles (Scheme 18). Therefore, we decided to expand the scope of carbonates/carbamates by examination of epoxy alcohols and amines with more challenging substitution patterns, using **1C** as the catalyst. In general the product scope, for the carbonates/carbamates that can be attained through this substrate-mediated CO_2 activation is diverse and the targeted products **71–83** (Figure 16) were obtained in good to excellent yields of up to 95%, and with high chemoselectivity.
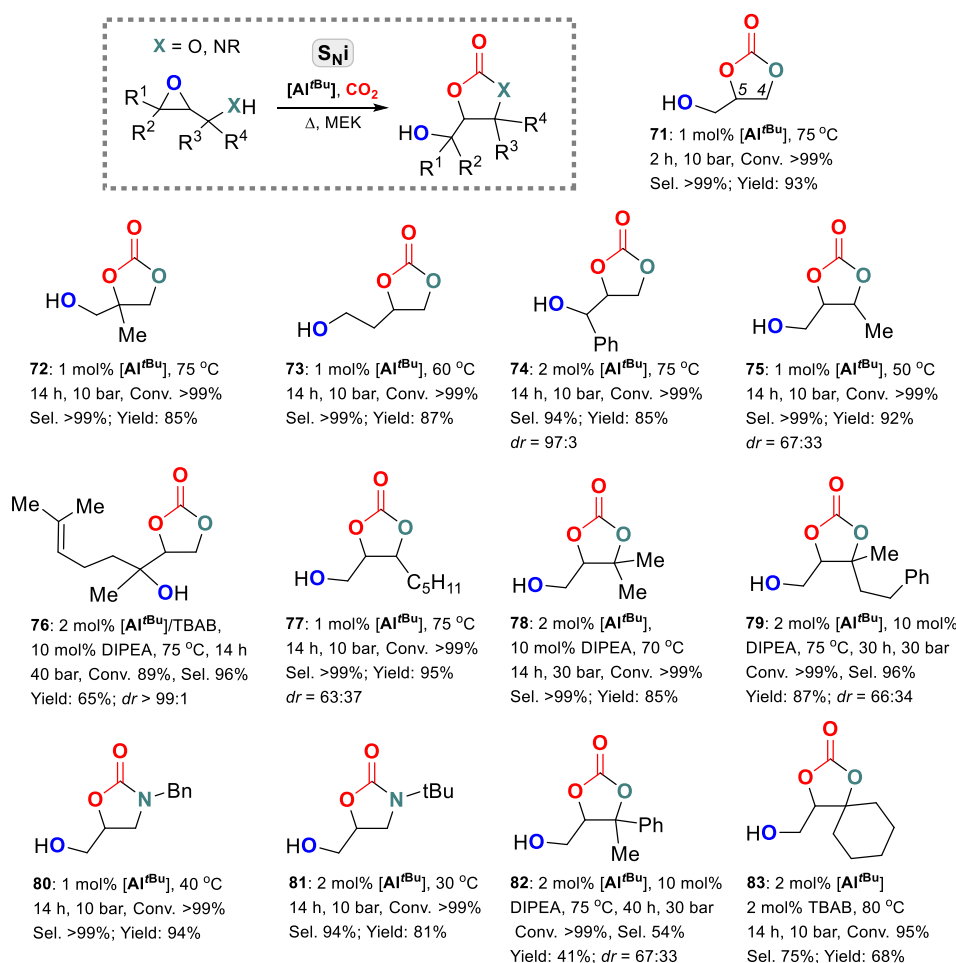

Figure 16. Synthesis of highly substituted organic carbonates and carbamates (*71-83*) from epoxy alcohols/amines and CO_2. Reported yields are isolated ones.

Notably, this alternative synthetic method for carbonates allows formation of highly challenging 4,5-di- (**75** and **77**) and 4,4,5-tri-substitutions (**78**, **79**, **82** and the spiro-compound **83**) on the cyclic carbonate ring, including the use of terpene-based scaffolds (**76** derived from 2,3-epoxy-geraniol **63**). Addition of DIPEA was required for the conversion of some of the sterically challenging substrates to increase the selectivity towards the desired product by further activation of the alcohol group. Catalytic amounts of base led to excellent selectivity and yields for products **76**, **78** and **79**, however in the case of **82** the chemoselectivity was compromised by the competitive formation of the carbonate product mediated through the conventional mechanism (Scheme 18). Note that the base itself does not act as nucleophile to ring-open the epoxide, as no conversion could be observed when DIPEA was used in the reaction with propylene oxide. For the spiro-compound **83** no reaction was observed even in the presence of DIPEA and a small amount of nucleophile was added in this case. While the use of a nucleophile by itself favors the direct insertion of CO_2 into the epoxide, it can also serve to facilitate the reaction towards the desired product (Scheme 19, *vide infra*).

Interestingly, when epoxy amines are used as substrates only the 5-substituted isomer is formed (**80** and **81**), and this in contrast to the known (catalytic) couplings between aziridines and CO_2 which often result in the formation of regioisomeric mixtures.[120] To the best of our knowledge, the trisubstituted carbonates cannot be obtained by using a conventional approach based on catalytic CO_2/epoxide couplings, thus demonstrating the added value of this new methodology.

4.3.3   Product divergence

Having validated that an alternative mechanism towards organic carbonate formation through the use of epoxy alcohols/amines can be selectively induced, we next set out to explore the possibility of an unprecedented product divergence from a single epoxy alcohol/amine substrate (Figure 17). In essence, the different mechanisms leading to the formation of organic carbonates should be triggered under different reaction (temperature) conditions and by using different additives. We were pleased to find that indeed access to both types of carbonate products from simple and accessible precursors (**84–87**) could be achieved in good yields. Notably, the use of a natural product (sclareol, a bicyclic diterpenol) shows that the approach is also feasible with more complicated scaffolds. For both sclareol carbonates **86** (X-ray molecular structure determined, see experimental section) and **87** the formation of diastereoisomeric

Chapter 4

mixtures arises from the sclareol epoxidation stage, with apparently some higher degree of stereocontrol in the preparation of **87**.
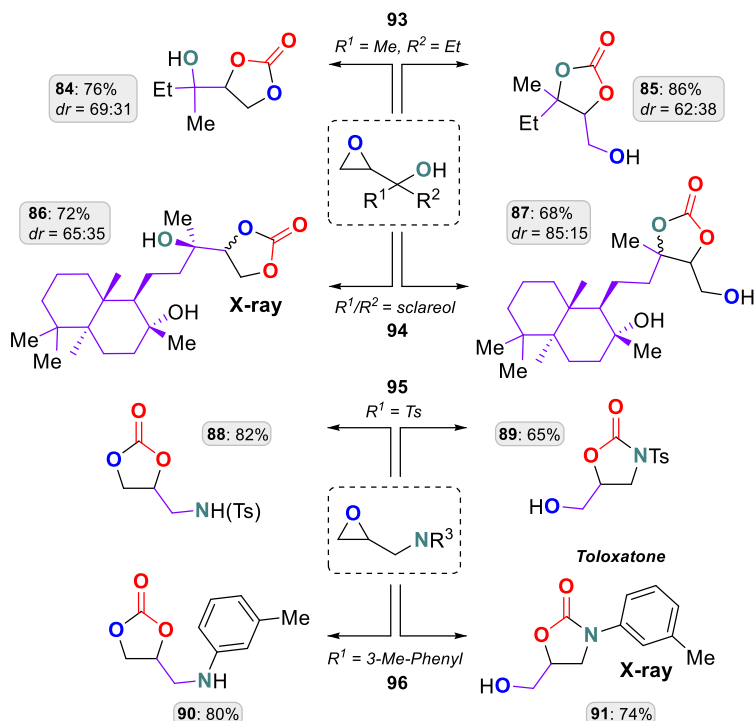

*Figure 17. Product divergence from four epoxy alcohols/amines, giving access to the compounds **84–91**. For all reactions 2 mol% **Al^{tBu}** and 10 bar initial CO_2 pressure were used unless indicated otherwise. Details: **84**, 5 mol% TBAB, 25 ºC, 60 h, conv. 95%, sel. 85%; **85**, 80 ºC, 40 h, 30 bar, conv. >99%, sel. 93%; **86**, 5 mol% TBAB, 50 ºC, 14 h, 30 bar, conv. >99%, sel. 79%; **87**, 10 mol% TBACl, 75 ºC, 14 h, conv. >99%, sel. 79%; **88**, 5 mol% TBAB, 75 ºC, 14 h, conv. >99%, sel. 97%; **89**, 10 mol% DIPEA, 50 ºC, 40 h, 30 bar, conv. >99%, sel. 77%; **90**, 5 mol% TBAB, 30 ºC, 40 h, conv. >99%, sel. 81%; **91**, 2 mol% TBAB, 75 ºC, 14 h, conv. >99%, sel. 81%. Ts = 4-toluenesulfonyl.*

The use of epoxy amines (Figure 17, lower part) also allows for product divergence (**88–91**), and leads to the formation of either cyclic carbonate or carbamate scaffolds. The use of tosyl-protected epoxy amines is challenging since the amine will be rather unreactive toward the formation of a nucleophilic intermediate based on CO_2 (Scheme 18, alternative pathway). However, we found that the addition of a suitable base (DIPEA) allows to access the carbamate **89** in an appreciable yield of 65% with full selectivity towards the 5-substituted isomer in line with the proposed intramolecular pathway presented in Scheme 18. The presence of an N-aryl group in the epoxy amine

Chapter 4

substrate expands the potential of this chemistry as it provides a simple entry to pharmaceutically relevant 5-substituted oxazolidinones such as Toloxatone (**91**; 74% yield; X-ray structure determined, see experimental section), which is a known antidepressant. Note that in the case of **91** full selectivity towards the carbamate product is obtained when using DIPEA, however the yield remains rather low even after prolonged reaction times (55% after 60 h). To overcome this issue, an external nucleophile was added to accelerate the reaction, though with some loss of selectivity (see Scheme 19).
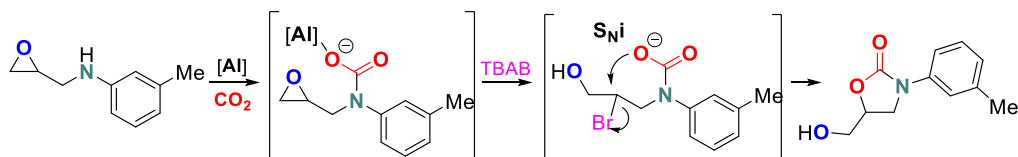
Scheme 19. Use of external nucleophile in combination with a substrate derived nucleophile.

After formation of the nucleophilic species that arises from binding of CO_2 to the amine, the external nucleophile (bromide in this case) can ring-open the epoxide. This further activates the substrate towards intramolecular attack and formation of the oxazolidinone ring in **91**. Interestingly, there are several structurally highly related oxazolidinone molecules (see Figure 18) which are used as antibacterials[121] or antidepressants.[32] The easy formation of **91** gives promise to the synthesis of new types of bioactive compounds using CO_2 as a co-reactant.
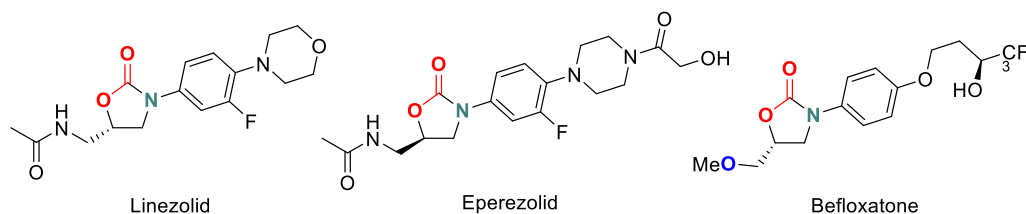

Figure 18. Pharmaceutical compounds based on the 5-substituted oxazolidinone scaffold.

4.3.4   Mechanistic support

To support the formation of a nucleophile derived from an epoxy alcohol and CO_2, we closely examined the formation of the carbonate product **74** (Figure 19). Enantiopure (2R,3R)-(+)-3-phenylglycidol (96%) was converted with 94% diastereoselectivity into **74**

Chapter 4

(86% yield for the major diastereoisomer). The other two components of the reaction mixture were the other diastereoisomer (3%) and the standard carbonate product (3%), which were separated from **74** by chromatography. Note that this reaction also proceeds in the presence of cesium carbonate, though with preferential formation of the expected, disubstituted carbonate product.[117a]
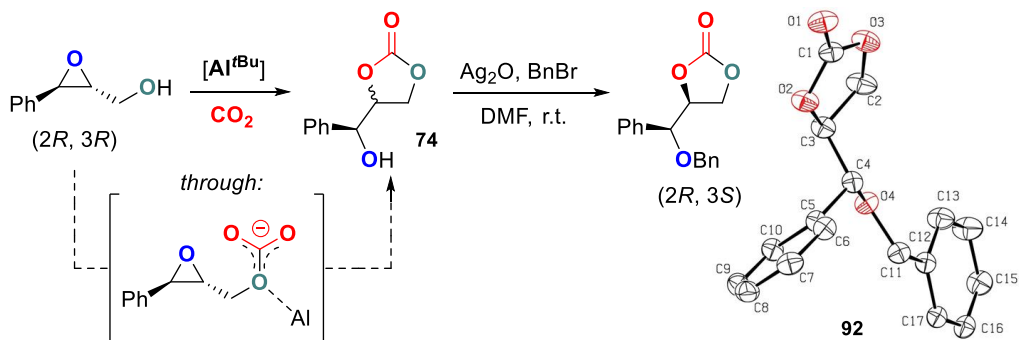

*Figure 19. A more detailed investigation into the diastereoselective formation of cyclic carbonate **74** and its benzyl-protected derivative **92**.*

Overall, the reaction follows a diastereoselective pathway (*d.r.* = 97:3). The absolute configuration [(2*R*,3*S*)] of **74** was determined by X-ray crystallographic analysis of its *O*-benzyl-protected derivative **92** (see Experimental) and showed a formal inversion at one of the carbon centers. This inversion suggests that a nucleophilic substitution takes place prior to isolation (Walden inversion), and is in line with the mechanistic proposal in Scheme 18 and Figure 19 which present a formal 5-*exo*-tet-type cyclization. Moreover, the selective formation of the 5-substituted oxazolidinone products **80**, **81**, and **91** additionally supports the involvement of an intramolecular nucleophilic attack on the epoxide prior to product formation.

4.4 Conclusion

In summary, we report a simple and practical method for a new substrate-controlled CO_2 conversion process which allows product divergence from epoxy alcohols/amines. The different carbonate/carbamate products can be accessed through different mechanistic manifolds which are simply triggered by tuning of the reaction temperature/pressure and use of suitable nucleophilic/base additives. Such control allows new, unexplored uses of CO_2 in organic synthesis through substrate-driven
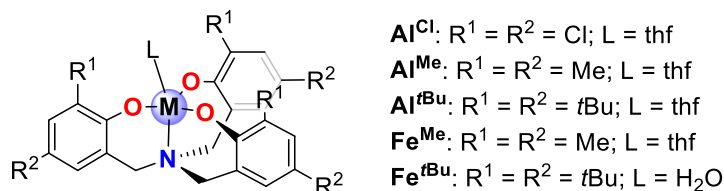
Chapter 4

activation of this renewable carbon feedstock. Notably, such reactivity herein has proven to be useful to access extremely challenging substitution patterns on the cyclic carbonate/carbamate ring. Further work is in progress to expand this principle to other readily available organic scaffolds to further capitalize on the potential of this alternative raw carbon material in chemical synthesis. In chapter 5 of this thesis a detailed mechanistic investigation is presented using glycidol as a model substrate.

4.5 Experimental

4.5.1 General comments

Both the ligands[77] and catalysts[44] (see figure below) were synthesized according to previously reported procedures. ^{1}H and ^{13}C NMR spectra were recorded on a Bruker AV-300, AV-400 or AV-500 spectrometer. Mass spectrometric analysis and X-ray diffraction studies were performed by the Research Support Group at the ICIQ. Carbon dioxide was purchased from PRAXAIR and used without further purification. Solvents used in the synthesis of the complexes were dried using an Innovative Technology PURE SOLV solvent purification system. *D.r.* values of all products are also provided in Figures 16 and 17.

$\mathbf{Al^{Cl}}$: $R^1 = R^2$ = Cl; L = thf
$\mathbf{Al^{Me}}$: $R^1 = R^2$ = Me; L = thf
$\mathbf{Al^{tBu}}$: $R^1 = R^2$ = tBu; L = thf
$\mathbf{Fe^{Me}}$: $R^1 = R^2$ = Me; L = thf
$\mathbf{Fe^{tBu}}$: $R^1 = R^2$ = tBu; L = H$_2$O

4.5.2 Preparation of substrates
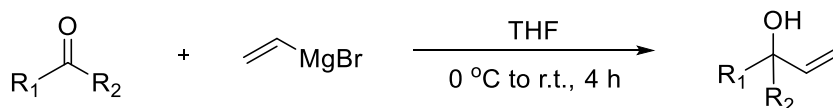
Allylic alcohols (**A1-A3**; see below) were synthesized according to a general procedure.[122] To a stirred solution of the carbonyl precursors (10.0 mmol) in dry THF (30 mL) was added vinyl magnesium bromide (1.0 M in THF, 12.0 mL, 12.0 mmol) dropwise through a syringe at 0 °C. After stirring for 20 min, the reaction mixture was

Chapter 4

allowed to warm to room temperature. The resulting mixture was stirred for additional 4 h and then quenched by saturated NH₄Cl solution (40 mL). The organic phase was extracted with ethyl acetate (50 mL × 3). The combined organic layers were washed with brine, dried over MgSO₄, and concentrated under vacuum to afford the crude product. It was further purified by flash silica gel column chromatography.
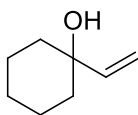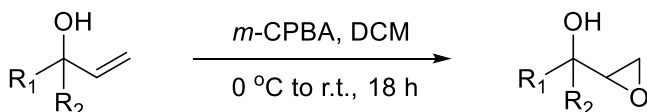
2-phenylbut-3-en-2-ol (A1)
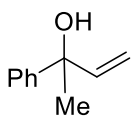
Prepared according to the general procedure for allylic alcohols described above. Purification by column chromatography (EtOAc:hexane, 1:10) gave the product as a colorless liquid in 78% yield (1.16 g, 7.8 mmol). NMR spectra/data are in agreement with the literature.[122] **¹H NMR** (300 MHz, CDCl₃) δ 7.52 – 7.30 (m, 5H), 6.20 (dd, J = 17.2 and 10.6 Hz, 1H), 5.50 – 5.06 (m, 2H), 1.89 (s, 1H), 1.68 (s, 3H).

3-methyl-5-phenylpent-1-en-3-ol (A2)
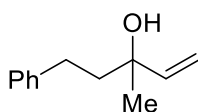
Prepared according to the general procedure for allylic alcohols described above. Purification by column chromatography (EtOAc:hexane, 1:15) gave the product as a colorless liquid in 74% yield (1.30 g, 7.4 mmol). NMR spectra/data are in agreement with the literature.[122] **¹H NMR** (500 MHz, CDCl₃) δ 7.30 (s, 2H), 7.23 – 7.18 (m, 3H), 6.00 (dd, J = 17.3, 10.8 Hz, 1H), 5.30 (dd, J = 17.4 and 1.2 Hz, 1H), 5.14 (dd, J = 10.8, 1.2 Hz, 1H), 2.76 – 2.60 (m, 2H), 1.88 (m, 2H), 1.47 (s, 1H), 1.37 (s, 3H).
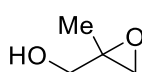
1-vinylcyclohexanol (A3)

Prepared according to the general procedure for allylic alcohols described above (20.0 mmol scale). Purification by column chromatography (EtOAc:hexane, 1:15) gave the product as a colorless liquid in 41% yield (1.02 g, 8.1 mmol). NMR spectra/data are in agreement with the literature.[122] **¹H NMR** (500 MHz, CDCl₃) δ 6.00 (dd, J = 17.4 and 10.8 Hz, 1H), 5.27 (dd, J = 17.4, 1.3 Hz, 1H), 5.06 (dd, J = 10.7 and 1.3 Hz, 1H), 1.75 – 1.64 (m, 6H), 1.56 – 1.44 (m, 4H).

Chapter 4

Epoxy alcohols were synthesized according to the standard procedure for alkene epoxidation using *m*-CPBA. To a stirred solution of epoxy alcohol (10.0 mmol) in DCM (25 mL) at 0 °C was added 3-chloroperbenzoic acid (2.80 g, 12.5 mmol, 1.25 equiv.) in small portions and the mixture was stirred for 18 h at rt. A white precipitate was filtered off after the reaction and the mixture was concentrated to obtain the crude product. Purification was done by basic alumina column chromatography (Et$_2$O:hexane).

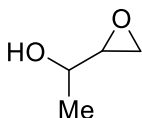### (2-methyloxiran-2-yl)methanol (59)

Prepared according to the general procedure for epoxy alcohols described above. Purification by basic alumina column chromatography (Et$_2$O:hexane, 1:1) gave the product as a colorless liquid in 83% yield (0.73 g, 8.3 mmol). **^{1}H NMR** (500 MHz, CDCl$_3$) δ 3.74 (m, 1H), 3.66 – 3.58 (m, 1H), 2.92 (d, J = 4.7 Hz, 1H), 2.67 (d, J = 4.7 Hz, 1H), 2.00 (s, 1H), 1.37 (s, 3H). **^{13}C NMR** (126 MHz, CDCl$_3$) δ 64.23, 57.24, 51.03, 18.07.

2-(oxiran-2-yl)ethanol (60)
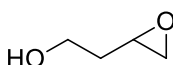
Prepared according to the general procedure for epoxy alcohols described above. Purification by basic alumina column chromatography (Et$_2$O:hexane, 1:1) gave the product as a colorless liquid in 79% yield (0.70 g, 7.9 mmol). **^{1}H NMR** (400 MHz, CDCl$_3$) δ 3.80 (m, 2H), 3.14 – 3.04 (m, 1H), 2.81 (t, J = 4.4 Hz, 1H), 2.65 – 2.52 (m, 1H), 2.23 (s, 1H), 2.03 – 1.90 (m, 1H), 1.70 (m, 1H). **^{13}C NMR** (126 MHz, CDCl$_3$) δ 59.80, 50.48, 46.63, 34.70.
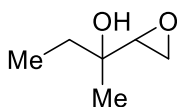
1-(oxiran-2-yl)ethanol (62)

Prepared according to the general procedure for epoxy alcohols described above. Purification by basic alumina column chromatography (Et$_2$O:hexane, 1:1) gave the product (a mixture of diastereoisomers) as a colorless liquid in 82% yield (0.72 g, 8.2 mmol). **^{1}H NMR** (500 MHz, CDCl$_3$) δ 4.06 – 3.56 (m, 1H), 3.05 – 2.95 (m, 1H), 2.85 – 2.78 (m, 1H), 2.72 (m, 1H), 2.44 – 2.02 (m, 1H), 1.29 (m, 3H). **^{13}C NMR** (126 MHz, CDCl$_3$) δ 68.07, 64.73, 56.28, 55.32, 45.11, 43.47, 19.71, 18.62.
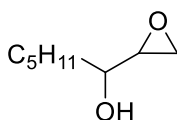
Chapter 4

2-(oxiran-2-yl)butan-2-ol (93)

Prepared according to the general procedure for epoxy alcohols described above. Purification by basic alumina column chromatography (Et$_2$O:hexane, 1:2) gave the product (a mixture of diastereoisomers) as a colorless liquid in 86% yield (1.00 g, 8.6 mmol).

^{1}H NMR (500 MHz, CDCl$_3$) δ 2.95 (m, 1H), 2.82 (m, 1H), 2.73 (m, 1H), 1.81 – 1.56 (m, 3H), 1.24 (s, 3H), 0.99 (m, 3H). **^{13}C NMR** (126 MHz, CDCl$_3$) δ 69.40, 69.31, 57.71, 57.43, 44.21, 43.28, 33.92, 31.32, 25.64, 22.16, 7.78, 7.64.
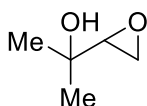
1-(oxiran-2-yl)hexan-1-ol (64)

Prepared according to the general procedure for epoxy alcohols described above. Purification by basic alumina column chromatography (Et$_2$O:hexane, 1:2) gave the product (a mixture of diastereoisomers) as a colorless liquid in 95% yield (1.37 g, 9.5 mmol).

^{1}H NMR (500 MHz, CDCl$_3$) δ 3.90 – 3.42 (m, 1H), 3.07 – 2.97 (m, 1H), 2.88 – 2.72 (m, 2H), 1.84 – 1.77 (m, 1H), 1.61 – 1.31 (m, 8H), 0.95 – 0.90 (m, 3H). **^{13}C NMR** (101 MHz, CDCl$_3$) δ 71.72, 68.46, 55.43, 54.56, 45.17, 43.42, 34.33, 33.43, 31.84, 31.78, 24.96, 22.55, 22.53, 13.98.
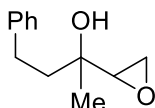
2-(oxiran-2-yl)propan-2-ol (65)

Prepared according to the general procedure for epoxy alcohols described above (20.0 mmol scale). Purification by basic alumina column chromatography (Et$_2$O:hexane, 1:1) gave the product as a colorless liquid in 81% yield (1.65 g, 16.1 mmol). **^{1}H NMR** (500 MHz, CDCl$_3$) δ 2.97 (m, 1H), 2.83 (m, 1H), 2.75 (m, 1H), 1.68 (s, 1H), 1.35 (s, 3H), 1.26 (s, 3H). **^{13}C NMR** (126 MHz, CDCl$_3$) δ 67.61, 58.45, 44.14, 27.69, 24.79.
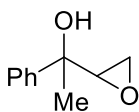
2-(oxiran-2-yl)-4-phenylbutan-2-ol (66)

Prepared according to the general procedure for epoxy alcohols described above (7.3 mmol scale). Purification by basic alumina column chromatography (Et$_2$O:hexane, 1:4) gave the product (a mixture of diastereoisomers) as a colorless liquid in 94% yield (1.33 g, 6.9 mmol).

^{1}H NMR (500 MHz, CDCl$_3$) δ 7.36 – 7.18 (m, 5H), 3.02 (m, 1H), 2.93 – 2.74 (m, 4H), 2.00 – 1.86 (m, 2H), 1.66 – 1.59 (s, 1H), 1.35 (s, 3H). **^{13}C NMR** (126 MHz, CDCl$_3$) δ 142.19, 142.09, 128.46, 128.44, 128.30, 128.28, 125.88, 69.20, 69.14, 57.79, 57.66, 44.36,

Chapter 4

43.37, 43.35, 40.53, 29.87, 29.66, 26.34, 22.89. **HRMS** (ESI+): calcd. m/z 215.1043 [M+ H]$^+$; found: 215.1038.
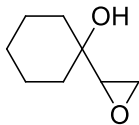
1-(oxiran-2-yl)-1-phenylethanol (69)

Prepared according to the general procedure for epoxy alcohols described above (6.7 mmol scale). Purification by basic alumina column chromatography (Et$_2$O:hexane, 1:2) gave the product (a mixture of diastereoisomers) as a colorless liquid in 91% yield (1.0 g, 6.1 mmol). **¹H NMR** (500 MHz, CDCl$_3$) δ 7.59 – 7.29 (m, 5H), 3.32 (m, 1H), 2.92 (m, 1H), 2.88 – 2.69 (m, 1H), 2.36 (s, 1H), 1.64 (s, 3H). **¹³C NMR** (126 MHz, CDCl$_3$) δ 145.35, 143.57, 128.44, 128.38, 127.43, 124.99, 71.45, 70.68, 58.69, 58.15, 44.54, 44.41, 27.86, 25.50.
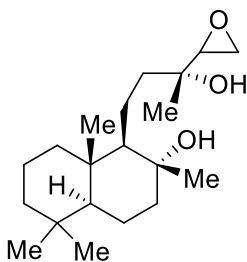
1-(oxiran-2-yl)cyclohexanol (70)

Prepared according to the general procedure for epoxy alcohols described above (8.1 mmol scale). Purification by basic alumina column chromatography (Et$_2$O:hexane, 1:2) gave the product as a colorless liquid in 88% yield (1.0 g, 7.1 mmol). **¹H NMR** (400 MHz, CDCl$_3$) δ 2.99 – 2.93 (m, 1H), 2.88 – 2.81 (m, 1H), 2.74 – 2.68 (m, 1H), 1.62 (m, 8H), 1.47 – 1.26 (m, 2H). **¹³C NMR** (101 MHz, CDCl$_3$) δ 68.01, 58.08, 43.52, 36.30, 33.51, 25.73, 21.39, 21.37.

Sclareol epoxide (94)

Prepared according to the general procedure for epoxy alcohols described above (4.4 mmol scale). Purification by basic alumina column chromatography (Et$_2$O:hexane, 1:1) gave the product (a mixture of diastereoisomers) as a white powder in 94% yield (1.34 g, 4.13 mmol). **¹H NMR** (500 MHz, Chloroform-d) δ 2.96 (m, 1H), 2.85 (m, 1H), 2.74 (m, 1H), 2.52 – 2.07 (m, 1H), 1.91 – 1.85 (m, 1H), 1.83 – 1.64 (m, 6H), 1.61 – 1.54 (m, 2H), 1.48 – 1.38 (m, 4H), 1.25 (m, 3H), 1.18 (m, 3H), 1.15 (m, 2H), 1.04 – 0.92 (m, 2H), 0.89 (s, 3H), 0.83 – 0.80 (m, 6H). **¹³C NMR** (101 MHz, CDCl$_3$) δ 74.63, 74.51, 70.02, 69.63, 62.02, 61.78, 58.28, 58.22, 56.13, 56.10, 44.51, 44.32, 43.96, 43.55, 42.00, 41.98, 41.28, 39.77, 39.71, 39.30, 39.24, 33.38, 33.24, 29.70, 25.39, 24.21, 24.02, 23.08, 21.49, 20.56, 20.50, 18.56, 18.45, 18.43, 18.23, 15.39, 15.37.

Chapter 4

2,3-epoxygeraniol (63)
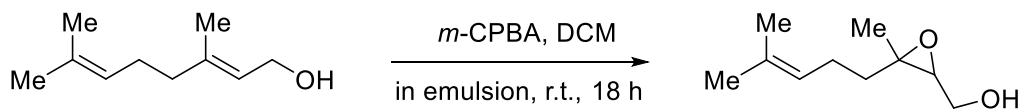
Synthesized according to a modified literature procedure.[123] Additional purification (silica gel chromatography, EtOAc:hexane, 1:4) was performed to obtain the pure product as a slightly yellow liquid. **^{1}H NMR** (500 MHz, CDCl$_3$) δ 5.11 (m, 1H), 3.85 (m, 1H), 3.72 (m, 1H), 3.00 (m, 1H), 2.17 – 2.07 (m, 2H), 1.71 (m, 4H), 1.64 (s, 3H), 1.50 (m, 1H), 1.33 (s, 3H). **^{13}C NMR** (101 MHz, CDCl$_3$) δ 132.15, 123.33, 62.93, 61.45, 61.17, 38.49, 25.66, 23.68, 17.64, 16.75.

N-benzyl-1-(oxiran-2-yl)methanamine (67)
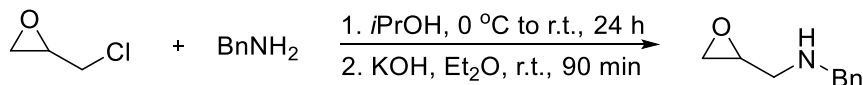
Synthesized according to a modified literature procedure.[124] To a stirred solution of benzylamine (0.64 g, 6.0 mmol) in *iso*-propylalcohol (15 mL) at 0 °C was slowly added epichlorohydrin (0.46 g, 0.40 mL, 5.0 mmol) and stirred for 18 h at rt. The mixture was concentrated after the reaction, re-dissolved in ether and filtered to remove any solid. Dehydrohalogenation was performed by stirring for 90 min with KOH in diethyl ether. Afterwards the ether layer was concentrated and the crude purified by column chromatography to yield the final product as a slightly yellow liquid in 46% yield. **^{1}H NMR** (300 MHz, CDCl$_3$) δ 7.34 (m, 5H), 3.86 (s, 2H), 3.14 (m, 1H), 3.00 (m, 1H), 2.79 (m, 1H), 2.71 – 2.61 (m, 2H). **^{13}C NMR** (75 MHz, CDCl$_3$) δ 140.16, 128.39, 128.09, 126.99, 77.87, 77.45, 77.02, 53.80, 51.68, 50.85, 45.28.

2-methyl-N-(oxiran-2-ylmethyl)propan-2-amine (68)
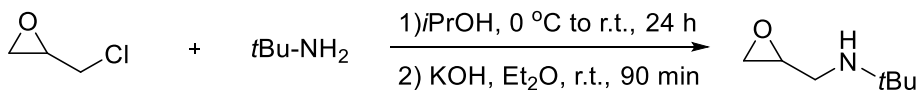
Synthesized according to a modified literature procedure.[124] To a stirred solution of *tert*-butylamine (0.80 g, 11.0 mmol) in *iso*-propylalcohol (25 mL) at 0 °C was slowly added epichlorohydrin (0.93 g, 0.79 mL, 10.0 mmol) and stirred for 18 h at rt. The mixture was concentrated after the reaction, re-dissolved in ether and filtered to remove solids. Dehydrohalogenation was performed by stirring for 90 min with KOH in diethyl ether. Afterwards the ether layer was concentrated and the crude purified by

column chromatography (ether:triethyl amine, 100:1) to yield the final product as a slightly yellow liquid in 57% yield. **^{1}H NMR** (500 MHz, CDCl$_3$) δ 3.14 – 3.07 (m, 1H), 2.86 (m, 1H), 2.79 (m, 1H), 2.64 – 2.59 (m, 2H), 1.11 (s, 9H). **^{13}C NMR** (126 MHz, CDCl$_3$) δ 52.35, 50.13, 45.84, 44.99, 28.96.

3-methyl-*N*-(oxiran-2-ylmethyl)aniline (96)
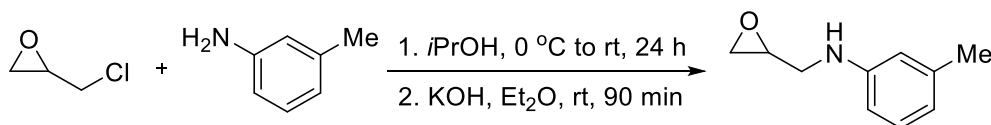
To a stirred solution of *m*-toluidine (1.07 g, 10.0 mmol) in *iso*-propanol (25 mL) at 0°C was slowly added epichlorohydrin (1.86 g, 1.58 mL, 20.0 mmol) and further stirred at rt for 18 h. The solvent was evaporated and the mixture was purified by column chromatography over silica (EtOAC:hexane, 1:10) to obtain the crude halohydrin product. Dehydrohalogenation was performed by stirring for 90 min with KOH in diethyl ether. Afterwards the ether layer was washed with water and brine, dried over MgSO$_4$ and concentrated to yield the final product as a slightly orange liquid in 47% yield (0.94 g, 4.7 mmol). **^{1}H NMR** (500 MHz, CDCl$_3$) δ 7.16 (m, 1H), 6.64 (m, 1H), 6.54 (m, 2H), 3.89 (s, 1H), 3.61 – 3.52 (m, 1H), 3.28 (m, 2H), 2.87 (m, 1H), 2.75 (m, 1H), 2.40 – 2.33 (m, 3H). **^{13}C NMR** (101 MHz, CDCl$_3$) δ 148.04, 139.12, 129.26, 118.86, 113.87, 110.18, 51.12, 45.44, 45.14, 21.70. **HRMS** (ESI+): calcd. *m/z* 164.1070 [M+H]$^+$; found: 164.1075.

4-methyl-N-(oxiran-2-ylmethyl)benzenesulfonamide (95)
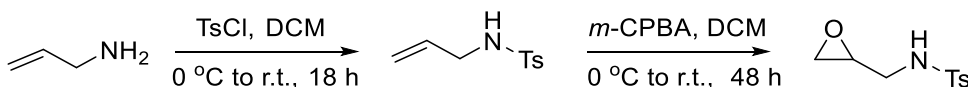
Synthesized according to literature procedure.[125] **^{1}H NMR** (300 MHz, CDCl$_3$) δ 7.76 (d, *J* = 8.3 Hz, 2H), 7.34 (d, *J* = 7.7 Hz, 2H), 4.63 (s, 1H), 3.37 (m, 1H), 3.13 – 2.99 (m, 2H), 2.77 (t, *J* = 4.3 Hz, 1H), 2.65 (m, 1H), 2.45 (s, 3H). **^{13}C NMR** (126 MHz, CDCl$_3$) δ 143.69, 136.78, 129.82, 127.04, 50.35, 45.19, 44.39, 21.54.

### 4.5.3   Typical catalytic coupling of substituted epoxides and CO$_2$

The respective epoxide, Al-complex, co-catalyst (TBAI, TBACl or TBAB) and 1 mL of MEK (2-butanone) were charged into a 30 mL stainless steel autoclave. The autoclave was

Chapter 4

then subjected to three cycles of pressurization and depressurization with carbon dioxide (5 bar), before final stabilization of the pressure to 10–40 bar. The autoclave was sealed and heated to the required temperature and left stirring. At the end of the reaction an aliquot of the resulting mixture was taken and the conversion was determined by means of ^{1}H NMR spectroscopy using CDCl$_3$ as the solvent. The pure cyclic carbonate product was then isolated by column chromatography and the solvent removed under vacuum. The identities of the cyclic carbonate products were confirmed by comparison to literature data or where unavailable, characterized by ^{1}H/^{13}C NMR, IR and HRMS. For compounds **86**, **91** (toloxatone) and **92** the molecular structures were determined by single crystal X-ray crystallography (*vide infra*).

4.5.4 Analytical data for the carbonate/carbamate products
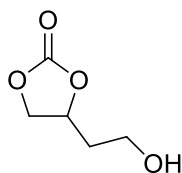
4-(hydroxymethyl)-1,3-dioxolan-2-one (71)
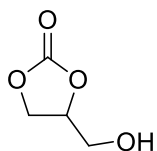
Al^{tBu} (1 mol%), 75 °C, 10 bar, 2 h; conversion: 99%. Isolated by column chromatography (EtOAc:hexane, 1:1) in 93% yield. **^{1}H NMR** (400 MHz, CDCl$_3$) δ 4.83 (m, 1H), 4.58 – 4.44 (m, 2H), 4.00 (m, 1H), 3.73 (m, 1H), 2.91 (t, *J* = 6.2 Hz, 1H). **^{13}C NMR** (101 MHz, CDCl$_3$) δ 155.45, 76.68, 65.82, 61.65. **IR** (neat): 1765 cm^{-1} (C=O).

4-(hydroxymethyl)-4-methyl-1,3-dioxolan-2-one (72)
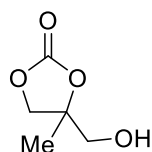
Al^{tBu} (1 mol%), 75 °C, 10 bar, 14 h; conversion: 99%. Isolated by column chromatography (EtOAc:hexane, 1:1) in 85% yield. **^{1}H NMR** (400 MHz, CDCl$_3$) δ 4.53 (d, *J* = 8.3 Hz, 1H), 4.10 (d, *J* = 8.3 Hz, 1H), 3.77 (s, 1H), 3.74 (m, 1H), 3.53 (m, 1H), 1.44 (s, 3H). **^{13}C NMR** (101 MHz, CDCl$_3$) δ 155.48, 84.05, 71.51, 65.80, 21.28. **IR** (neat): 1757 cm^{-1} (C=O). **HRMS** (ESI+): calcd. *m/z* 155.0315 [M+Na]$^+$; found: 155.0313.

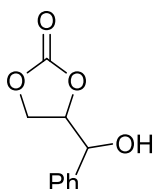**4-(2-hydroxyethyl)-1,3-dioxolan-2-one (73)**

Al^{tBu} (1 mol%), 60 °C, 10 bar, 14 h; conversion: 99%. Isolated by column chromatography (EtOAc:hexane, 1:1) in 87% yield. **^{1}H NMR** (400 MHz, CDCl$_3$) δ 4.93 (m, 1H), 4.60 (m, 1H), 4.20 (m, 1H), 3.79 (m, 2H), 2.95 (s, 1H), 2.09 – 1.84 (m, 2H). **^{13}C NMR** (101 MHz, CDCl$_3$) δ 155.54, 75.40, 69.97, 57.91, 36.08. **IR** (neat): 1774 cm^{-1} (C=O).

Chapter 4

### 4-(hydroxy(phenyl)methyl)-1,3-dioxolan-2-one (74)

Al^{tBu} (2 mol%), 60 °C, 10 bar, 14 h; conversion: 99%; selectivity: 94%. Isolated by column chromatography (EtOAc:hexane, 1:2) as one diastereoisomer (*dr* 97:3) in 85% yield. **^{1}H NMR** (500 MHz, CDCl$_3$) *δ* 7.48 − 7.32 (m, 5H), 5.17 (t, *J* = 3.8 Hz, 1H), 4.86 (m, 1H), 4.56 (m, 1H), 4.26 (m, 1H), 3.04 (d, *J* = 4.1 Hz, 1H). **^{13}C NMR** (126 MHz, CDCl$_3$) *δ* 155.31, 137.05, 128.97, 128.66, 125.85, 79.08, 71.78, 64.55. **IR** (neat): 1784 cm^{-1} (C=O). **HRMS** (ESI+): calcd. *m/z* 217.0471 [M+Na]$^+$; found: 217.0472.

4-(hydroxymethyl)-5-methyl-1,3-dioxolan-2-one (75)
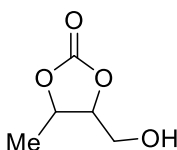
Al^{tBu} (1 mol%), 50 °C, 10 bar, 14 h; conversion: 99%; selectivity: 99%. Isolated by column chromatography (EtOAc:hexane, 1:1) as a mixture of diastereoisomers (*dr* 67:33) in 92% yield. Major diastereoisomer: **^{1}H NMR** (500 MHz, CDCl$_3$) *δ* 5.00 − 4.89 (m, 1H), 4.74 - 4.69 (m, 1H), 3.89 − 3.60 (m, 3H), 1.47 (d, *J* = 6.4 Hz, 3H). **^{13}C NMR** (126 MHz, CDCl$_3$) *δ* 155.38, 79.38, 75.86, 59.77, 14.13. Minor diastereoisomer: **^{1}H NMR** (500 MHz, CDCl$_3$) *δ* 4.74 − 4.69 (m, 1H), 4.33 − 4.26 (m, 1H), 3.89 − 3.60 (m, 3H), 1.47 (d, J = 6.4 Hz, 3H). **^{13}C NMR** (126 MHz, CDCl$_3$) *δ* 155.28, 83.34, 75.16, 60.91, 19.29. **IR** (neat): 1770 cm^{-1} (C=O). **HRMS** (ESI+): calcd. *m/z* 155.0315 [M+Na]$^+$; found: 155.0319.

4-(2-hydroxy-6-methylhept-5-en-2-yl)-1,3-dioxolan-2-one (76)
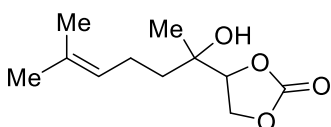
Al^{tBu} (2 mol%), TBAB (2 mol%), DIPEA (10 mol%), 75 °C, 10 bar, 14 h; conversion: 89%; selectivity: 96%. Isolated by column chromatography (ether:hexane, 1:3) as one diastereoisomer (*dr* >99:1) in 65% yield. **^{1}H NMR** (400 MHz, CDCl$_3$) *δ* 5.14 − 5.06 (m, 1H), 4.56 − 4.49 (m, 2H), 4.45 (m, 1H), 2.21 − 2.08 (m, 2H), 1.71 (d, *J* = 1.4 Hz, 3H), 1.64 (d, *J* = 1.3 Hz, 3H), 1.54 − 1.39 (m, 2H), 1.34 (s, 3H). **^{13}C NMR** (101 MHz, CDCl$_3$) *δ* 155.10, 132.98, 123.22, 81.05, 72.10, 65.40, 37.09, 25.67, 22.29, 21.63, 17.70. **IR** (neat): 1779 cm^{-1} (C=O). **HRMS** (ESI+): calcd. *m/z* 237.1097 [M+Na]$^+$; found: 237.1100.

Chapter 4

4-(hydroxymethyl)-5-pentyl-1,3-dioxolan-2-one (77)
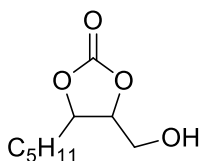
Al^{tBu} (1 mol%), 75 °C, 10 bar, 14 h; conversion: 99%; selectivity: 99%. Isolated by column chromatography (EtOAc:hexane, 1:1) as a mixture of diastereoisomers (*dr* 63:37) in 95% yield. **¹H NMR** (500 MHz, CDCl$_3$) *δ* 4.78 – 4.30 (m, 2H), 3.96 – 3.63 (m, 2H), 3.38 (m, 1H), 1.92 – 1.74 (m, 1H), 1.73 – 1.63 (m, 1H), 1.60 – 1.43 (m, 1H), 1.43 – 1.26 (m, 5H), 0.95 – 0.84 (m, 3H). **¹³C NMR** (126 MHz, CDCl$_3$) *δ* 155.29, 155.25, 81.92, 79.83, 79.33, 78.52, 61.44, 59.91, 33.80, 31.29, 31.26, 28.51, 25.71, 24.06, 22.38, 22.36, 13.88, 13.87. **IR** (neat): 1776 cm^{-1} (C=O).
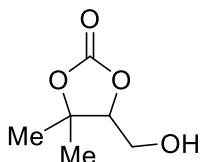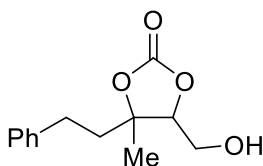
5-(hydroxymethyl)-4,4-dimethyl-1,3-dioxolan-2-one (78)

Al^{tBu} (2 mol%), DIPEA (10 mol%), 70 °C, 30 bar, 14 h; conversion: 99%; selectivity: 99%. Isolated by column chromatography (EtOAc:hexane, 1:1) in 85% yield. **¹H NMR** (500 MHz, CDCl$_3$) *δ* 4.37 (m, 1H), 3.91 – 3.80 (m, 2H), 3.24 (s, 1H), 1.54 (s, 3H), 1.48 (s, 3H). **¹³C NMR** (126 MHz, CDCl$_3$) *δ* 154.49, 84.43, 83.75, 60.10, 27.29, 20.98. **IR** (neat): 1765 cm^{-1} (C=O). **HRMS** (ESI+): calcd. *m/z* 169.0471 [M+Na]$^+$; found: 169.0468.

### 5-(hydroxymethyl)-4-methyl-4-phenethyl-1,3-dioxolan-2-one (79)

Al^{tBu} (2 mol%), DIPEA (10 mol%), 80 °C, 30 bar, 14 h; conversion: >99%; selectivity: >96%. Isolated by column chromatography (EtOAc:hexane, 1:2) as a mixture of diastereoisomers (*dr* 66:34) in 87% yield. Major diastereoisomer: **¹H NMR** (400 MHz, CDCl$_3$) *δ* 7.31 (m, 2H), 7.27 – 7.18 (m, 3H), 4.45 (m, 1H), 3.90 (m, 2H), 2.78 (m, 2H), 2.69 (m, 1H), 2.27 – 1.92 (m, 2H), 1.62 (s, 3H). **¹³C NMR** (101 MHz, CDCl$_3$) *δ* 154.22, 140.25, 128.70, 128.25, 126.42, 85.26, 83.14, 60.49, 42.31, 29.35, 19.12. Minor diastereoisomer: **¹H NMR** (400 MHz, CDCl$_3$) *δ* 7.31 (m, 2H), 7.27 – 7.18 (m, 3H), 4.42 (m, 1H), 3.90 (m, 2H), 2.78 (m, 2H), 2.63 (m, 1H), 2.27 – 1.92 (m, 2H), 1.55 (s, 3H). **¹³C NMR** (101 MHz, CDCl$_3$) *δ* 154.22, 140.71, 128.67, 128.30, 126.37, 85.21, 83.14, 59.84, 35.91, 29.77, 24.14. **IR** (neat): 1771 cm^{-1} (C=O). **HRMS** (ESI+): calcd. *m/z* 231.0628 [M+Na]$^+$; found: 231.0620.
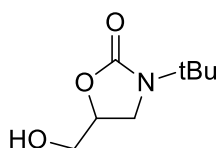
Chapter 4
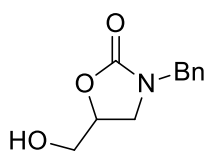
3-benzyl-5-(hydroxymethyl)oxazolidin-2-one (80)

Al^{tBu} (1 mol%), 40 °C, 10 bar, 14 h; conversion: 99%; selectivity: 99%. Isolated by column chromatography (EtOAc:hexane, 1:1) in 94% yield. **^{1}H NMR** (400 MHz, Acetone-d_6) δ 7.40 − 7.24 (m, 5H), 4.60 − 4.51 (m, 1H), 4.40 (s, 2H), 4.31 (m, 1H), 3.76 − 3.57 (m, 2H), 3.54 − 3.31 (m, 2H). **^{13}C NMR** (101 MHz, Acetone-d_6) δ 205.67, 157.85, 136.76, 128.63, 127.80, 127.51, 73.65, 62.49, 47.61, 45.22. **IR** (neat): 1719 cm^{-1} (C=O).

### 3-(*tert*-butyl)-5-(hydroxymethyl)oxazolidin-2-one (81)

Al^{tBu} (1 mol%), 30 °C, 10 bar, 14 h; conversion: 99%; selectivity: 94%. Isolated by column chromatography (EtOAc:hexane, 1:1) in 81% yield. **^{1}H NMR** (500 MHz, CDCl$_3$) δ 4.51 − 4.45 (m, 1H), 3.84 (d, J = 12.5 Hz, 1H), 3.66 (d, J = 12.5 Hz, 1H), 3.63 (m, 1H), 3.54 (m, 1H), 2.93 (s, 1H), 1.40 (s, 9H). **^{13}C NMR** (126 MHz, CDCl$_3$) δ 156.78, 72.29, 62.95, 53.55, 44.54, 27.39. **IR** (neat): 1713 cm^{-1} (C=O). **HRMS** (ESI+): calcd. *m/z* 196.0944 [M+Na]$^+$; found: 196.0943.

5-(hydroxymethyl)-4-methyl-4-phenyl-1,3-dioxolan-2-one (82)
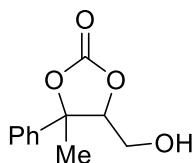
Al^{tBu} (2 mol%), 80 °C, 30 bar, 40 h; conversion: 99%; selectivity: 54%. Isolated by column chromatography (EtOAc:hexane, 1:2) as a mixture of diastereoisomers (*dr* 67:33) in 41% yield. Major diastereoisomer: **^{1}H NMR** (400 MHz, CDCl$_3$) δ 7.48 − 7.34 (m, 5H), 4.71-4.68 (m, 1H), 4.06 (m, 2H), 2.36 (m, 1H), 1.81 (s, 3H). **^{13}C NMR** (101 MHz, CDCl$_3$) δ 153.72, 142.04, 129.03, 128.59, 123.86, 85.86, 85.53, 60.55, 22.29. Minor diastereoisomer: **^{1}H NMR** (400 MHz, CDCl$_3$) δ 7.48 − 7.34 (m, 5H), 4.66-4.63 (m, 1H), 3.88 (m, 2H), 1.92 (s, 3H), 1.76 (m, 1H). **^{13}C NMR** (101 MHz, CDCl$_3$) δ 153.87, 137.04, 128.88, 128.82, 124.75, 85.48, 85.20, 61.61, 27.66. **IR** (neat): 1784 cm^{-1} (C=O). **HRMS** (ESI+): calcd. *m/z* 231.0628 [M+Na]$^+$; found: 231.0620.
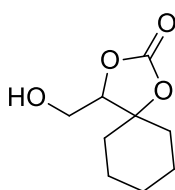
4-(hydroxymethyl)-1,3-dioxaspiro[4.5]decan-2-one (83)

Al^{tBu} (2 mol%), TBAB (5 mol%), 80 °C, 10 bar, 14 h; conversion: 96%; selectivity: 75%. Isolated by column chromatography (EtOAc:hexane, 1:2) in 68% yield. **^{1}H NMR** (500 MHz, CDCl$_3$) δ 4.30 (t, J = 5.0 Hz, 1H), 3.87 (m, 2H), 2.85 (t, J = 6.1 Hz, 1H), 2.04 − 1.91 (m, 2H), 1.71 − 1.59 (m, 6H), 1.36 − 1.20 (m, 2H). **^{13}C NMR** (126 MHz, CDCl$_3$) δ 154.39, 84.95, 84.50, 60.03, 36.32, 29.97, 24.72, 21.88, 21.85. **IR** (neat): 1767 cm^{-1} (C=O). **HRMS** (ESI+): calcd. *m/z* 209.0784 [M+Na]$^+$; found: 209.0779.

Chapter 4

4-(2-hydroxybutan-2-yl)-1,3-dioxolan-2-one (84)
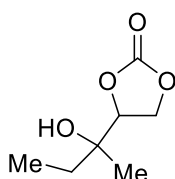
Al^{tBu} (2 mol%), TBAB (5 mol%), 25 °C, 10 bar, 60 h; conversion: 95%; selectivity: 85%. Isolated by column chromatography (EtOAc:hexane, 1:1) as a mixture of diastereoisomers (*dr* 69:31) in 76% yield. **^{1}H NMR** (500 MHz, CDCl$_3$) *δ* 4.60 − 4.51 (m, 2H), 4.50 − 4.42 (m, 1H), 2.11 − 2.10 (s, 1H), 1.75 − 1.40 (m, 2H), 1.32 − 1.10 (s, 3H), 1.03 − 0.94 (m, 3H). **^{13}C NMR** (75 MHz, CDCl$_3$) *δ* 155.21, 81.12, 80.63, 72.10, 65.43, 65.37, 31.22, 29.88, 21.85, 20.13, 7.73, 7.21. **IR** (neat): 1775 cm^{-1} (C=O). **HRMS** (ESI+): calcd. *m/z* 183.0628 [M+Na]$^+$; found: 183.0627.

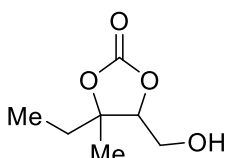### 4-ethyl-5-(hydroxymethyl)-4-methyl-1,3-dioxolan-2-one (85)

Al^{tBu} (2 mol%), 80 °C, 10 bar, 40 h; conversion: 99%; selectivity: 93%. Isolated by column chromatography (EtOAc:hexane, 1:1) as a mixture of diastereoisomers (*dr* 62:38) in 86% yield. **^{1}H NMR** (500 MHz, CDCl$_3$) *δ* 4.39 (m, 1H), 3.85 (m, 2H), 3.16 (m, 1H), 1.98–1.61 (m, 2H), 1.47 (m, 3H), 1.03 (m, 3H). **^{13}C NMR** (75 MHz, CDCl$_3$) *δ* 154.58, 86.06, 85.95, 85.33, 82.96, 60.52, 59.78, 33.26, 26.60, 23.40, 18.61, 7.81, 7.33. **IR** (neat): 1766 cm^{-1} (C=O). **HRMS** (ESI+): calcd. *m/z* 183.0628 [M+Na]$^+$; found: 183.0626.

Sclareol carbonate – conventional carbonate product (86)
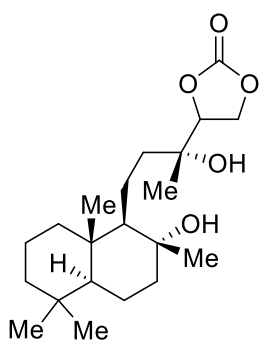
Al^{tBu} (2 mol%), TBAB (5 mol%), 50 °C, 30 bar, 14 h; conversion: >99%; selectivity: 79%. Isolated by column chromatography (acetone:hexane, 1:5) as a mixture of diastereoisomers (*dr* 52:48) in 72% yield. **^{1}H NMR** (500 MHz, CDCl$_3$) *δ* 4.60 − 4.51 (m, 1H), 4.49 − 4.40 (m, 2H), 2.31 (s, 1H), 1.91 − 1.72 (m, 2H), 1.71 − 1.36 (m, 10H), 1.29 (s, 3H), 1.22 − 1.20 (m, 3H), 1.13 (s, 3H), 1.01 − 0.91 (m, 2H), 0.89 (m, 3H), 0.81 (m, 6H). **^{13}C NMR** (126 MHz, CDCl$_3$) *δ* 155.28, 155.24, 81.95, 81.90, 75.52, 75.39, 72.75, 72.03, 65.61, 65.39, 61.90, 61.42, 55.99, 44.30, 44.02, 41.89, 41.88, 39.93, 39.88, 39.65, 39.53, 39.23, 39.20, 33.33, 33.32, 33.23, 33.21, 24.45, 24.00, 21.46, 21.03, 20.68, 20.48, 20.42, 18.35, 17.94, 17.76, 15.42, 15.32. **IR** (neat): 1783 cm^{-1} (C=O). **HRMS** (ESI+): calcd. *m/z* 391.2455 [M+Na]$^+$; found: 391.2454.

Chapter 4

Sclareol carbonate - carbonate product via substrate-assisted route (87)
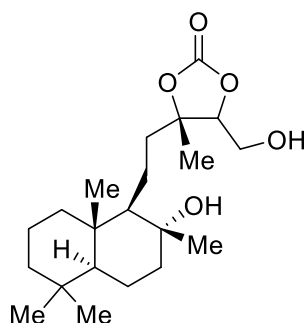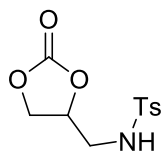
Al^{tBu} (2 mol%), TBACl (10 mol%), 75 °C, 10 bar, 14 h; conversion: >99%; selectivity: 79%. Isolated by column chromatography (acetone:hexane, 1:5) as a mixture of diastereoisomers (*dr* 85:15) in 68% yield. **^{1}H NMR** (500 MHz, CDCl$_3$) *δ* 4.53 (t, *J* = 5.4 Hz, 1H), 3.96 – 3.77 (m, 2H), 3.54 (s, 1H), 1.97 – 1.80 (m, 3H), 1.70 – 1.48 (m, 5H), 1.46 (s, 3H), 1.44 – 1.22 (m, 5H), 1.19 (m, 3H), 1.16 – 1.03 (m, 2H), 0.92 (m, 2H), 0.88 (m, 3H), 0.80 (m, 6H). **^{13}C NMR** (126 MHz, CDCl$_3$) *δ* 154.64, 154.52, 86.02, 83.54, 81.97, 74.79, 74.74, 61.90, 61.63, 61.48, 60.51, 60.25, 59.48, 56.06, 56.02, 44.44, 44.10, 43.83, 43.14, 41.90, 41.88, 39.70, 39.47, 39.19, 39.15, 37.28, 33.36, 33.23, 24.57, 24.22, 24.12, 24.01, 23.92, 23.80, 21.45, 20.47, 20.40, 19.88, 18.38, 18.28, 15.53, 15.48. **IR** (neat): 1775 cm^{-1} (C=O). **HRMS** (ESI+): calcd. *m/z* 391.2455 [M+Na]$^+$; found: 391.2450.

4-methyl-*N*-((2-oxo-1,3-dioxolan-4-yl)methyl)benzenesulfonamide (88)

Al^{tBu} (2 mol%), TBAB (5 mol%), 75 °C, 10 bar, 14 h; conversion: >99%; selectivity: 97%. Isolated by column chromatography (EtOAc:hexane, 1:2) in 89% yield. **^{1}H NMR** (500 MHz, Acetone-*d$_6$*) *δ* 7.79 (m, 2H), 7.47 – 7.38 (m, 2H), 7.00 (m, 1H), 4.98 – 4.89 (m, 1H), 4.64 (m, 1H), 4.43 (m, 1H), 3.40 – 3.20 (m, 2H), 2.44 (s, 3H). **^{13}C NMR** (126 MHz, Acetone-*d$_6$*) *δ* 154.47, 143.34, 137.81, 129.68, 126.89, 75.16, 66.53, 44.56, 20.49. **IR** (neat): 1770 cm^{-1} (C=O). **HRMS** (ESI+): calcd. *m/z* 294.0407 [M+Na]$^+$; found: 294.0404.

5-(hydroxymethyl)-3-tosyloxazolidin-2-one (89)
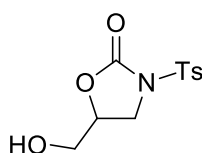
Al^{tBu} (2 mol%), DIPEA (10 mol%), 50 °C, 30 bar, 40 h; conversion: >99%; selectivity: 77%. Isolated by column chromatography (EtOAc:hexane, 1:1) in 65% yield. **^{1}H NMR** (400 MHz, Acetone-*d$_6$*) *δ* 7.96 – 7.90 (m, 2H), 7.50 – 7.45 (m, 2H), 4.75 (m, 1H), 4.50 – 4.36 (m, 1H), 4.21 (t, *J* = 8.8 Hz, 1H), 4.05 (m, 1H), 3.82 (m, 1H), 3.68 (m, 1H), 2.47 (s, 3H). **^{13}C NMR** (101 MHz, Acetone-*d$_6$*) *δ* 205.47, 151.67, 145.43, 134.89, 129.68, 128.10, 74.71, 61.50, 45.64, 20.66. **IR** (neat): 1763 cm^{-1} (C=O). **HRMS** (ESI+): calcd. *m/z* 294.0407 [M+Na]$^+$; found: 294.0410.
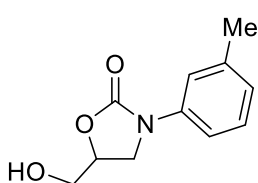
Chapter 4

4-((*m*-tolylamino)methyl)-1,3-dioxolan-2-one (90)
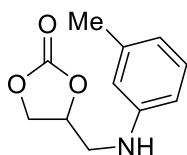
Al^{tBu} (2 mol%), TBAB (5 mol%), 30 °C, 10 bar, 40 h; conversion: >99%; selectivity: 81%. Isolated by column chromatography (EtOAc:hexane, 1:2) in 80% yield. **^{1}H NMR** (400 MHz, CDCl$_3$) δ 7.12 (t, J = 8.0 Hz, 1H), 6.64 (d, J = 7.4 Hz, 1H), 6.49 (m, 2H), 4.99 − 4.87 (m, 1H), 4.55 (t, J = 8.4 Hz, 1H), 4.30 (m, 1H), 4.20 − 3.73 (m, 1H), 3.54 (m, 1H), 3.44 (m, 1H), 2.32 (s, 3H). **^{13}C NMR** (101 MHz, CDCl$_3$) δ 154.86, 147.04, 139.39, 129.37, 119.73, 114.10, 110.32, 75.45, 67.17, 45.91, 21.60. **IR** (neat): 1809 cm^{-1} (C=O). **HRMS** (ESI+): calcd. *m/z* 208.0968 [M+Na]$^+$; found: 208.0966.

5-(hydroxymethyl)-3-(m-tolyl)oxazolidin-2-one (Toloxatone) (91)

Al^{tBu} (2 mol%), TBAB (2 mol%), 75 °C, 10 bar, 14 h; conversion: >99%; selectivity: 81%. Isolated by column chromatography (EtOAc:hexane, 1:1) in 74% yield. **^{1}H NMR** (500 MHz, CDCl$_3$) δ 7.40 (s, 1H), 7.34 (m, 1H), 7.28 (m, 1H), 6.98 (m, 1H), 4.78 − 4.71 (m, 1H), 4.07 − 3.96 (m, 3H), 3.78 (m, 1H), 2.66 (t, J = 6.6 Hz, 1H), 2.38 (m, 3H). **^{13}C NMR** (126 MHz, CDCl$_3$) δ 154.86, 139.03, 138.02, 128.88, 125.06, 119.13, 115.51, 72.87, 62.84, 46.50, 21.62. **IR** (neat): 1721 cm^{-1} (C=O).

4.5.5 Benzylation of 4-(hydroxy(phenyl)methyl)-1,3-dioxolan-2-one

The alcohol group of cyclic carbonate **74** was benzylated to obtain crystals suitable for X-ray diffraction in order to determine the absolute stereochemistry of the product. NMR analysis revealed a mixture of two diastereo-isomers for product **74**, with a *dr* of approximately 30:1. X-ray analysis revealed the major product to be the (*R,S*)-isomer (**92**).
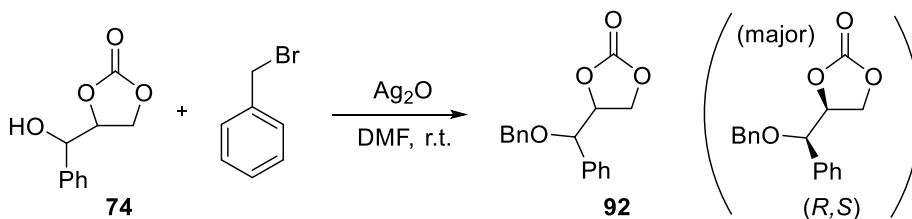
To a solution of the cyclic carbonate **74** in DMF was added silver(I)oxide and benzyl bromide at rt and the mixture was stirred for 18 h. Hereafter the mixture was washed

Chapter 4

with water and extracted with ether to remove the DMF. The solvent was evaporated to give the crude product which was purified using column chromatography (silica stationary phase) to obtain the pure product as a white solid in 46% yield (64 mg, 0.23 mmol). **^{1}H NMR** (400 MHz, CDCl$_3$): δ = 7.50 – 7.30 (m, 10H), 4.77 (m, 1H), 4.73 – 4.64 (m, 2H), 4.59 (m, 1H), 4.44 (d, J = 11.7 Hz, 1H), 4.34 (t, J = 8.4 Hz, 1H). **^{13}C NMR** (101 MHz, CDCl$_3$) δ 154.87, 136.98, 135.47, 129.14, 129.00, 128.57, 128.09, 127.92, 126.90, 79.46, 78.50, 71.27, 65.26, 53.45, 31.60, 22.66, 14.12. **IR** (neat): 1797 cm^{-1} (C=O). **HRMS** (ESI+): calcd. m/z 307.0941 [M+Na]$^+$; found: 307.0944.

4.5.6 Crystallographic studies

The measured crystals were stable under atmospheric conditions; nevertheless they were treated under inert conditions immersed in perfluoro-polyether as protecting oil for manipulation. Data Collection: measurements were made on a Bruker-Nonius diffractometer equipped with an APPEX II 4K CCD area detector, a FR591 rotating anode with Mo Kα radiation, Montel mirrors and a Kryoflex low temperature device (T = −173 °C). Full-sphere data collection was used with ω and φ scans. Programs used: Data collection Apex2 V2011.3 (Bruker-Nonius 2008), data reduction Saint+Version 7.60A (Bruker AXS 2008) and absorption correction SADABS V. 2008−1 (2008). Structure Solution: SHELXTL Version 6.10 (Sheldrick, 2000) was used. Structure Refinement: SHELXTL-97-UNIX VERSION. CCDC-1441881 (**86**), CCDC-1441880 (**91**) and CCDC-1441879 (**92**) contain the supplementary crystallographic data for this paper. These data can be obtained free of charge from The Cambridge Crystallographic Data Centre via www.ccdc.cam.ac.uk/data_request/cif.

Crystallographic Data for Compound 86:

C$_{22}$H$_{39}$Cl$_3$O$_5$, M_r = 495.88, triclinic, $P2(1)2(1)2(1)$, a = 13.5715(6) Å, b = 15.6227(7) Å, c = 23.8600(12) Å, α = β = γ = 90°, V = 5058.9(4) Å^3, Z = 8, ρ = 1.302 mg·M^{-3}, μ = 0.392 mm^{-1}, λ = 0.71073 Å, T = 100(2) K, F(000) = 2120, crystal size = 0.35 × 0.10 × 0.07 mm, θ(min) = 1.988°, θ(max) = 32.738°, 84371 reflections collected, 18653 reflections unique (R_{int} = 0.0331), GoF = 1.063, R_1 = 0.0403 and wR_2 = 0.1034 [$I > 2\sigma(I)$], R_1 = 0.0482 and wR_2 = 0.1078 (all indices), min/max residual density = −0.386/0.330 [e·Å^{-3}]. Completeness to θ(32.738°) = 99.9%. Flack parameter x = 0.023(9).

Chapter 4

86
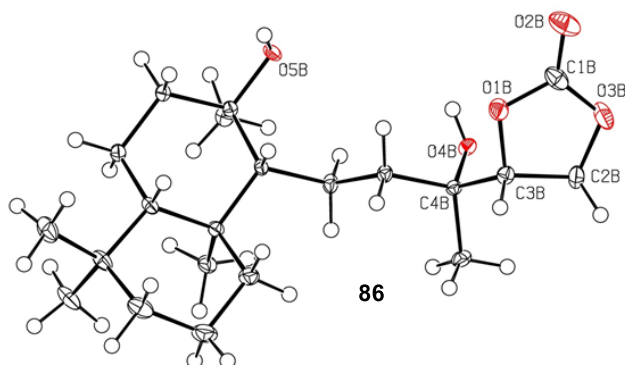
Crystallographic Data for Compound 91:

$C_{11}H_{13}NO_3$, M_r = 207.22, monoclinic, $P2(1)/c$, a = 10.4299(13) Å, b = 10.5784(11) Å, c = 9.2246(13) Å, $\alpha = \gamma = 90°$, $\beta = 83.022(4)°$, V = 1010.2(2) Å³, Z = 4, ρ = 1.362 mg·M⁻³, μ = 0.100 mm⁻¹, λ = 0.71073 Å, T = 100(2) K, $F(000)$ = 440, crystal size = 0.60 × 0.50 × 0.40 mm, θ(min) = 1.967°, θ(max) = 32.451°, 18857 reflections collected, 3445 reflections unique (R_{int} = 0.0449), GoF = 1.049, R_1 = 0.0447 and wR_2 = 0.1156 [$I > 2\sigma(I)$], R_1 = 0.0563 and wR_2 = 0.1232 (all indices), min/max residual density = −0.457/0.287 [e·Å⁻³]. Completeness to θ(32.451°) = 94.6%.


91

Chapter 4
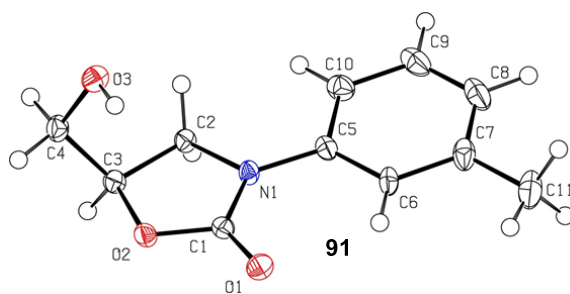
4.6 References

[30]   M. M. Heravi, V. Zadsirjan, *Tetrahedron: Asymmetry* **2013**, *24*, 1149-1188.

[31]   L. Aurelio, R. T. C. Brownlee, A. B. Hughes, *Chem. Rev.* **2004**, *104*, 5823-5846.

[32]   Z. Giovanni, M. Pilar, M. Giuliano Delle, M. Domenico, N. Laura, B. Bruno, *Mini-Rev. Med. Chem.* **2007**, *7*, 389-409.

[33]   A. Sarkar, S. Bhattacharyya, S. K. Dey, S. Karmakar, A. Mukherjee, *New J. Chem.* **2014**, *38*, 817-826.

[44]   C. J. Whiteoak, N. Kielland, V. Laserna, F. Castro-Gómez, E. Martin, E. C. Escudero-Adán, C. Bo, A. W. Kleij, *Chem. Eur. J.* **2014**, *20*, 2264-2275.

[61]   a) J. Klankermayer, S. Wesselbaum, K. Beydoun, W. Leitner, *Angew. Chem. Int. Ed.* **2016**, *55*, 7296-7343; b) Q. Liu, L. Wu, R. Jackstell, M. Beller, *Nat. Commun.* **2015**, *6*, 5933.

[77]   M. Kol, M. Shamis, I. Goldberg, Z. Goldschmidt, S. Alfi, E. Hayut-Salant, *Inorg. Chem. Commun.* **2001**, *4*, 177-179.

[102] S. Minakata, I. Sasaki, T. Ide, *Angew. Chem. Int. Ed.* **2010**, *49*, 1309-1311.

[110] M. Aresta, A. Dibenedetto, A. Angelini, *Chem. Rev.* **2014**, *114*, 1709-1742.

[111] N. Homs, J. Toyir, P. R. de la Piscina, in *New and Future Developments in Catalysis*, Elsevier, Amsterdam, **2013**, pp. 1-26.

[112] a) S. Yoshida, K. Fukui, S. Kikuchi, T. Yamada, *J. Am. Chem. Soc.* **2010**, *132*, 4072-4073; b) Z. Yang, B. Yu, H. Zhang, Y. Zhao, Y. Chen, Z. Ma, G. Ji, X. Gao, B. Han, Z. Liu, *ACS Catal.* **2016**, *6*, 1268-1273.

[113] J. Rintjema, W. Guo, E. Martin, E. C. Escudero-Adán, A. W. Kleij, *Chem. Eur. J.* **2015**, *21*, 10754-10762.

[114] B. A. Vara, T. J. Struble, W. Wang, M. C. Dobish, J. N. Johnston, *J. Am. Chem. Soc.* **2015**, *137*, 7302-7305.

[115] J. Rintjema, A. W. Kleij, *Synthesis* **2016**, *48*, 3863-3878.

[116] a) R. M. Hanson, *Chem. Rev.* **1991**, *91*, 437-475; b) A. Riera, M. Moreno, *Molecules* **2010**, *15*, 1041; c) J. L. Olivares-Romero, Z. Li, H. Yamamoto, *J. Am. Chem. Soc.* **2013**, *135*, 3411-3413; d) C. Wang, H. Yamamoto, *J. Am. Chem. Soc.* **2014**, *136*, 1222-1225.

[117] a) A. G. Myers, K. L. Widdowson, *Tetrahedron Lett.* **1988**, *29*, 6389-6392; b) A. G. Myers, P. J. Proteau, T. M. Handel, *J. Am. Chem. Soc.* **1988**, *110*, 7212-7214; c) J. A. H. Inkster, I. Ling, N. S. Honson, L. Jacquet, R. Gries, E. Plettner, *Tetrahedron: Asymmetry* **2005**, *16*, 3773-3784; d) P. Yan, X. Tan, H. Jing, S. Duan, X. Wang, Z. Liu, *J. Org. Chem.* **2011**, *76*, 2459-2464.

[118] a) O. Hauenstein, M. Reiter, S. Agarwal, B. Rieger, A. Greiner, *Green Chem.* **2016**, *18*, 760-770; b) C. M. Byrne, S. D. Allen, E. B. Lobkovsky, G. W. Coates, *J. Am. Chem. Soc.* **2004**, *126*, 11404-11405; c) L. Peña Carrodeguas, J. González-Fabra, F. Castro-Gómez, C. Bo, A. W. Kleij, *Chem. Eur. J.* **2015**, *21*, 6115-6122.

[119]   a) G. Fiorani, M. Stuck, C. Martín, M. M. Belmonte, E. Martin, E. C. Escudero-Adán, A. W. Kleij, *ChemSusChem* **2016**, *9*, 1304-1311; b) L. Pena Carrodeguas, A. Cristofol, J. M. Fraile, J. A. Mayoral, V. Dorado, C. I. Herrerias, A. W. Kleij, *Green Chem.* **2017**, *19*, 3535-3541.

[120]   a) A. W. Miller, S. T. Nguyen, *Org. Lett.* **2004**, *6*, 2301-2304; b) Z.-Z. Yang, Y.-N. Li, Y.-Y. Wei, L.-N. He, *Green Chem.* **2011**, *13*, 2351-2353.

[121]   M. R. Barbachyn, C. W. Ford, *Angew. Chem. Int. Ed.* **2003**, *42*, 2010-2023.

[122]   Z. Deng, J. Wei, L. Liao, H. Huang, X. Zhao, *Org. Lett.* **2015**, *17*, 1834-1837.

[123]   M. Nakamura, N. Tsutsui, T. Takeda, T. Tokoroyama, *Tetrahedron Lett.* **1984**, *25*, 3231-3232.

[124]   V. R. Gaertner, *Tetrahedron* **1967**, *23*, 2123-2136.

[125]   M. Sova, A. Kovač, S. Turk, M. Hrast, D. Blanot, S. Gobec, *Bioorg. Chem.* **2009**, *37*, 217-222.

Chapter 5.

Mechanistic Studies towards the Formation and Reactivity of Alkyl Carbonate Anions in Cyclic Carbonate Synthesis
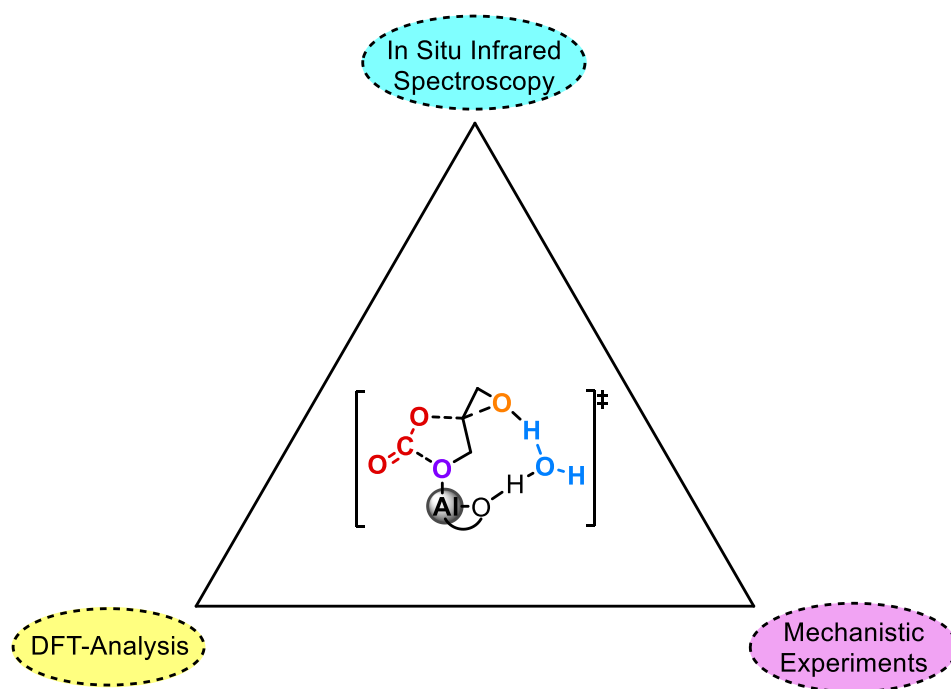
In collaboration with:
Joan González-Fabra and Prof. Carles Bo (DFT-calculations)
Dr. Rui Huang and Dr. Atsushi Urakawa (IR-spectroscopy)
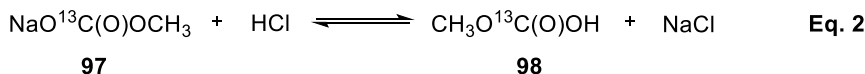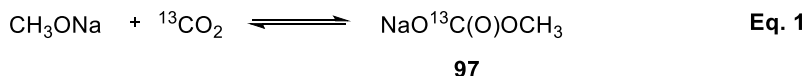
UNIVERSITAT ROVIRA I VIRGILI
ALUMINUM-CATALYZED COUPLING OF CARBON DIOXIDE AND CYCLIC ETHERS
Jeroen Rintjema Tanger

Chapter 5

5.1 Introduction

Carbonic acid and its derivatives such as the bicarbonate anion are important molecules that play a central role in many physiological and biological processes. As such, many groups have investigated the bicarbonate anion and related species using DFT calculations[126] and performing spectroscopic studies,[127] which show that even a seemingly simple system based on water and CO_2 displays rather complex properties and interactions. In the same way that carbonic acid is formed from CO_2 and water, the dissolvation of CO_2 in alcohols supposedly leads to the formation of carbonic acid monoalkyl esters. Compelling evidence for the interaction/activation of carbon dioxide with alcohols to form alkyl carbonic acid species comes, for instance, from its reaction with diazodiphenylmethane.[128] The latter is a compound that reacts with carboxylic acids forming related carbonate and ether species. Alcohols were found to react with diazodiphenylmethane in supercritical CO_2 forming the aforementioned product, which suggests the intermediacy of a carbonic acid species. In 2006 the group of Dibenedetto reported on the succesful room temperature preparation of the monomethyl ester of carbonic acid and analyzed this species by IR and NMR (see Equation 1 and 2).

$$CH_3ONa \ + \ {}^{13}CO_2 \ \rightleftharpoons \ NaO^{13}C(O)OCH_3 \qquad \textbf{Eq. 1}$$
$$\textbf{97}$$

$$NaO^{13}C(O)OCH_3 \ + \ HCl \ \rightleftharpoons \ CH_3O^{13}C(O)OH \ + \ NaCl \qquad \textbf{Eq. 2}$$
$$\textbf{97} \qquad\qquad\qquad\qquad\quad \textbf{98}$$

Upon reacting sodium methoxide with CO_2, species **97** is formed which is a white solid with an $\nu_{C=O}$ absorption of the carbonate moiety residing at 1631 cm^{-1}. Protonation with HCl in aqueous media leads to the formation of **98** with two carbonyl based peaks in the IR spectra present at 1730 and 1779 cm^{-1}. Moreover, two new signals can be found in the ^{1}H and ^{13}C NMR spectra: a singlet at 4.76 ppm which is attributed to the acidic species **98**, and a carbonyl based peak at 159.92 ppm. More recently, the group of Stoddart investigated the properties of a metal-organic framework (MOF) consisting of cyclodextrin units. This MOF was capable of reversibly binding CO_2 through its hydroxyl groups present in the cyclodextrin units, forming a carbonic acid species. Evidence for this formation was provided by solid state ^{13}C NMR, showing a diagnostic, new peak at $\delta = 158$ (cf., formation of a carbonate) upon exposure of the MOF to CO_2 (Figure 20).[129]
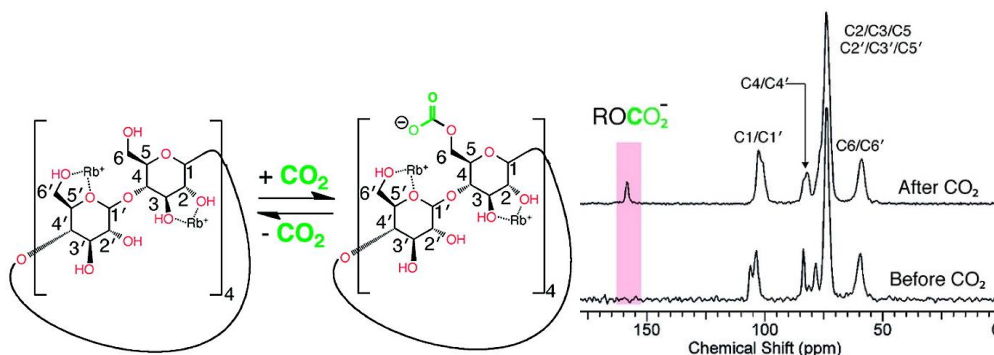
Chapter 5

Figure 20. Reversible chemisorption of CO_2 by the cyclodextrin based MOF (left) and the occurrence of a new peak in ^{13}C-NMR assigned to the alkyl carbonate anion (right).

While there is a substantial amount of reports on the mechanism and reaction intermediates associated with the chemisorption of CO_2,[130] there are very few studies on the involvement of alkyl carbonic acids in catalysis.[131] A recent example by Park *et al.* reported on the beneficial effect of added water in the DMAP-mediated formation of cyclic carbonates, where water is proposed to form a bicarbonate species that acts as a catalyst.[132] In the aforementioned examples however, quaternary ammonium salts or nitrogen bases are added to stabilize the bicarbonate species. Recently we reported on the halide-free reaction between epoxy alcohols and CO_2 (chapter 4 of this thesis) where we proposed the formation of an alkyl carbonate anion that acts as an internal nucleophile to ring-open the epoxide.[133]

In contrast to the chemisorption of CO_2, the alkyl carbonate anion acts in this latter example as an intermediate that leads to a carbonate product. As a result, the concentration is comparatively low which makes it difficult to detect by spectroscopic means. However, *in-situ* IR spectroscopy has emerged in recent years as a powerful technique in organic synthesis. By combining IR-spectroscopy with both experimental work and DFT calculations we herein provide a detailed mechanistic analysis of the Al-aminotriphenolate mediated coupling of glycidol and CO_2. Understanding the mechanism of chemical transformations under turnover conditions has become a crucial part of catalyst design as well as in the development and improvement of synthetic methodologies.[134] The results presented in this chapter provide useful mechanistic insight for other common substrates such as allylic and propargylic amines/alcohols or aziridines that follow a similar reaction pathway.

When considering epoxy alcohols as substrates, there is an additional epoxide moiety that can interact with CO_2 as well, leading to two possible reaction pathways (see Scheme 18). While the mechanism related to conventional (external) nucleophile-

Chapter 5

assisted ring-opening of epoxides has been well documented in the literature,[44, 72] there is only one report that reports the mechanism associated with the coupling of an epoxy alcohol and CO_2. The group of Capacchione investigated the coupling of glycidol with CO_2 by comparing its reactivity with other epoxides both experimentally and via DFT analysis.[135] Much higher yields are found when comparing glycidol to methyl glycidyl ether (that does not contain a free hydroxy group), consistent with a lower activation energy for glycidol. Interestingly, they found that glycidol itself is a hydrogen bond donor and acts as a catalyst in the conversion of several terminal epoxides. A main difference is, however, that an external nucleophile was required for decent turnover kinetics and the hydroxy group of glycidol served to activate the epoxide and stabilize reaction intermediates. In this chapter, the mechanism investigated does not imply the use of an external nucleophile and glycidol is supposed to primarily interact with CO_2 to generate a nucleophilic species *in-situ*.

5.2 Objectives

In this chapter we aim to elucidate the mechanism related to the halide-free formation of cyclic carbonates from CO_2 and epoxy alcohols using glycidol as a model substrate. The reaction mechanism is investigated by DFT analysis supported by experimental data and kinetics, labeling experiments, NMR and *operando* IR spectroscopy. The main aspects we wish to adress are the role of the aluminum catalyst, the activation mode of CO_2 and the nature of the nucleophilic ring-opening step. The outcome of this work can be useful in a wider context as related substrates such as allylic and propargylic alcohols activate CO_2 in a rather similar fashion.

5.3 Results and discussion

As a starting point for our mechanistic investigations we used the catalytic cycle that was proposed in the previous chapter (see Scheme 20). Glycidol is used as a model substrate in our studies, however in some cases substituted epoxy alcohols are used for comparison to see the influence of steric and electronic effects. The first step of the initial manifold is the loss of a coordinated THF from the aluminum center forming **I**, which creates a vacant position to coordinate the epoxide. The aluminum center in this case coordinates to the alcohol unit rather than activating the epoxide moiety in conventional epoxides (**II**). Binding of CO_2 generates the alkyl carbonate species that

Chapter 5

acts as an internal nucleophile to ring-open the epoxide (**III**), leading to formation of glycidol carbonate and regeneration of the free Al complex.
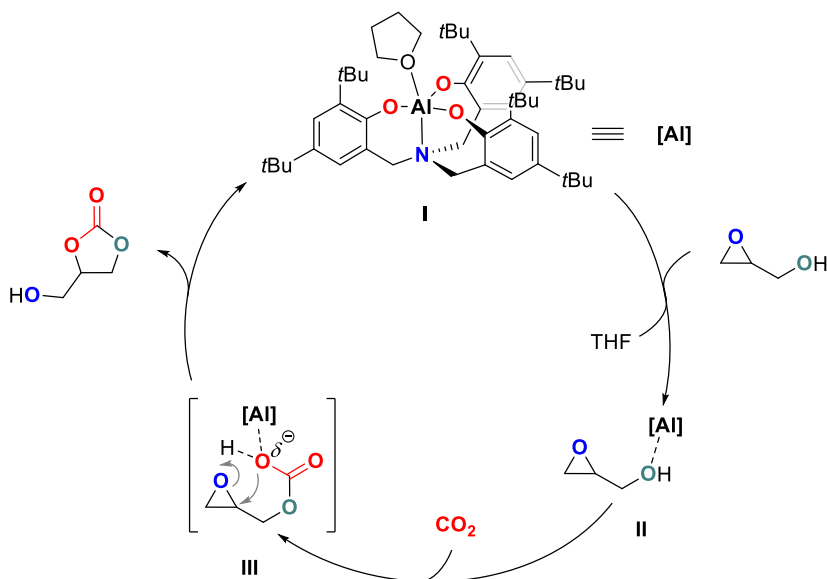
Scheme 20. Proposed initial catalytic cycle for the aluminum-aminotriphenolate catalyzed coupling of glycidol with CO_2.

5.3.1 Substrate activation by the catalyst

Epoxides are generally activated for nucleophilic ring-opening by coordination of a Lewis acid to the epoxide oxygen atom. In the case of glycidol however, there is an additional coordination mode possible through the alcohol group. In order to differentiate between these two possibilities we performed ^{1}H NMR experiments to see the preferred coordination mode of the substrate to the Al complex. We further compared the coordination mode of glycidol with that of glycidyl methyl ether, with the latter not having a free alcohol group. Chemical shifts changes in ^{1}H NMR were measured for both glycidol and glycidyl methyl ether upon addition of the Al complex to a solution containing the epoxide (Figure 21).
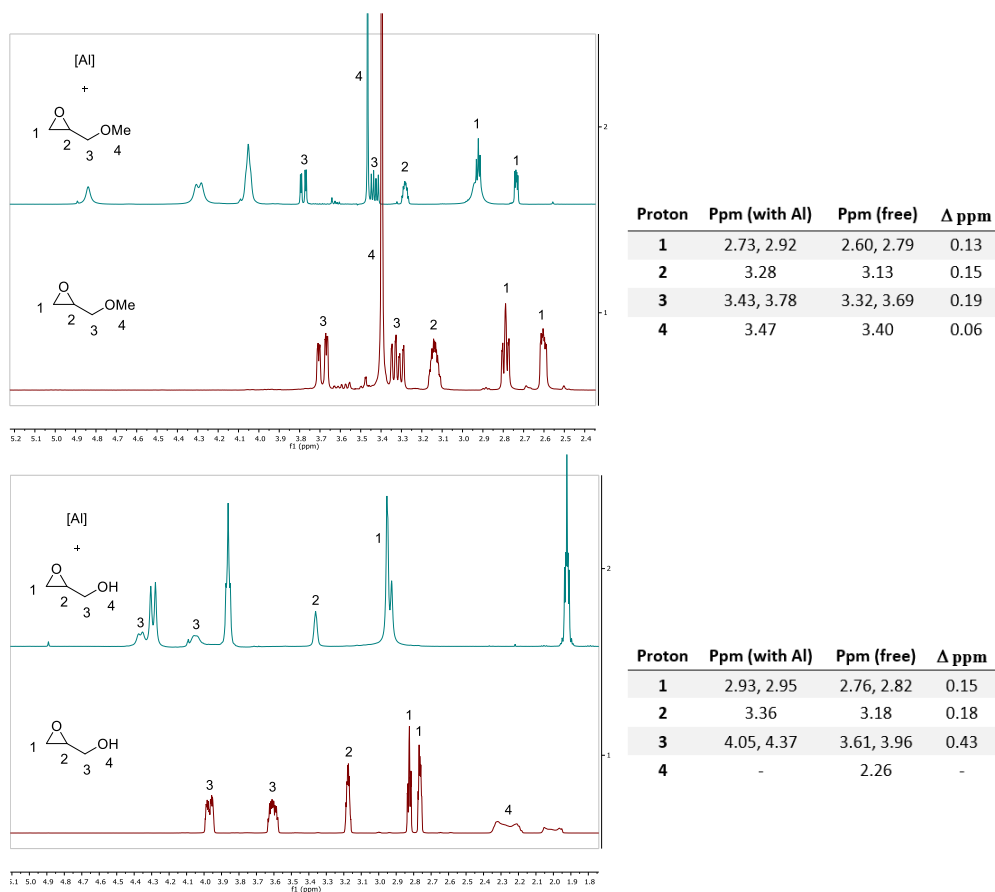
Chapter 5

Proton	Ppm (with Al)	Ppm (free)	Δ ppm
1	2.73, 2.92	2.60, 2.79	0.13
2	3.28	3.13	0.15
3	3.43, 3.78	3.32, 3.69	0.19
4	3.47	3.40	0.06

Proton	Ppm (with Al)	Ppm (free)	Δ ppm
1	2.93, 2.95	2.76, 2.82	0.15
2	3.36	3.18	0.18
3	4.05, 4.37	3.61, 3.96	0.43
4	-	2.26	-

Figure 21. Part of the ^1H NMR spectra for glycidyl methyl ether (top) and glycidol (bottom) in CDCl₃. Free substrate traces in red, and in the presence of Al complex in green.

For methyl glycidyl ether (Figure 21, top) moderate changes in chemical shift values are observed after addition of the Al complex. All hydrogens undergo a shift of about 0.15 ppm with respect to the free substrate, implying that the aluminum most likely preferentially interacts with the epoxide unit. When using glycidol, a significant larger shift of 0.43 ppm is observed for the methylene-H adjacent to the hydroxy group, hinting at prefered alcohol coordination to the aluminum center. Further evidence for this activation mode was obtained in the solid state by X-ray analysis of a glycidol bound aluminum complex that shows indeed coordination of the alcohol group to the metal center (Figure 22).
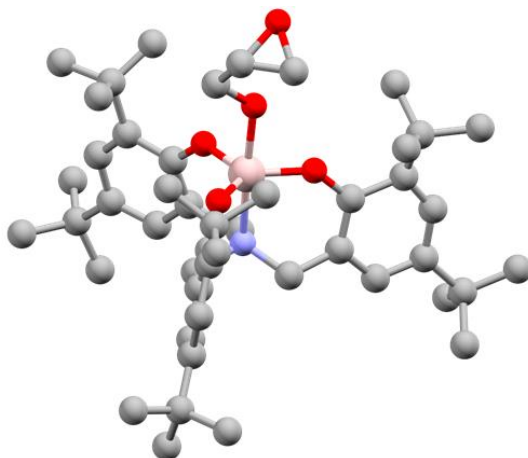
Chapter 5

Figure 22. X-ray molecular structure showing a glycidol-bound aluminum complex with coordination of the hydroxy group to the metal center.

After substrate coordination to the catalyst, the next step is most likely to involve alkoxide formation by deprotonation of the alcohol unit in glycidol. Theoretically, CO_2 could insert directly into the O-H bond to form the alkyl carbonic acid intermediate, however this reaction was found to be disfavored with a calculated activation energy of more than 50 kcal/mol.[136] Studies on the formation of bicarbonate from water and CO_2 show that the involvement of a second molecule of water greatly lowers the activation energy for this process.[137] The role of the additional water molecule is to act as a proton shuttle to transfer the proton from the alcohol to the newly formed bicarbonate anion.

In our case, proton transfer could also occur via residual water that is in the reaction media, although this seems less likely since its concentration is much lower compared to an aqueous bicarbonate system. Another option is through an additional molecule of glycidol, where the hydroxyl group can aid in the proton relay process. An interesting third method of proton transfer involves participation of the aminotriphenolate ligand, with one of the phenolate oxygen atoms acting as a basic unit able to deprotonate the substrate (see **99**, Scheme 21). Not only is the phenolate-*O* more basic than glycidol, it also is in close proximity to the hydroxyl group of the bound substrate. Similar type of non-innocent ligand behavior, where the ligand mediates proton shuttling, has been previously reported for aluminum (III) complexes bearing tridentate bis(amino)pyridine ligands.[106] In addition, we recently reported on the isolation of a vanadium(V)-epoxide complex where one of the phenolate donors served as an internal nucleophile to ring-open the bound epoxide.[138]

Chapter 5
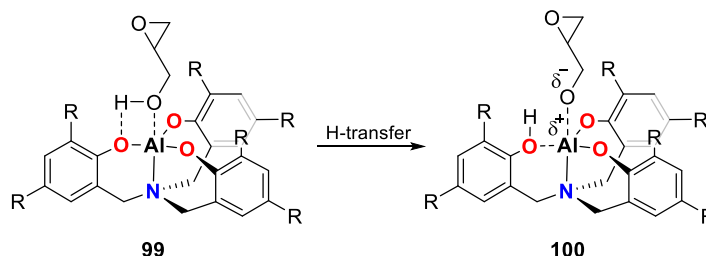
Scheme 21. Formation of a metal-bound alkoxide via deprotonation of the substrate by one of the phenolate donors of the ligand.

The ligand-mediated proton transfer depicted in Scheme 21 furnishes a metal-bound alkoxide species (**100**). Desymmetrization of the ligand system due to protonation could not be observed by NMR, and elongation of one of the Al–O bonds in the crystal structure was also not noted. This is not surprising as the charge-separated intermediate **100** presumably lies higher in energy than the neutral adduct and therefore the former cannot easily be observed under these conditions.

5.3.2   Formation of an alkyl carbonate species

The aluminum-bound alkoxide should be able to activate CO_2 to form an alkyl carbonate anion, which can be reprotonated to form the corresponding alkyl carbonic acid. DFT-calculations on the related formation of carbonic acid show that initial coordination of CO_2 to water is a stabilizing interaction that leads to a low lying-intermediate.[136] Based on previous analyses of alkyl carbonic acid species,[129, 139] we intented to detect the glycidol-CO_2 adduct by NMR. However, neither the acidic proton nor the carbonyl carbon of the presumed intermediate species could be detected by ^1H or ^{13}C NMR. This can be ascribed to a combination of a too low sensitivity of NMR spectroscopy compared to other spectroscopic techniques and unfavorable conditions inside the NMR-tube, compared to the standard catalytic conditions: in particular, there is a much lower gas-to-liquid ratio inside the NMR tube and in addition there is no efficient mixing feasible to dissolve the CO_2.

Inspired by the successful application of IR spectroscopy in related studies,[127b] we decided to focus on this technique in order to observe a CO_2-based intermediate. A major difference between our Al-glycidol based system and the previously described examples is that the alkyl carbonic acid species is an actual intermediate in the catalytic cycle rather than an adsorption-desorption process. In order to analyze our system with

Chapter 5

in-situ IR spectroscopy we needed to deviate from the standard reaction conditions and switch to cyclohexane as medium, using a lower concentration (20 mM vs 1 M) and atmospheric CO_2 pressure at rt. Following this experimental setup, we observed the appearance of a new peak in IR at 1650 cm^{-1}, though no product formation took place under these specific conditions. In order to achieve catalytic turnover it was necessary to add TBAI as an external nucleophile, as the formation of glycidol carbonate at rt is too slow especially in cyclohexane. When TBAI was introduced to the reacion mixture, we quickly observed a growing signal at 1790 cm^{-1} corresponding to the carbonate product (Figure 23 - red traces).
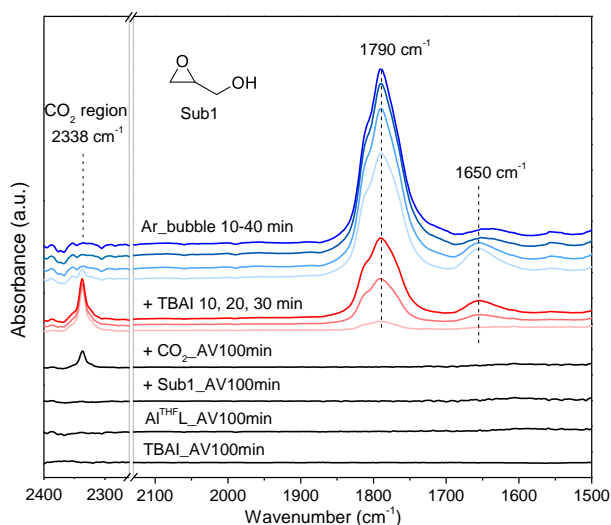

Figure 23. Formation of an intermediate in the reaction between glycidol and CO_2, owing to the appearance of a new signal in IR along with that of the product.

Initially we attributed the peak at 1650 cm^{-1} to the alkyl carbonic acid derived from glycidol and CO_2, however the calculated IR-spectrum of the glycidol based carbonic acid intermediate predicts a peak around 1880-1900 cm^{-1}. The value that we obtained resembles more that of an anionic species, which has been described for the bicarbonate system with absorptions ranging between 1630-1650 cm^{-1}.[139-140] Interestingly, when the CO_2 atmosphere was replaced with argon during the experiment, the intermediate species disappeared over time while product formation continued (Figure 23 – blue line). This supports that there is indeed an intermediate formed between glycidol and CO_2, which converts to the product even in the absence of free (unbound) CO_2. To rule out the possibility of a different CO_2-adduct arising for instance from an interaction with the catalyst, we performed several control

120

experiments. No interactions could be observed by IR analysis between CO_2 and either the catalyst, the solvent, TBAI or a combination of them. This is especially relevant as in the case of the ammonium halide it contradicts the previously suggested partial decomposition of the salt forming tributylamine which can activate CO_2.[72]

5.3.3   Epoxide ring-opening

After coordination of CO_2 to the alkoxide species, an alkyl carbonate anion is formed that can act as internal nucleophile to ring-open the epoxide. In the conventional formation of cyclic carbonates from epoxides and CO_2, the epoxide ring-opening and cyclization with CO_2 are two separate steps in the catalytic cycle. With epoxy alcohols both processes can happen simultaneously, making it reasonable to assume that this is the rate determining step also when considering the steric implications in the complex at this stage. First of all we analyzed the initial kinetics to determine the dependence of each component on the reaction rate. Under conditions close to the actual catalytic process (chapter 4), we found a first order dependence on both Al-catalyst and glycidol concentration (Figure 24).
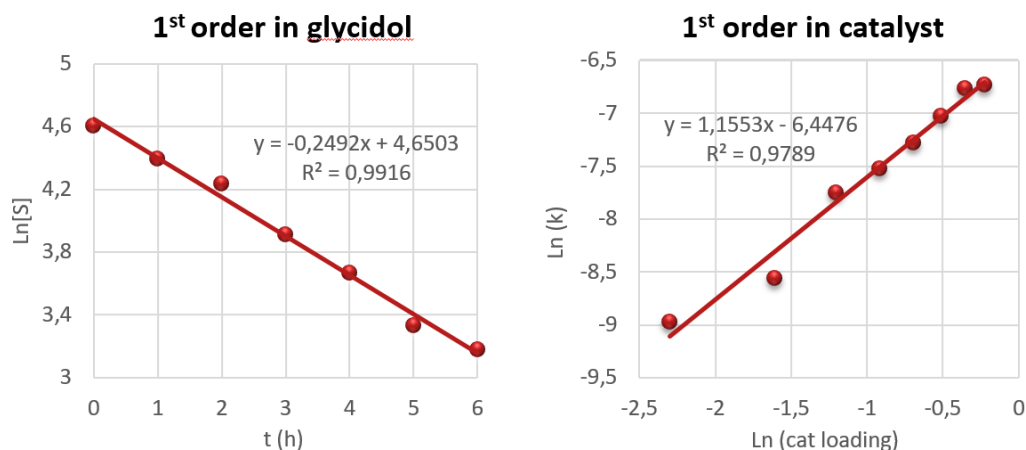

1st order in glycidol

$y = -0,2492x + 4,6503$
$R^2 = 0,9916$

1st order in catalyst

$y = 1,1553x - 6,4476$
$R^2 = 0,9789$

Figure 24. Initial rate kinetic studies showing a first order dependence on both the Al catalyst and substrate.

The influence of CO_2 on the reaction yield was measured over a range between 1–80 bar of pressure (Figure 25 – left). Initially the yield goes up with increasing CO_2 pressure, closely approaching a first order in CO_2 in the range of 1–10 bar (Figure 25 – right). Probably the solvent already reaches CO_2 saturation levels at relatively low pressure.

Chapter 5

Identical results were obtained for reactions performed between 10–30 bar of CO_2, suggesting that under these conditions there is basically a zero order in CO_2. At higher pressures than 30 bar the yield decreases, probably due to a reduced solubility of the catalyst in an increasingly rich CO_2 phase. This is supported by the fact that under supercritical conditions (>70 bar CO_2) very poor results were obtained compared to reactions performed at lower pressures.
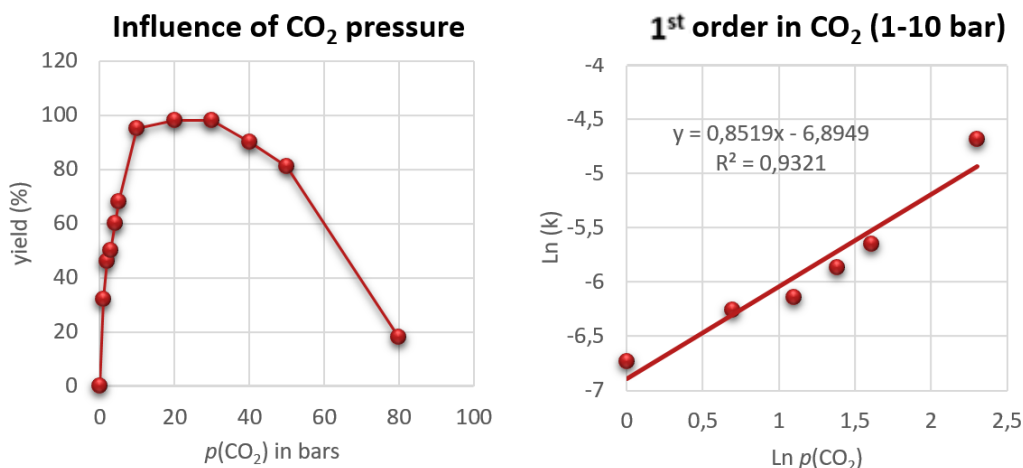

Figure 25. Influence of CO_2 pressure on the yield over a range of 1–80 bar at 50 °C for (left) and a kinetic plot to determine the order in CO_2 at lower pressures (1–10 bar).

The activation energy of the reaction was determined experimentally by using a Van 't Hoff plot and was found to be 23.3 kcal/mol. This value corresponds well to a reaction that is very slow at rt (<1 turnover per hour) and smoothly runs to completion at 50 °C. We wanted to investigate whether product formation indeed occurs via the mechanism proposed in Scheme 20 and if further details could be obtained. While the impact of both possible pathways (see Scheme 18) for subsituted epoxy alcohols can be easily determined by looking at the product distribution, the use of glycidol would afford the same product irrespective of the manifold involved. To determine if indeed only one mechanistic manifold is operative for glycidol, we introduced a deuterium label in the glycidol substrate (Scheme 22).

Chapter 5
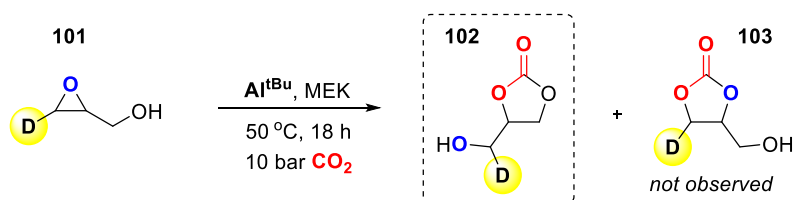
Scheme 22. Exclusive formation of carbonate **102** from deuterium-labeled glycidol **101**.

When the deuterated substrate **101** was subjected to the standard reaction conditions, the cyclic carbonate **102** was obtained exclusively. This is in line with our mechanistic proposal, where an internal nucleophile is formed via coupling of CO_2 with the hydroxy group, which ring-opens the epoxide. Formation of **103** was not observed, indicating that there is indeed no observable classical coupling of CO_2 and the epoxide substrate under these conditions.
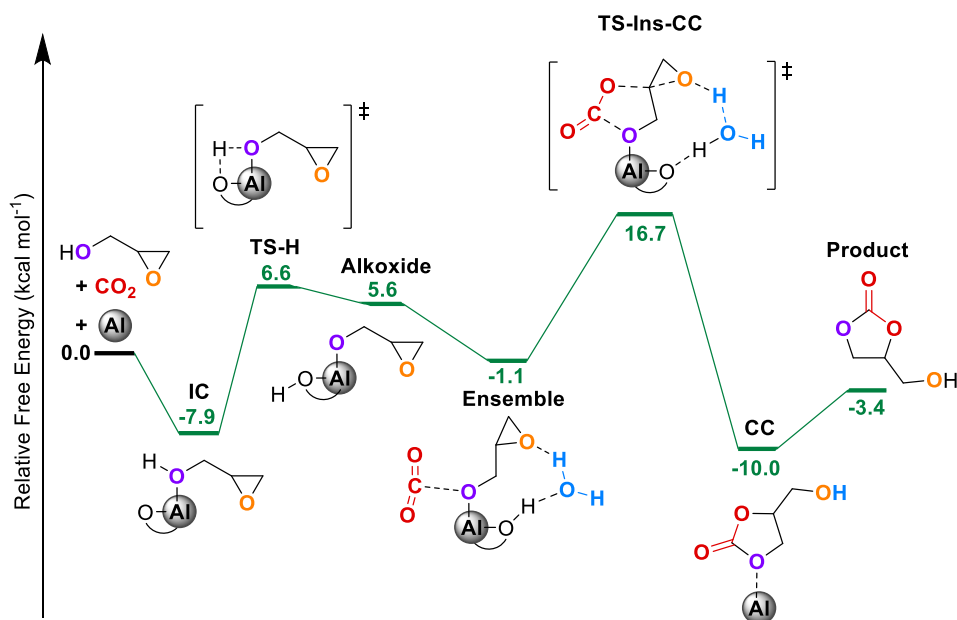

Figure 26. Gibbs free-energy profile of glycidol carbonate formation via a concerted mechanism.

5.3.4   DFT-analysis

To gain further insight into the reaction mechanism, stability of reaction intermediates

Chapter 5

and the energy barriers associated with their formation, we performed computational studies using DFT-based methods. The 6-311G(d,p) basis set was used along with the B97-D3 functional to calculate the gibbs free energies under standard conditions (323 K and 1 atm CO_2). The resulting energy profile for the formation of glycidol carbonate is depicted in Figure 26).

The first step is the coordination of glycidol to the axial coordinative vacancy of the aluminum catalyst, forming the most stable intermediate (**IC**) before the highest transition state **TS-Ins-CC** making **IC** the rate-determining intermediate (RDI). This coordination was found to be a favorable interaction with a lower energy for coordination via the alcohol unit, in agreement with the obtained X-ray structure. Deprotonation of the substrate by the ligand is associated with a barrier of 14.5 kcal/mol leading to the **Alkoxide** species. Subsequent coordination of CO_2 is a stabilizing interaction that leads to the relatively low-lying **Ensemble** intermediate, followed by simultaneous epoxide ring-opening and formation of the cyclic carbonate time via a concerted mechanism.

An absolute barrier of 24.6 kcal/mol was found, which is in good agreement with the 23.3 kcal/mol found experimentally. Interestingly, it was computed that water facilitates the proton transfer from the ligand to the epoxide oxygen in the rate-determining step (Figure 26, **TS-Ins-CC**). Although water is not added to the reaction mixture, small amounts of water can come from the solvent, substrate or directly from the air. To test this experimentally, we prepared a reactor under anhydrous conditions inside the glovebox, using a freshly prepared batch of Al-catalyst and distilled solvents. When running the reaction for 4 h under standard conditions a lower yield was indeed found when using anhydrous conditions (32% vs 62%). Another important feature arising from the DFT-calculations is that the ring-opening step occurs via an S_N2 mechanism. This should give a formal inversion of configuration, which was indeed confirmed experimentally using a chiral substrate (chapter 4).

5.3.5   Chiral glycidol

In order to verify whether product formation indeed occurs exclusively via an S_N2 pathway we studied the conversion of chiral (*S*)-glycidol. In the previous chapter we found almost full retention of stereochemical information for the conversion of (2*R*,3*R*)-(+)-3-phenylglycidol (see Figure 19). As this is an internal epoxide with an additional stereocenter, the same outcome is not necessarily the case for glycidol. Initially we tried to analyze the chiral glycidol carbonate directly, however no suitable
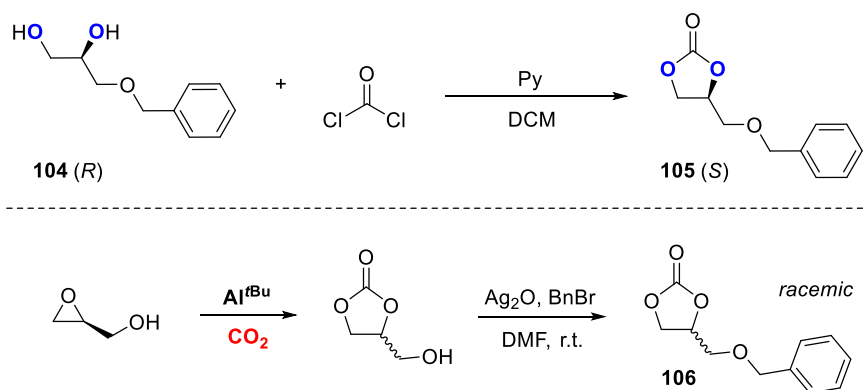
Chapter 5

data could be obtained owing to a complicated analysis/detection of this compound. Instead, we decided to perform an aminolysis of the formed carbonate from chiral glycidol leading to the formation of two linear carbamates, from which the enantiomeric excess can be determined (Scheme 23).
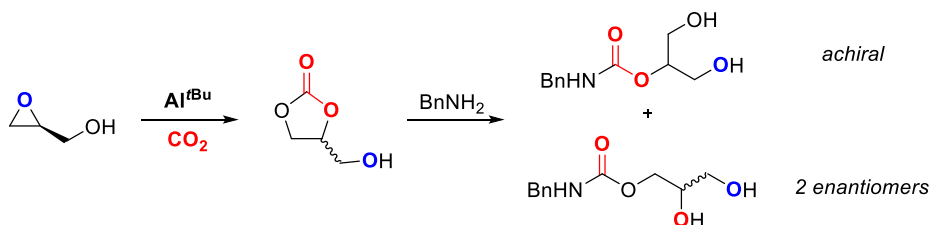
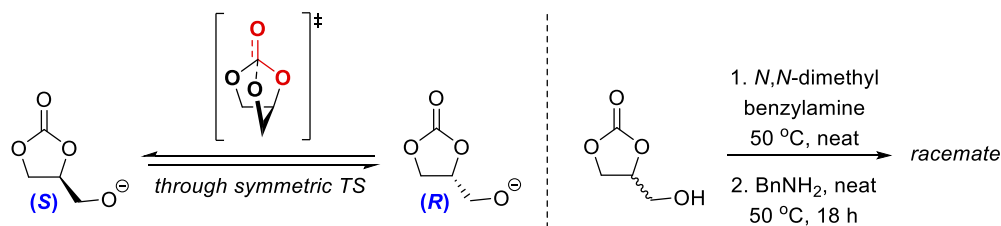Scheme 23. Aminolysis of glycidol carbonate leading to the formation of two linear carbamates.

The aminolysis with benzylamine gives two regioisomeric products with a 65:35 ratio in favor of the chiral compound. To our surprise an *ee* of only 45% was determined by UPC2 for this linear carbamate, instead of the expected retention of stereochemistry associated with the proposed S_N2 type mechanism. Changing the temperature, catalyst loading or reaction times had no obvious effect on the outcome, as the ee´s remained between 40-45% in each of these investigated cases. To see whether the aminolysis reaction somehow affected the stereochemical purity of the product, an *O*-benzylated derivative of glycidol carbonate was prepared. In addition, chiral reference compound **105** was also synthesized from the enantiomerically pure diol **104**, which may be used to confirm the stereochemistry of our chiral carbonate (Scheme 24 – top).

Scheme 24. Synthesis of the chiral reference **105** (top) and benzylation of glycidol carbonate (bottom).

125

Chapter 5

Following the synthesis of the benzylated glycidol carbonate **106** (Scheme 24 – bottom), we obtained a completely racemic product. Seemingly the glycidol carbonate racemizes under basic conditions through an intramolecular trans-esterification reaction (Scheme 25 - left). The silver(I) oxide and the benzylamine can both act as base to favor deprotonation of the glycidol carbonate. DFT-analysis shows that this pathway is indeed feasible under basic conditions and goes through a symmetrical transition state. This implies that the benzylation of the carbonate competes with the racemization, and as the latter process is apparently much faster a racemic mixture is produced. The rate of the aminolysis reaction described in Scheme 23 seems competitive with the intramolecular transesterification, and as such only partial racemization occurs.

Scheme 25. Racemization of glycidol carbonate under basic conditions (left) and formation of a racemic carbamate upon aminolysis of glycidol carbonate that was pre-treated with a base (right).

Further support for these competing reactions was found when glycidol carbonate was treated with a tertiary amine prior to aminolysis, leading to the formation of racemic linear carbamate (Scheme 25 – right). As shown before, the phenolate units from the ligand can act as a base that could potentially cause racemization of the product and loss of *ee*. For the substrate, this can happen through a Payne rearrangement,[141] which is the isomerization of 2,3-epoxy alcohols under basic conditions However, this was not observed even when using 10 mol% of Al-catalyst (Scheme 26, **b**). When the deuterated glycidol carbonate **102** was treated with 10% of either **Al^tBu** or *N,N*-dimethyl benzylamine, isomerization only took place in the latter case leading to a 1:1 ratio of both deuterated carbonates (Scheme 26, **d**).

Chapter 5
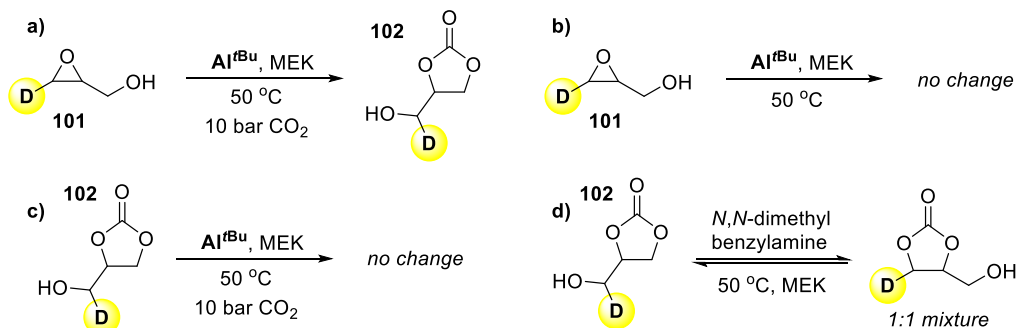
*Scheme 26. Control experiments using deuterium labeled substrate/carbonate **101** and **102** showing that no substrate or product racemization occurs under the catalytic conditons.*

The experiments described in Schemes 23-26 show that glycidol carbonate can racemize through a transesterification process in the presence of a base, but does not occur under catalytic conditions. This suggests that the formation of glycidol carbonate indeed follows an S_N2 type cyclization with full retention of stereochemistry, in line with the control experiment using a chiral substrate in chapter 4.

5.3.6   CO$_2$-trapping

The series of experiments depicted in Figure 23 shows that the intermediate species formed from glycidol and CO_2 can be converted into the product in the absence of a CO_2 atmosphere. This suggests that CO_2 is somehow trapped by the substrate and is not removed while flushing the system with argon. Intrigued by this result we decided to further investigate this effect of "CO_2-trapping" by glycidol. It was found that using 3,4-epoxy-1-butanol (**107**) that has an additional CH$_2$ unit, is more efficient in trapping CO_2 than glycidol. When a solution of **107** in cyclohexane was exposed to an atmosphere of CO_2 the appearance of a new species at 1650 cm^{-1} (Figure 27) was detected, in line with the *in-situ* IR analysis described previously for the interaction of glycidol and CO_2.
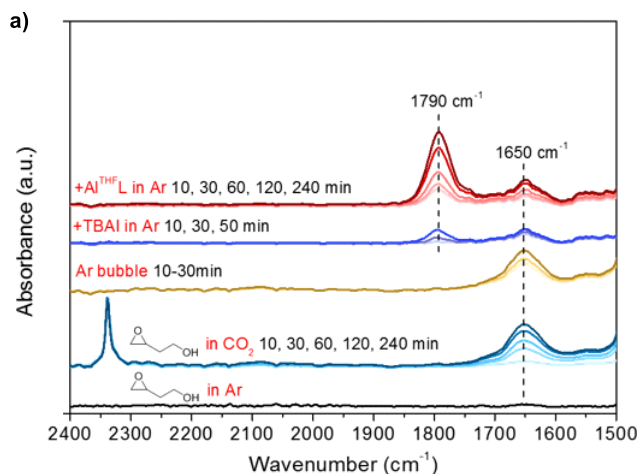
Chapter 5

*Figure 27. Trapping of CO$_2$ by 3,4-epoxy-1-butanol (**107**) and subsequent addition of TBAI and Al-catalyst, resulting in conversion of the intermediates into cyclic carbonate products.*

Complete removal of CO$_2$ was achieved by bubbling argon through the solution for 30 min, after which the signal of free CO$_2$ at 2330 cm^{-1} completely disappeared (Figure 27 – orange/brown line). The intensity of the peak belonging to the intermediate does not decrease much over time, meaning that the interaction of the substrate with CO$_2$ is rather strong. As was mentioned before, TBAI is required for product formation to occur, although the aluminum complex does speed up the reaction in combination with TBAI. If the Al complex is added directly to the solution containing the intermediate, no product formation is observed until an external nucleophile is added. To get a better understanding of how CO$_2$ can be trapped by epoxy alcohols we performed the control experiments outlined in Scheme 27. No CO$_2$ is trapped by the catalyst either with or without coordinated THF (**d** and **e**). Epoxides that lack an alcohol group (**a** and **b**; propylene oxide and *O*-methyl-glycidol) are also not capable of trapping CO$_2$. Additionally, a combination of glycidyl methyl ether and methanol also did not lead to any product formation (**c**), suggesting that the alcohol and epoxide moieties need to be present in the same molecule for succesful trapping of CO$_2$.

128

Chapter 5
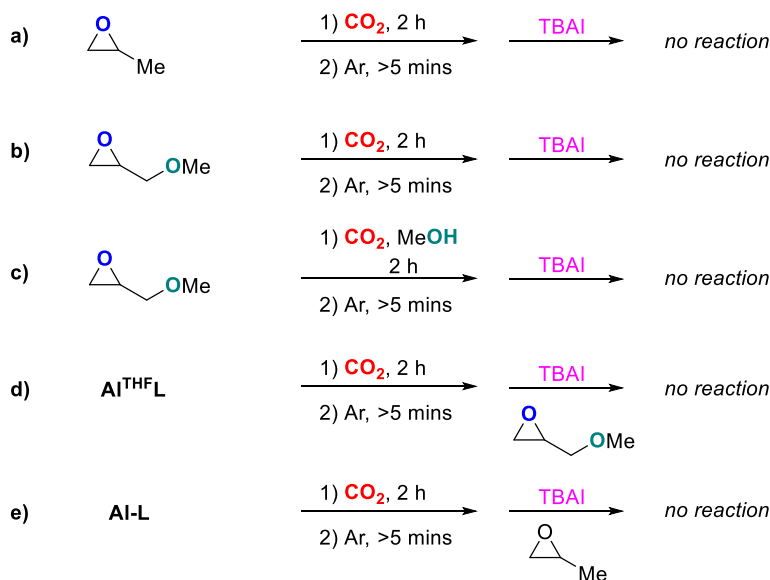
Scheme 27. Control experiments showing that CO2 trapping does not occur by other type of epoxides, alcohols or the aluminum catalyst.

Similar trapping of CO_2 has been observed for alcohols in combination with bases such as DBU, forming a carbonate salt.[142] In these cases DBU does not interact directly with CO_2, as no evidence of a carbamate species could be detected.[143] DBU instead serves as base to form a salt with the otherwise unstable alkyl carbonic acid species derived from the alcohol and CO_2 (Scheme 28).[144] A TBD–CO_2 adduct has been isolated and characterized under strictly anhydrous conditions.[145]
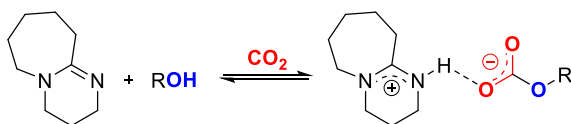
Scheme 28. Formation of a carbonate salt from an alcohol, DBU and CO2.

5.4 Conclusion

Experiments described in this chapter show that the activation of glycidol by the aluminum catalyst occurs through coordination of the hydroxyl group to the metal center. Subsequent activation of CO_2 by a metal-alkoxide species leads to the formation of a low-lying intermediate resembling an alkyl carbonate anion, which is supported by
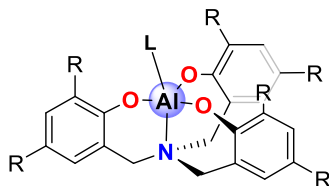
Chapter 5

DFT analysis. Further evidence for this intermediate comes from *in-situ* IR spectroscopy, where the formation of a new species (peak at 1650 cm^{-1}) can be observed upon pressurizing with CO_2. The nucleophilic species that is generated can intramolecularly attack the epoxide leading to the formation of the cyclic carbonate product. A first order rate dependence was found for the Al catalyst, substrate and CO_2 (the latter only at low pressure). Deuterium labeling experiments reveal that only one product is formed under the reaction conditions. However, under basic conditions product racemization can take place via an intramolecular transesterification reaction. Furthermore, we showed that epoxy alcohols can trap small quantities of CO_2, a feature previously only seen using strong bases such as DBU. The combined experimental and theoretical results provide a rather complete picture of the Al-mediated conversion of epoxy alcohols and key structural information of some of the intermediates, and supports the view that the reactions are mediated by *in-situ* produced nucleophiles reminiscent of elusive carbonic acid derived species.

5.5 Experimental

5.5.1 General comments

Both the ligand[77] and catalyst[44] (see Figure below) were synthesized according to previously reported procedures. ^1H and ^{13}C NMR spectra were recorded on a Bruker AV-300, AV-400 or AV-500 spectrometer. Mass spectrometric analysis and X-ray diffraction studies were performed by the Research Support Group at the ICIQ. Carbon dioxide was purchased from PRAXAIR and used without further purification. Solvents used in the synthesis of the complexes were dried using an Innovative Technology PURE SOLV solvent purification system.

Al^{tBu}: R = *t*Bu; L = thf

Chapter 5

5.5.2   Typical catalytic experiment

The respective epoxide, Al complex, internal standard and solvent were charged into a 30 mL stainless steel autoclave. The autoclave was then subjected to three cycles of pressurization and depressurization with carbon dioxide (5 bar), before final stabilization of the pressure to 10 bar. The autoclave was sealed and heated to the required temperature and left stirring. At the end of the reaction an aliquot of the resulting mixture was taken and the conversion was determined by means of ^1H NMR spectroscopy using $CDCl_3$ as the solvent. The identities of the cyclic carbonate products were confirmed by comparison to literature data.
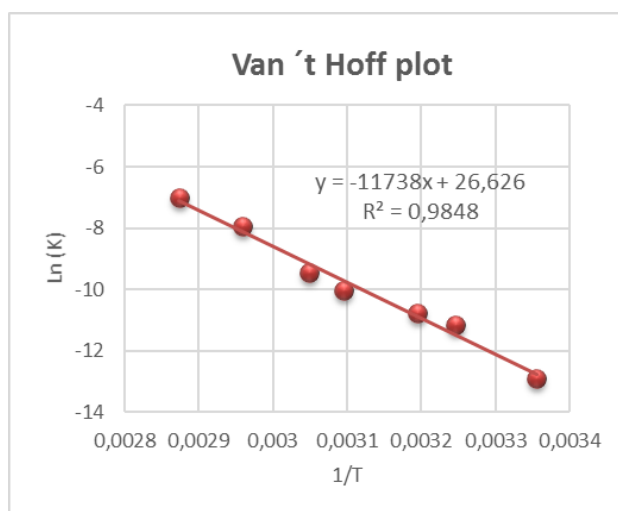
5.5.3   Energy of activation

The activation energy of the reaction was determined from a Van ´t Hoff plot. Using the Arrhenius equation $K = Ae^{-Ea/RT}$ to plot the natural logarithm versus 1/T, a straight line was obtained of which the slope is related to the activation energy.

$$Slope = - E_a / R$$

$$E_a = -R * slope$$

$$E_a = - (1.987 * 10^{-3}) * -11738$$

$$\mathbf{E_a = 23.3 \text{ kcal/mol}}$$

Van ´t Hoff plot

y = -11738x + 26,626
R² = 0,9848

Ln (K)

1/T

Chapter 5

5.5.4 Deuterium labeling experiments

Deuterium labeled glycidol was synthesized according to the procedure shown below in Scheme 29. The key step is the formation of compound **C**, which was prepared according to a previously published procedure.[146] Spectra of the compounds **C–F** show around 15% of their non-deuterated analogues as impurities in NMR.
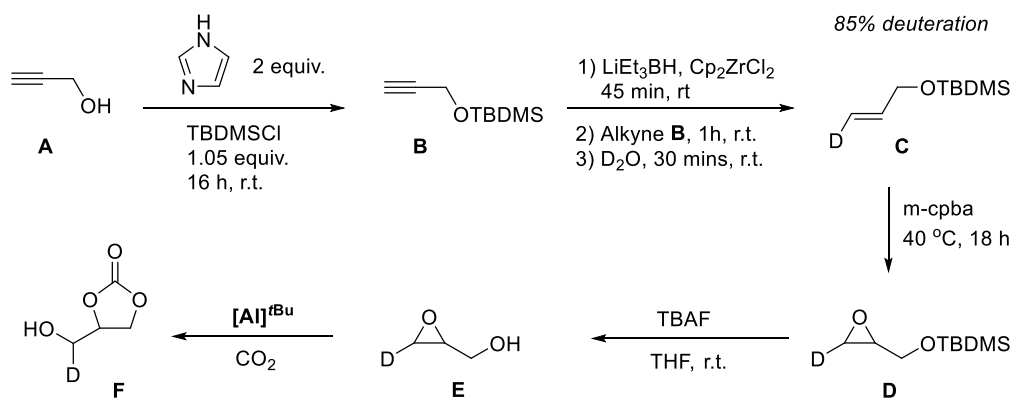

Scheme 29. Synthesis of deuterium labeled glycidol and its carbonate derivative F.

Compound B[147]
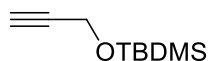
To a solution of propargylic alcohol (1.12 g, 20.0 mmol) in DCM (40 mL) was added TBDMS-Cl (3.16 g, 21.0 mmol) and imidazole (2.72 g, 40.0 mmol). After stirring for 16 h the mixture was washed with water, dried over $MgSO_4$ and concentrated under vacuum to yield the product as a slightly yellow liquid in 99% yield (3.37 g, 19.8 mmol). **1H NMR** (400 MHz, $CDCl_3$) δ 4.33 (d, J = 2.4 Hz, 2H), 2.40 (t, J = 2.4 Hz, 1H), 0.93 (s, 9H), 0.14 (s, 6H). **13C NMR** (101 MHz, $CDCl_3$) δ 82.42, 72.81, 51.50, 25.78, 18.27, -5.21.

Compound C[146]
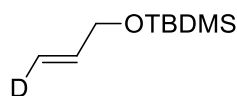
In a dried Schlenk-flask protected from light by aluminum foil, were added Cp_2ZrCl_2 (2.92 g, 10.0 mmol) and THF (60 mL) under nitrogen atmosphere. $LiEt_3BH$ (10 mL, 10.0 mmol) was slowly added and the mixture stirred for 45 min at rt before adding the alkyne **B** (1.70 g, 2.10

Chapter 5

mL, 10.0 mmol, previously distilled over CaH_2) and stirring for an additional 1 h. Afterwards, D_2O (2.0 mL) was added and the mixture further stirred for 30 min. Diethyl ether was added after the reaction and the mixture was dried over $MgSO_4$ and the solvent evaporated. The crude product was purified by neutral alumina column chromatography (hexane) to obtain the product as a colorless liquid in 65% yield (1.13 g, 6.5 mmol). **^{1}H NMR** (500 MHz, CDCl$_3$) δ 5.99 – 5.89 (m, 1H), 5.28 (m, 1H), 4.20 (m, 2H), 0.94 (s, 9H), 0.10 (s, 6H). **^{13}C NMR** (126 MHz, CDCl$_3$) δ 137.40, 113.65, 64.07, 25.93, 18.41, -5.26.
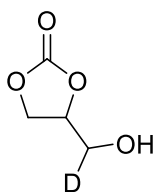
Compound D
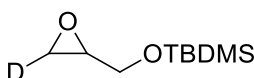
To a solution of **C** (0.80 g, 4.6 mmol) in DCM (10 mL) was added *m*-CPBA (0.95 g, 5.5 mmol) and the mixture was than stirred for 24 h at 45 °C. Hereafter the mixture was isolated by basic alumina column chromatography (Hexane: Et$_2$O, 10:1) to yield the product as a colorless liquid in 83% yield (0.73 g, 3.8 mmol). **^{1}H NMR** (500 MHz, CDCl$_3$) δ 3.87 (m, 1H), 3.68 (m, 1H), 3.12 – 3.08 (m, 1H), 2.64 (d, *J* = 2.7 Hz, 1H), 0.92 (s, 9H), 0.10 (d, *J* = 4.5 Hz, 6H). **^{13}C NMR** (126 MHz, CDCl$_3$) δ 63.73, 52.33, 44.36, 25.86, 18.36, -5.32.

Compound E[148]
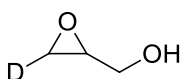
To a solution of **D** (0.36 g, 1.9 mmol) in THF (1 mL) was added a 1 M solution of TBAF in THF (2.0 mL, 2.0 mmol) and the mixture stirred for 18 h at rt. Hereafter the mixture was purified by neutral alumina column chromatography (Pentane: Et$_2$O, 1:1) to yield the final product as colorless liquid in 99% yield (0.14 g, 1.9 mmol). **^{1}H NMR** (500 MHz, CDCl$_3$) δ 3.89 (dd, *J* = 12.7 and 2.5 Hz, 1H), 3.52 (dd, *J* = 12.7 and 4.9 Hz, 1H), 3.23 – 3.11 (m, 1H), 3.11 (m, 1H), 2.68 (d, *J* = 2.8 Hz, 1H). **^{13}C NMR** (126 MHz, CDCl$_3$) δ 62.07, 52.36, 44.02, 25.56, -3.74.

Compound F

This compound was obtained following the general catalytic procedure described in this chapter. After the reaction, the solvent was evaporated and the mixture was purified by silica gel column chromatography to yield the final product as slightly yellow oil in 93% yield. **^{1}H NMR** (500 MHz, CDCl$_3$) δ 4.83 (m, 1H), 4.55 (t, *J* = 8.4 Hz, 1H), 4.48 (m, 1H), 4.00 (m 1H), 2.39 (d, *J* = 5.6 Hz, 1H). **^{13}C NMR** (126 MHz, CDCl$_3$) δ 155.12, 76.38, 65.69, 61.39.

133

Chapter 5

5.5.5   Aminolysis
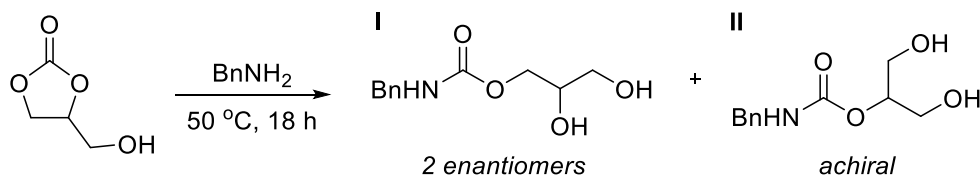
Scheme 30. Aminolysis of glycidol carbonate leading to two regio-isomeric linear carbamates.

Chiral glycidol carbonate (0.5 mmol) and benzylamine (0.5 mmol) were stirred at 50 °C for 18 h. The product solidified upon cooling down the reaction mixture to rt, and a sample was taken for chiral UPC2 analysis. Table 12 lists the regio-selectivity and *ee* obtained from different samples of the chiral glycidol carbonate after aminolysis.

entry	subs.	cat (mol%)	T (°C)	t (h)	regio-sel(I:II)[a]	yield (%)[a]	ee (%)[a]
1	(*rac*)	Al (1)	50	18	69:35	92	0
2	(*S*)	Al (3)	25	66	62:38	91	43
3	(*S*)	Al (1)	50	18	64:36	97	44
4	(*S*)	Al (1)	75	2	58:42	94	39

Table 12. Reaction conditions: 1 mmol glycidol (S or rac), Al^tBu catalyst, solvent is MEK (1 mL). [a] Average from three runs. Conditions in this table refer to the formation of cyclic carbonate. Conditions for the aminolysis are shown in Scheme 30.
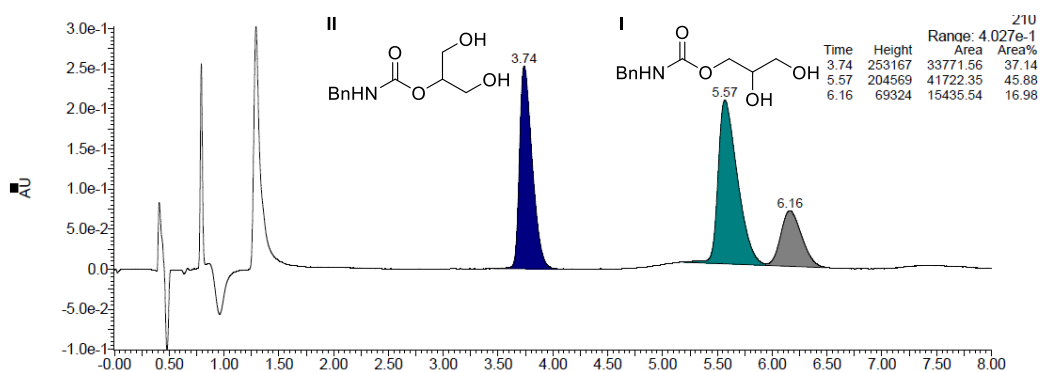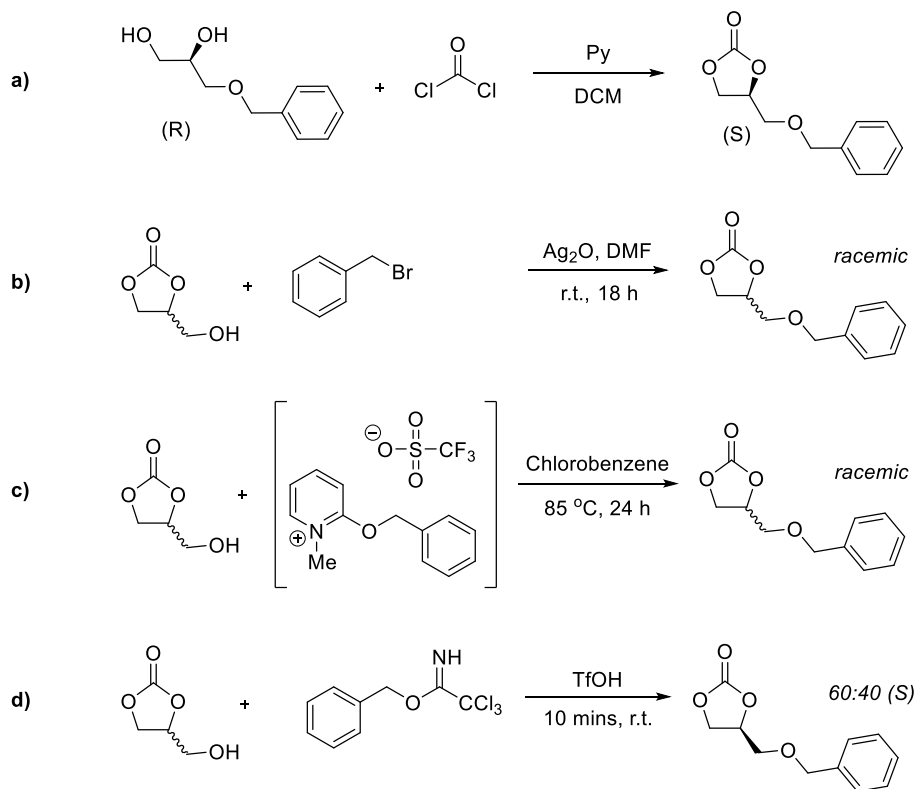

*Figure 28. UPC2-analysis showing both linear carbamates with an enantiomeric excess of 46% for **I**.*

134

Chapter 5

5.5.6   Benzylation of glycidol carbonate

*Scheme 31. Synthesis of chiral reference (**a**) and benzylation of glycidol carbonate under basic (**b**), neutral (**c**) and acidic conditions (**d**).*

a) To a solution of (*R*)-3-(benzyloxy)propane-1,2-diol in DCM was added pyridine (4 equiv) and triphosgene (equal to 1.5 equiv of phosgene). The reaction was stirred under a N_2 atmosphere at rt for 2 h. The reaction mixture was then quenched with saturated aqueous NH_4Cl, washed with H_2O, and extracted with DCM. The combined organic layers were dried over anhydrous Na_2SO_4, filtered and concentrated. The residue was purified by flash chromatography on silica to afford the corresponding carbonate.

b) To a solution of glycidol carbonate (82 mg, 0.69 mmol) in DMF (2.0 mL) was added silver(I) oxide (239 mmol, 1.04 mmol) and benzyl bromide (142 mg, 0.83 mmol) and the mixture stirred for 18 h at rt. Hereafter the mixture was washed with water and extracted with diethyl ether to remove DMF. The crude product was purified by silica gel column chromatography to obtain the pure product.

Chapter 5

c) The product was prepared according to a modified literature procedure.[149] A mixture of 2-benzyloxy-1-methyl-pyridinium triflate (276 mg, 0.79 mmol) and glycidol carbonate (59 mg, 0.50 mmol) in chlorobenzene (1.5 mL), was heated at 80 °C for 24 h. The reaction mixture was cooled to rt and filtered through Celite. The filtrate was concentrated under vacuum and purified on silica gel to yield the product.

d) Product was prepared according to a modified literature procedure.[150] To an ice-cooled solution of glycidol carbonate (58 mg. 0.49 mmol) and benzyl trichloroacetimidate (161 mg, 0.64 mmol) in anhydrous dioxane (2 mL) was added triflic acid (2 drops). <u>Note</u>: enough acid should be added to ensure that the mixture is strongly acidic. The reaction had gone to completion within 10 min at rt. The mixture was diluted with diethyl ether (20 mL) and washed with a saturated aquous solution of $NaHCO_3$ (20 mL). The organic phase was dried over K_2CO_3, concentrated, and the residue purified by flash chromatography to yield the pure product.

5.5.7 Kinetic experiments

The kinetic experiments were performed using a parallel reactor system The substrate, Al complex and internal standard (mesitylene) were charged into stainless-steel inserts. The reactor system was then heated to the required temperature while stirring. After reaching the selected reaction temperature, the parallel reactor system was pressurized with CO_2 to the desired pressure and left stirring. At the end of the chosen time interval, the system was cooled to rt and depressurized. An aliquot of the reaction mixtures were taken for analysis and the yield was determined by ^1H NMR spectroscopy in $CDCl_3$.

Chapter 5

5.6 References

[44]   C. J. Whiteoak, N. Kielland, V. Laserna, F. Castro-Gómez, E. Martin, E. C. Escudero-Adán, C. Bo, A. W. Kleij, *Chem. Eur. J.* **2014**, *20*, 2264-2275.

[72]   M. North, R. Pasquale, *Angew. Chem. Int. Ed.* **2009**, *48*, 2946-2948.

[77]   M. Kol, M. Shamis, I. Goldberg, Z. Goldschmidt, S. Alfi, E. Hayut-Salant, *Inorg. Chem. Commun.* **2001**, *4*, 177-179.

[106]   L. A. Berben, *Chem. Eur. J.* **2015**, *21*, 2734-2742.

[126]   W. W. Rudolph, D. Fischer, G. Irmer, *Appl. Spectrosc.* **2006**, *60*, 130-144.

[127]   a) W. W. Rudolph, G. Irmer, E. Konigsberger, *Dalton Trans.* **2008**, 900-908; b) E. Garand, T. Wende, D. J. Goebbert, R. Bergmann, G. Meijer, D. M. Neumark, K. R. Asmis, *J. Am. Chem. Soc.* **2010**, *132*, 849-856.

[128]   K. N. West, C. Wheeler, J. P. McCarney, K. N. Griffith, D. Bush, C. L. Liotta, C. A. Eckert, *J. Phys. Chem. A* **2001**, *105*, 3947-3948.

[129]   J. J. Gassensmith, H. Furukawa, R. A. Smaldone, R. S. Forgan, Y. Y. Botros, O. M. Yaghi, J. F. Stoddart, *J. Am. Chem. Soc.* **2011**, *133*, 15312-15315.

[130]   a) D. D. Miller, S. S. C. Chuang, *J. Phys. Chem. C* **2016**, *120*, 25489-25504; b) P. V. Kortunov, L. S. Baugh, M. Siskin, D. C. Calabro, *Energy & Fuels* **2015**, *29*, 5967-5989; c) H.-B. Xie, X. Wei, P. Wang, N. He, J. Chen, *J. Phys. Chem. A* **2015**, *119*, 6346-6353; d) K. I. Assaf, A. K. Qaroush, A. a. F. Eftaiha, *Phys. Chem. Chem. Phys.* **2017**, *19*, 15403-15411.

[131]   a) T. Ema, K. Fukuhara, T. Sakai, M. Ohbo, F.-Q. Bai, J.-y. Hasegawa, *Catal. Sci. Technol.* **2015**, *5*, 2314-2321; b) C. Carvalho Rocha, T. Onfroy, J. Pilmé, A. Denicourt-Nowicki, A. Roucoux, F. Launay, *J. Catal.* **2016**, *333*, 29-39.

[132]   K. R. Roshan, R. A. Palissery, A. C. Kathalikkattil, R. Babu, G. Mathai, H.-S. Lee, D.-W. Park, *Catal. Sci. Technol.* **2016**, *6*, 3997-4004.

[133]   J. Rintjema, R. Epping, G. Fiorani, E. Martín, E. C. Escudero-Adán, A. W. Kleij, *Angew. Chem. Int. Ed.* **2016**, *55*, 3972-3976.

[134]   G.-J. Cheng, X. Zhang, L. W. Chung, L. Xu, Y.-D. Wu, *J. Am. Chem. Soc.* **2015**, *137*, 1706-1725.

[135]   F. Della Monica, A. Buonerba, A. Grassi, C. Capacchione, S. Milione, *ChemSusChem* **2016**, *9*, 3457-3464.

[136]   T. Nguyen Minh, T. K. Ha, *J. Am. Chem. Soc.* **1984**, *106*, 599-602.

[137]   a) C. A. Wight, A. I. Boldyrev, *J. Phys. Chem.* **1995**, *99*, 12125-12130; b) K. R. Liedl, S. Sekušak, E. Mayer, *J. Am. Chem. Soc.* **1997**, *119*, 3782-3784.

[138]   C. Miceli, J. Rintjema, E. Martin, E. C. Escudero-Adán, C. Zonta, G. Licini, A. W. Kleij, *ACS Catal.* **2017**, *7*, 2367-2373.

[139]   A. Dibenedetto, M. Aresta, P. Giannoccaro, C. Pastore, I. Pápai, G. Schubert, *Eur. J. Inorg. Chem.* **2006**, 908-913.

[140]   R. Srivastava, D. Srinivas, P. Ratnasamy, *J. Catal.* **2005**, *233*, 1-15.

[141]   G. B. Payne, *J. Org. Chem.* **1962**, *27*, 3819-3822.

Chapter 5

[142] P. Munshi, A. D. Main, J. C. Linehan, C.-C. Tai, P. G. Jessop, *J. Am. Chem. Soc.* **2002**, *124*, 7963-7971.

[143] D. J. Heldebrant, P. G. Jessop, C. A. Thomas, C. A. Eckert, C. L. Liotta, *J. Org. Chem.* **2005**, *70*, 5335-5338.

[144] D. J. Heldebrant, C. R. Yonker, P. G. Jessop, L. Phan, *Energy Environ. Sci.* **2008**, *1*, 487-493.

[145] C. Villiers, J.-P. Dognon, R. Pollet, P. Thuéry, M. Ephritikhine, *Angew. Chem. Int. Ed.* **2010**, *49*, 3465-3468.

[146] D. Orain, J.-C. Guillemin, *J. Org. Chem.* **1999**, *64*, 3563-3566.

[147] A. Köpfer, B. Breit, *Angew. Chem. Int. Ed.* **2015**, *54*, 6913-6917.

[148] S. S. Higashibayashi, K.; Ishizu, T.; Hashimoto, K.; Shirahama, H.; Nakata, M., *Synlett* **2000**, 1306-1308.

[149] K. W. C. Poon, G. B. Dudley, *J. Org. Chem.* **2006**, *71*, 3923-3927.

[150] P. R. Skaanderup, C. S. Poulsen, L. Hyldtoft, M. R. Jørgensen, R. Madsen, *Synthesis* **2002**, 1721-1727.

General conclusions

Carbon dioxide represents a cheap and sustainable C1 building block for organic transformations such as the synthesis of cyclic carbonates and carbamates. The former are versatile compounds that have found application in many fields of chemistry, for instance as additives for plasticizers, as electrolytes, building blocks for polymerization reactions or pharmaceutical compounds. Aluminum catalysis plays a prominent role within the field of cyclic carbonate formation which has led to some of the most effective catalytic systems to date. In the first chapter we report a comparative study on the activity of various aluminum-based complexes, providing a benchmarking of their initial reaction rates in the coupling of epoxides with CO_2 (Figure 29). These investigations provide a useful framework for how to realistically valorize relative reactivities and which features are important when considering the ideal operational window of each binary catalytic system.
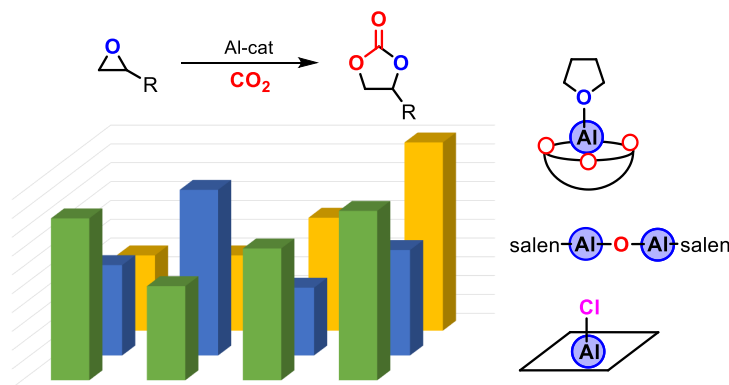

Figure 29. Benchmarking catalytic performances of Al-based catalysts in the field of cyclic carbonate formation.

The chemoselective coupling of oxetanes and carbon dioxide to afford functional, heterocyclic organic compounds known as six-membered cyclic carbonates remains a challenging topic. Making use of Al-aminotriphenolate catalysis, we presented the first general approach towards the formation of six-membered cyclic carbonates (6MCCs) through oxetane/CO_2 coupling chemistry (Figure 30). Excellent selectivity for the cyclic carbonate product was obtained as well as a broad product scope allowing substitution at both the 2- and 3-position(s) of the carbonate. Apart from a series of substituted six-membered cyclic carbonates, also the unprecedented room-temperature coupling of

General conclusion

oxetanes and CO_2 was discovered giving, depending on the structural features of the substrate, a variety of five- and six-membered heterocyclic products. The developed methodology was applied in the one-pot synthesis of linear carbamates from oxetanes, amines and CO_2.
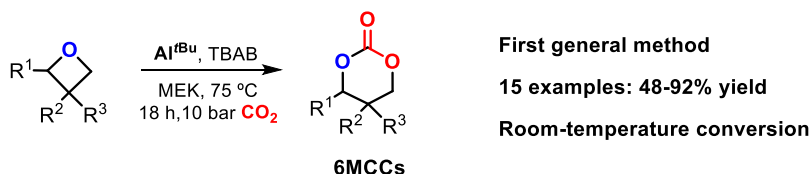

Figure 30. Chemoselective coupling of oxetanes and CO_2 to afford functional 6MCCs

Substituted epoxy alcohols and amines allow substrate-assisted conversion of CO_2 in the absence of a halide nucleophile. This new approach results in an unusual scope of CO_2-derived products by initial activation of CO_2 through either the amine or alcohol unit, thus providing nucleophiles for intramolecular epoxy ring opening under mild reaction conditions. Challenging di-substituted carbonates can be accessed by this method under very mild conditions and a unique approach towards the synthesis of tri-substituted carbonates is reported herein. Furthermore we can trigger both mechanistic manifolds under different conditions, thereby allowing for product divergence from a single substrate (Figure 31). The presented methodology proved exceptionally useful for epoxy amines, giving easy access to 5-substituted oxazolidinones that are common scaffolds in pharmaceutical compounds.
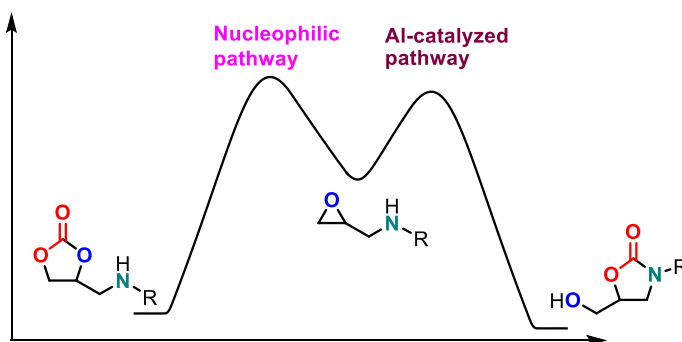

Figure 31. Selective triggering of both mechanistic manifolds leads to product divergence from a single substrate.

General conclusion

In the last part we provide a mechanistic investigation on the novel halide-free coupling of epoxides and CO_2. An alkyl carbonate species is proposed as the key intermediate, which has been investigated in the context of CO_2-trapping though its role in catalytic conversions remains virtually unexplored. We combined mechanistic experiments, *in-situ* IR spectroscopy and DFT-calculations in order to provide a complete description of the coupling of epoxy alcohols and CO_2, in which we were able to identify and characterize multiple crucial reaction intermediates via X-ray analysis and *in-situ* IR spectroscopy. The current findings can provide useful mechanistic insight into related processes where alkyl carbonates participate in catalytic reactions.
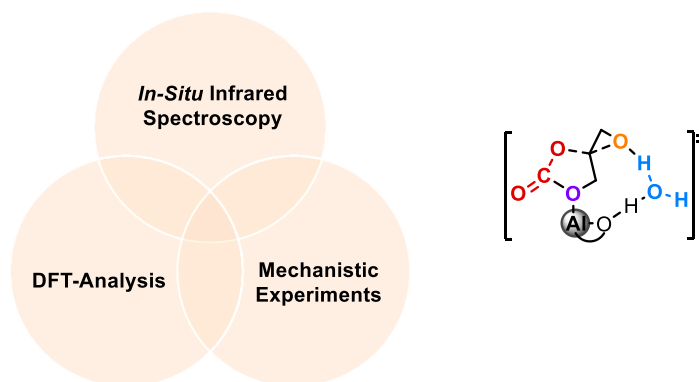

Figure 32. Mechanistic studies on the halide-free coupling of epoxy-alcohols and CO_2.

Overall, the results presented in this thesis show that Al-aminotriphenolate complexes are highly efficient systems in the context of existing epoxide/CO_2 coupling reactions, that can compete with the current state of the art in this area. Moreover, these Al-aminotriphenolate based catalysts are highly versatile systems that have provided a solution to important challenges such as the synthesis of 6MCCs from oxetanes and CO_2, and to explore new reactivity in the novel halide-free coupling of epoxy alcohols and amines with CO_2. The diverse substrate scope shows the generality of the methods described herein, which is further supported by application of the developed methodologies as a key step in the synthesis of several drug molecules.

UNIVERSITAT ROVIRA I VIRGILI
ALUMINUM-CATALYZED COUPLING OF CARBON DIOXIDE AND CYCLIC ETHERS
Jeroen Rintjema Tanger

UNIVERSITAT ROVIRA I VIRGILI
ALUMINUM-CATALYZED COUPLING OF CARBON DIOXIDE AND CYCLIC ETHERS
Jeroen Rintjema Tanger